The Effect of High Intensity Conditioning on Surface Oxidation with Processed Sudbury Nickel Ore

by

Jonathan Daniel Malainey

A thesis submitted in partial fulfillment of the requirements for the degree of

Master of Science

in

Chemical Engineering

Department of Chemical and Materials Engineering
University of Alberta

Abstract

In the Sudbury Basin, froth flotation is commonly used to recover Pentlandite (Pn), and Chalcopyrite (Cp), while rejecting Pyrrhotite (Po), and other gangue minerals typically found in the region. However, as the sulfide minerals flow through the plant the surfaces continually oxidize, allowing hydrophilic species to form on the surface. Thus, the selectivity of Pn, Cp and Po during flotation separation in a plant is reduced. To create new pentlandite surfaces, the slurry is reground, and a final flotation is performed to recover as much pentlandite as possible before the tails. The challenge is that pentlandite floats poorly in the fine particle size range so grinding creates additional fines and renders pentlandite less floatable. Additionally, pentlandite fines oxidize faster, resulting in a hydrophilic surface and poor dixanthogen formation. Finding a means of surface cleaning without the use of chemicals would be a helpful tool in improving nickel recovery in a sulfide processing mill.

High intensity conditioning (HIC) is a technique that has been successfully used in removing slimes from minerals that would otherwise be difficult to separate. The shear force generated from HIC can overcome the force of adhesion from both slimes and oxides, cleaning the mineral surface. In addition, a mechanism known as shear flocculation can occur under certain conditions, that agglomerates fine hydrophobic particles into larger, more floatable particles. The simultaneous dixanthogen formation during surface cleaning and aggregation of fines is responsible for the increased recovery of the minerals tested in the few studies available. The main purpose of this paper is to illuminate the benefits of High Intensity Conditioning (HIC) on oxidized slurries and clarify the challenges that hinder the implementation of HIC into plants. With the use of a Rushton impeller, the high shear fields can clean the mineral surface of slimes and oxides while still allowing for xanthate adsorption on Cp and Pn. Due to the lack of studies

combining HIC and sulfide minerals, fundamental tests were performed to determine each mineral's response to HIC. Oxide layers formed on concentrates and tails were removed and analyzed to determine metal oxidation levels.

The effect of high intensity conditioning on the oxidized sulfide ore is dramatic. When 10 or 20 g/ton of xanthate were used, chalcopyrite recovery with HIC was 4.5% higher than with no HIC while pentlandite recovery was 12% and 8.5% higher with HIC, respectively. However, pyrrhotite recovery with HIC was shown to increase by 22% and 14% for 10 and 20 g/ton of xanthate respectively. Solution analysis of the dissolved oxide layers from the concentrates showed that the immediately floatable minerals had high levels of oxidized copper and nickel. Ion activation is believed to be the cause. Based on the metal levels, with copper activation being more prevalent in the first few minutes of flotation and nickel activation playing a lesser role initially but becomes more rampant as time progresses. The HIC, while able to remove oxide surfaces, did nothing to hinder the oxidation of the sulfide surfaces. The combination of the oxidation and subsequent removal by HIC likely increases the copper and nickel ion concentration in the solution, allowing for pyrrhotite to activate and become floatable. If steps to reduce oxidation can be made, it is likely that pyrrhotite activation could be diminished but not entirely removed. Additionally, results may improve if chalcopyrite is not present in the slurry and therefore only nickel activation was the primary catalyst for activation.

The parameters used for HIC reflected the state of the minerals when used. The initial flotation responses showed the mineral was much less floatable despite being a concentrate. Given this, it is quite likely that if the slurry was testing shortly after plant sampling, the parameters for HIC, including xanthate addition and duration of HIC, can be reduced. More

minute changes would allow for greater control and analysis of which mechanisms complete faster.

High intensity conditioning can reinvigorate pentlandite surfaces and flocculate fines. The sparse use of this technique means more work is needed before a complete process can be implemented. If more interest could be garnered and the experimental design improved, HIC could eventually be a means to slurry treatment to maximize recovery of valuable minerals, which will become scarcer over time.

Acknowledgements

I want to express my gratitude and sincerest appreciation to my supervisor, Dr. Qingxia Liu for the challenging direction he allowed me to pursue in this research project. You provided valuable insight, supported me in my research interests and used your experience to improve my experiments and my thought process when planning out experiments. I will always appreciate the many times you took to debate my experimental findings with me and really make me work to defend my position, cement my analytical skills and mature the way I present my information.

Within our research group, there were a few people who were indispensable and truly made my work a joy. Thank you to Jing Liu and Chao Qi for the enormous amount of time and patience you showed me when we sat together, and I would describe my thoughts and concerns on my experiments, findings, interests or fringe areas of interest in mineral processing. I cannot imagine what my work would look like without their companionship throughout my time in the master's program. Thank you to Caroline Gonclaves for all things you helped me improve in the lab that eventually culminated in vastly improved accuracy in my experiments. You helped me find inventive solutions to my problems and your fearless criticism forced me to improve how I conducted my work. Thank you to Carol Dwaik for helping me on multiple occasions and providing skillful help for demanding experiments in the lab.

Thank you to James Skwarok, for helping me in the lab with providing insight into how I could improve my experiments or helping me find an innumerable number of small items that made my experiments possible. Your kindness and patience were appreciated. Thank you to Mingda Li for helping me design parts with the 3D printer to continue improving with my experiments. Your speed and skill with AutoCAD meant I never waited long for parts so I could continue my work. Thank you to Shiraz Merali and Guangcheng Chen for using their labs to analyze my samples quickly and accurately. Thank you to Mingli Cao for the use of the grinding lab equipment and table space for sampling my filtered slurry.

A special thank you to Susie Woo with Bureau Veritas for their reliable services in analysis of my many mineral samples. Your expertise on ICP analysis and consideration in rushing my samples when I needed them quickly was greatly appreciated.

Finally, I want to thank our sponsor and research partner, Glencore, and more specific XPS Consulting in Sudbury, Ontario. I want to thank Curtis Deredin for his help in sending my

buckets of sampled slurry, without I could not do my work. As well, thanks for assisting me with my ICP and LECO analysis. Thank you to Ravi Multani and Gregg Hill for communicating with me over the course of the project and providing me with valuable information and experience. My appreciation is beyond words. A last thank you to Dominic Fragomeni for being instrumental in funding this project, granting me this opportunity in the first place, and inviting our group out to the Strathcona Mill for firsthand experience with the flotation process.

Table of Contents

List of Tables

Table of Figures

Chapter 1 Introduction

1.1 Background and Purpose

In the Sudbury Basin, the main minerals of interest are chalcopyrite, pentlandite and pyrrhotite. While chalcopyrite and pentlandite are important sources of copper and nickel, respectively, pyrrhotite is an unwanted gangue that must be separated at all costs. This is simply due to its negligible economic value in the Sudbury Basin. In other parts of the world, pyrrhotite can be valuable due to their association with platinum-group minerals (PGM) and are therefore not a gangue[1], [2]. When pyrrhotite is recovered, the result is a dilution of the concentrate grade and more sulfur dioxide expelled during smelting.

There have been strides in the depression of pyrrhotite in the last few decades. The faster oxidation rate of pyrrhotite lead to all flowsheets incorporating a basic environment during froth flotation, as well as the use of mild steel during the grinding process. These changes have led to a high depression of pyrrhotite and are now common practice in all plants.

In the last 20 years, the revelation of ion activation on pyrrhotite drove research into the use of chelation to counteract this new challenge. Even now, the incorporation of chelators into a plant's flowsheet is being studied due to their positive effect on pyrrhotite depression[3][4]. However, the best chelators are not environmentally friendly, due to their innate stability, so the use of current chelators is not viable in the long term.

Much of the work into sulfides is still establishing a better fundamental understanding. The difference between hexagonal and monoclinic pyrrhotite during processing is becoming more apparent, with recent publications focusing on the impact the differences have on flotation [5], [6]. While this body of work has been improved dramatically in the past few years, the individual effects of ion activation on monoclinic and hexagonal pyrrhotite still needs further investigation and will likely cause another shift in how pyrrhotite-containing sulfide ore is dealt with in the future.

While much of the focus is on depressing pyrrhotite, another equally important factor into the processing of sulfide ore is to maximize recovery of pentlandite and chalcopyrite. Without sounding cavalier, chalcopyrite is an extremely floatable mineral showing recoveries that exceed either of the other minerals, with and without the addition of a collector. Pentlandite is much more particular in the conditions that facilitate its high recovery. As the optimal environment for

pentlandite recovery often favors pyrrhotite, plant practice is often like balancing on the edge of a knife. Furthermore, pentlandite's ability to become hydrophobic with a collector is in direct competition with the formation of mineral lattice blocking species through normal oxidation. Considering that pyrrhotite is known as a slow floating mineral and the processing of sulfide ore becomes an incredibly time sensitive process. Lastly, given that most plants have been around for decades and have an established flowsheet, most alterations, beyond the use of a reagent, are difficult to implement and require a great deal of confidence before even preliminary consideration will be given.

Pentlandite is a mineral that is has a maximum opportunity for recovery with a clean surface that exposes nickel sites in the lattice, while in the optimal size range of 10 to 75 microns [7]. Therefore, the beginning of a flowsheet is scrutinized for providing the best environment to improve pentlandite's hydrophobicity. However, there will always be a varying amount of pentlandite that cannot be recovered in the early stages. This can either be to a lack of liberation from hydrophilic silicates resulting in their permanent disposal in rock tails or just unable to interact with the controlled levels of xanthate and end up in the pyrrhotite rejection circuit. While losses into the rock tails cannot be effectively solved without an overhaul in the grinding procedure, pentlandite in the pyrrhotite rejection circuit is likely present due to being in outside of the optimal particle size range or being overoxidized and unable to float effectively without excessive collector addition. Pentlandite recovery in this section of the flowsheet is dependent upon finding an option that can clean the surface of pentlandite particles and somehow improving the recovery of pentlandite fines while hopefully not improving the recovery of pyrrhotite.

This work within this thesis was first started when ways to improve the recovery of pentlandite fines were being investigated. Pentlandite fines, created during the grinding process, have abysmal recoveries and account for a great deal of pentlandite loss in the Sudbury Basin ore. This has been attributed to their fast oxidation and blocking of surface sites needed for pentlandite's recovery. While looking into work that had sought to study solutions into improving the recovery of pentlandite fines, work discussing a technique known as high intensity conditioning (HIC) was discovered. Srdjan Bulatovic had shown improvements in the recovery of pentlandite fines by creating high shear fields in a slurry. The early interpretation was that the fines had their surfaces cleaned, allowing for the adsorption of xanthate. This was only half the

story. This technique had been indirectly discussed over a decade prior by Leonard Warren, who used HIC to aggregate fines which resulting in their improved flotation. Dr. Warren's work completed the phenomenon observed by Srdjan, who hadn't considered shear flocculation in his own conclusions. Given this statement, HIC sounds promising. However, research in this direction was sparse and far too varied in the experimental design and choice of minerals to truly make a clear determination. While the benefits of using HIC has extending to a wide variety of minerals, most work focused on orebodies that had a single mineral that can be rendered hydrophobic with a collector. A system with pentlandite and pyrrhotite had never been investigated.

1.2 Research Objectives

The purpose of this thesis is to use HIC on a sulfide slurry containing pentlandite and pyrrhotite with the intent of determining whether HIC can improved the recovery of pentlandite while depressing pyrrhotite.

The objectives of this thesis are:

- To study the impact of different impellers during HIC on a chalcopyrite-pentlandite-pyrrhotite mixture
- To determine the effect of varying the power input of HIC on the recovery of each sulfide mineral
- To understand the oxidation of the sulfides during flotation but studying the metal oxides removed from their surface.

1.3 Structure of the Thesis

This thesis consists of 7 chapters:

- Chapter 1: Introduction of the current challenges of pentlandite recovery and pyrrhotite separation
- Chapter 2: Literature review that covers the fundamentals of mineral flotation, sulfide flotation with a xanthate collector, galvanic interaction between sulfide minerals, sulfide oxidation and sulfide recovery based on particle size. As well, the fundamentals that establish high intensity conditioning are discussed with shear flocculation and surface cleaning being the focus.

- Chapter 3: Description the samples used in this thesis, including the experimental methods, equipment and procedures. Mineralogy of the samples used in this work is described in this section.
- Chapter 4: HIC study using a hydrofoil impeller. Initial tests that tested various baseline experiments to understand the impact on the mineral sample.
- Chapter 5: HIC study using a Rushton turbine. Tests include analysis of the oxide surface after flotation to link recovery with metal oxidation on the surface.
- Chapter 6: Discussion of the results provided, considering previous work by other researchers.
- Chapter 7: Conclusion and Recommendations for Future Work

Chapter 2 Literature Review

2.1 Sulfide Mineral Processing

The separation of valuable metals from their sulfide constituents remains a process that can be improved. While the use of froth flotation along with a host of reagents have greatly increased the recovery of these precious minerals, there are still several issues that plague the mineral processing industry. With respect to sulfides, the flotation characteristics between the sulfides considered valuable and the sulfides largely regarded as unwanted (or gangue) are similar enough to affect their selective separation in a negative manner. This thesis specifically investigates ways to improve the selectivity between pentlandite and pyrrhotite, which is a continuing challenge due to their similar flotation chemistry.

Sulfide minerals are extracted worldwide and can be found in varying compositions[8]–[10]. The location of the sulfides that are investigated in this thesis are found in the Sudbury Basin, located in Ontario, Canada. The three sulfides considered are pentlandite, chalcopyrite and pyrrhotite.

The strategies used to recover pentlandite or separate pentlandite from accompanying minerals with vary in success based on the location. In the Sudbury Basin, the focus is more on the selective flotation of pentlandite and chalcopyrite while preventing the recovery of pyrrhotite. These sulfides are accompanied by various silicates that are naturally hydrophilic and are not overly challenging to segregate. Conversely in Australia or the Jinchuan province in China, sulfides are found with serpentine or magnesia-based minerals where slime coatings are a more prevalent challenge and require a different strategy.

2.1.1 Mineral Overview

2.1.1.1 Pentlandite Mineral

Pentlandite is a nickel sulfide, considered a valuable mineral due to the nickel metal contained within. The chemical formula for pentlandite is $(Fe,Ni)_9S_8$ where the ratio between iron and nickel will vary based on their geological location or if they were synthesized. Varying ratios can be achieved by using the solid solubility limits of pentlandite during cooling [11], [12].

The formation of pentlandite from the nickel content in pyrrhotite in solid solution can occur. When the solid solution is cooled slowly, the sulfur difference between pentlandite and pyrrhotite allows minor amounts of pentlandite to form at grain boundaries [11]. In recent years, the amount of nickel present in pyrrhotite is dependent upon the forms of pyrrhotite present [13]. The higher nickel content in pyrrhotite can lead to more pentlandite being formed. The ability to naturally form together shows the degree of intergrowth that can occur between pentlandite and pyrrhotite, illustrating the difficulty in their liberation even following crushing and grinding [14]. This locking of pentlandite and pyrrhotite is seen in analysis of feed ore for the Sudbury Basin mines, where pentlandite is locked with pyrrhotite more than any other mineral present.

2.1.1.2 Chalcopyrite Mineral

Chalcopyrite is a copper sulfide and the other sulfide that is recovered for the value of the copper metal. A very common mineral, the chemical formula is $CuFeS_2$. and the composition varies minimally. Chalcopyrite has a low nickel solubility which translates in easier liberation from pentlandite and pyrrhotite. This is reflected in the locking of chalcopyrite in the feed ore where the unliberated chalcopyrite appears locked with non-sulfide gangue than pentlandite and pyrrhotite combined. In the rock tails, where non-sulfide gangue is disposed of, 85% of chalcopyrite found in the stream was locked with non-sulfide gangue. In the pyrrhotite tails, 60% of the chalcopyrite was locked with NSG, while the rest was mostly still liberated with under 10% being locked with either pentlandite or pyrrhotite. In the Sudbury Basin, chalcopyrite is the most forgiving of the sulfide minerals and while maximized recovery of chalcopyrite is essential to the economic success of the plant, it is nowhere near as challenging to separate when compared to pyrrhotite and pentlandite.

2.1.1.3 Pyrrhotite Mineral

Pyrrhotite is an iron sulfide that has several compositions due to its non-stoichiometric formula $Fe_{1-x}S$ ($0 \leq x \leq 0.125$). In the Sudbury Basin, the two types of pyrrhotite that are present in the ore body are monoclinic (Fe_7S_8) and hexagonal (Fe_9S_{10}) pyrrhotite. The most notable difference between the two is the observed susceptibility to magnetism. When comparing vacancy distribution between the two pyrrhotites, hexagonal shows consecutive layers filled with iron while monoclinic only has single layers. This greatly affects the magnetic properties of the

two pyrrhotites, with monoclinic having ferromagnetic properties and hexagonal exhibiting ferromagnetic or nonmagnetic behavior [15], [16]. Nickel content in pyrrhotite has also been correlated to the type of pyrrhotite, where monoclinic pyrrhotite contains 0.4-0.5% nickel and hexagonal pyrrhotite contains 0.8-0.9% nickel. Recently, whether the pyrrhotite is either single phase or an intergrown mixture affects the nickel content was specifically linked to the deposit. While hexagonal pyrrhotite's nickel content was consistent, regardless of being a single phase or intergrown, monoclinic pyrrhotite showed a drastic change. As an intergrown mixture, nickel content was in previously reported range of 0.4-0.5 wt.% nickel. In a single phase, the nickel content could increase up to 2 wt.% Ni. These characteristics can drastically impact flotation or inferred success of a new technique, as depressing the pyrrhotite will impact the reported recovery of Ni. Given some feed ore, where pyrrhotite can be 7 times higher than the amount of pentlandite, the nickel losses can give a counterproductive impression when pyrrhotite is depressed.

2.1.2 Froth Flotation Overview

Froth flotation is a technique that has become commonplace in the mineral industry, due to its effectiveness in separating minerals based on their flotation characteristics. As the process has been described extensively in a multitude of literature [17], a short summary will be provided.

Froth flotation uses the innate surface chemistry of minerals to "float" specific minerals to the top of a liquid tank (known as froth or concentrate) while the remaining minerals stay in the solution (or slurry), to be either sent for storage as tails or to undergo additional flotations. The act of flotation is due to rendering the surface hydrophobic (dislikes water) and increasing the likelihood of attachment to air bubbles that are generated at the bottom of the tank and float upwards.

Collectors

There are several ways to preferentially float specific minerals. The use of a collector to preferentially adsorb onto the mineral surface is one method. Typically, the collector has two ends, one which can bond with the mineral surface and another which is hydrophobic and is responsible to attaching to the bubble [18]. There are many collectors and choosing the right one

is crucial to a successful flotation. With respect to sulfides, xanthates have shown to be an effective choice and will be explained in a later section[17].

Frothers

As the froth is used to transport the valuable minerals from the slurry, ensuring the stability of the bubbles is important. In this case, a frother is just another reagent typically found in the slurry. Frothers generally vary based on their application[4], [19]–[21].

pH Control

As the attachment of the collector is dependent upon the surface chemistry of the mineral, the importance of understanding how pH will affect the mineral surface cannot be overstated. Although this will be discussed further later, regarding the sulphide minerals previously mentioned, pH can have a profound effect on surface chemistry. Most, if not all, mineral processes are tuned to operate within a certain pH range to take advantage of surface chemistry. Although there is a wealth of information regarding the effect of pH on the flotation of various minerals [22]–[24], there are still configurations that haven't been investigated that could benefit selective flotation of multiple minerals.

Activators

Activators are reagents that allow for collectors to adsorb onto surfaces that may not be possible otherwise[25]. With respect to sulfides, cupric ions have a large effect on the surface, though not always for the benefit of the flotation. These will be described in Section 2.1.4.2.2.

Depressants

Depressants refer to any reagents that cause specific minerals, which would otherwise float, to sink [26]–[28]. This could be either through chelation (removing specific ions, which would activate a mineral surface, by forming a metal complex) or creating a passivating layer on the mineral surface.

2.1.3 Sulfide Flotation with a Collector

The surface of sulphide minerals can be hydrophobic, even without collectors. This behavior may still occur, in the presence of collectors, so it is important to know the electrochemical parameters that will induce flotation of the sulphides. This differs from natural floatability which refers to the ability to float without collectors, a specific Eh range and does not show a change in floatability if Eh is altered [29], [30]. The sulfides that are being investigated

do not exhibit natural floatability by this definition, so it will not be discussed further. Investigations regarding collectorless flotation of sulphides have been ongoing since the early 1940's with Ravitz in 1939 and Herd in 1940 suggesting the natural floatability of galena. In the 1970's, chalcopyrite was shown to have collectorless floatability [31], [32] which was supported by experiments performed by Heyes and Trahar [33] showing flotation in an oxidizing environment. Gardner and Woods corroborated Heyes and Trahar's findings using a Hallimond tube to control the mineral potential [34].

The species responsible for improving the hydrophobicity of sulfides without collector is elemental sulfur [34], [35]. Hydrophobic patch of elemental sulfur form due to an anodic oxidation reaction of the sulfide surface which can only occur under specific pulp potential and pH ranges in the system [36].

In an acidic environment:

$$MS = M^{n+} + S^0 + ne^- \qquad (1)$$

In a neutral or basic environment:

$$MS + nH_2O = M(OH)_n + S^0 + nH^+ + ne^- \qquad (2)$$

In competition with these oxidation reactions corresponding with improving the hydrophobicity of a mineral, there are oxidation reactions which will produce hydrophilic oxy-sulphur products. These have been described in previous studies on sulfides. Typically, oxy-sulphur compounds occur in more oxidizing conditions where elemental sulfur is considered a metastable product between the unoxidized sulfide surface. An Eh-pH or Pourbaix diagram can be used to determine these relative stabilities and metal ion concentrations will affect the placement of these stability lines[37]–[40].

Studies that investigate the collectorless flotation of pentlandite are scare compared to chalcopyrite and pyrrhotite[23], [41], [42]. Studies performed by Heiskanen et al. showed the collectorless flotation of pentlandite, chalcopyrite and pyrrhotite in noritic ore as a function of pH.

2.1.3.1 Collectorless Flotation of Chalcopyrite

Chalcopyrite had the best recovery of the three sulfides in Heiskanen's study, with recoveries about 80% below a pH of 6 and about a pH of 11 [43]. Chalcopyrite has shown strong collectorless floatability in other studies as well [29], [36], [44]–[49]. The pulp potential was

manipulated at various pH values. At lower pH values, the recovery of chalcopyrite is above 80% in both reducing and oxidizing conditions (0-800mV SHE). As the pH increases, the optimal pulp potential range decreases considerably. At a pH of 8, the range narrows to 250-550 mV SHE. At higher pH values, a further narrowing of this range is expected. In conclusion, chalcopyrite seems reasonably floatable regardless of the pH in typical plant setting.

2.1.3.2 Collectorless Flotation of Pentlandite

Pentlandite showed similar recoveries to chalcopyrite at a pH below 5, but quickly drop to 30-40% at high pH values [43]. Heiskanen et al. also showed that the collectorless flotation of pentlandite was quite slow, with recoveries more than doubling in the pH range of 6-9 when the collection time was increased from 8 minutes to 16 minutes. This changes the collectorless floatability of pentlandite from having a lower recovery in the neutral pH ranges and improving around a pH value of 10, to have a general decline in collectorless recovery as the environment becomes more basic. As most flotations in ore processing plants take time and are usually around a pH of 9, this means that pentlandite's collectorless recovery may account for its recovery than is currently assumed. In the studies performed by Chen in high intensity conditioning, pentlandite fines were able to aggregate together quite well without collector[50].

Pyrrhotite floats above 80% below at a pH of 5 or lower, but recovery drops to negligible values at high pH values [2], [43]. The study attributed the minimal recovery of pyrrhotite above a pH of 5 to only mechanical entrainment. At lower pHs, there is no selectivity between the sulfides. However, pyrrhotite floats poorly above 5 without collector, while pentlandite's recovery is severely reduced but still present. Pyrrhotite shows collectorless floatability over all pH ranges when the pulp potential was controlled [36]. Initially, a highly oxidizing potential range is needed for an acidic environment. However, as the environment becomes more basic, this optimal potential range become more reducing. At around a pH of 9, pyrrhotite is floatable without collector from approximately 300-425mV SHE [36], [51], [52].

2.1.3.3 Collectorless Flotation of Pyrrhotite

Pyrrhotite has the worst recovery without a collector and this is likely due to the aggressive oxidation of its surface compared to the other minerals[2], [5], [6], [41], [53]. Legrand compared the oxidation of pentlandite and pyrrhotite in environments with varying

amounts of dissolved oxygen [54]. Using argon purging, where dissolved oxygen was below the detectable limit of 0.01ppm, both minerals were reasonably clean and free of detectable oxidation. However, at 0.03ppm, pyrrhotite oxidized readily formed ferric oxyhydroxides while pentlandite showed only slight oxidation. Earlier studies treated pyrrhotite as a single mineral but is now being viewed as having a variety of forms. Regarding the Sudbury Basin, pyrrhotite can present with either a monoclinic or hexagonal crystal structure. Monoclinic pyrrhotite oxidizes faster than hexagonal pyrrhotite and therefore is more difficult to float with or without collector. This has been attributed to a few factors in the monoclinic structure compared to the hexagonal: higher vacancy concentration and ferric ions ratio in the lattice [13].

Overall, chalcopyrite is the most floatable without collector followed by pentlandite and finally pyrrhotite. The selective separation of these minerals is not possible without collector in typical flowsheets. Therefore, the interaction of xanthate with the sulfides needs to be discussed.

2.1.4 Sulfide Flotation using a Xanthate Collector

Collectors are typically used in all sulfide flotations to improve the hydrophobicity of the sulfides. Among the varied selection of collectors, xanthates are commonly used[4]. Their stability in basic solutions, as well as their solubility in water-based solutions, allow them to be used in typical sulfide environments [17]

However, their selectivity with sulfides is not ideal. Therefore, the use of other controls is required to improve the separation. Overall, xanthates are extremely convenient collectors that are excellent in orebodies where sulfide separation from other non- sulfide minerals is needed.

2.1.4.1 Xanthate Interaction with Pentlandite

Some of the earliest work performed on the use of xanthate to float pentlandite occurred in 1960s [55], where amyl xanthate was used to separate pentlandite and chalcopyrite from pyrrhotite. Studies in the late 70s [56] showed that xanthate adsorption on pentlandite was unaffected by the presence of serpentine slime, but the lack of hydrophobicity was expected to be due to slimes hindering the contact of dixanthogen with air bubbles. This is an issue seen today globally with orebodies in eastern Canada [23], [56], various Australian mines [10], [50], [57] and the Jinchuan mine in China [58].

A large gap in literature regarding the xanthate interaction with pentlandite from the 70s up until the 90s can be attributed to the difficulty in conserving early work and transitioning to electronic copies. As well, pure pentlandite is a difficult resource to procure, so much work with xanthate was performed on easier to acquire sulfide minerals such as galena, chalcopyrite, sphalerite and pyrite. Lastly, due to a large amount of work being performed by industrial research labs, much data likely remains internal and not easily accessible.

While pentlandite has been studied in recent decades when utilizing xanthate collectors, most of the work has been on depressing pyrrhotite in a pentlandite/pyrrhotite mixture. Therefore, much of the work has been less on fully understanding the interaction with xanthate, but more on the reasons for pyrrhotite's varying flotation response with xanthate. However, the consensus is that dixanthogen, an oxidized form of xanthate, is responsible for improving the hydrophobicity of pentlandite [22], [54], [59], [60]. In most cases, a combination of UV spectroscopy and ATR-FTIR can be used to confirm a transfer of xanthate in the solution into the formation of dixanthogen on the surface. UV spectroscopy is used to measure the xanthate concentration left in the solution [22] and been utilized to determine the adsorption of xanthate onto mineral surfaces. Extraction of the adsorbed species can be performed using hexane, following by UV spectroscopy as well.

Analysis of only the solution using UV spectroscopy does not provide a complete understanding, as previous work has shown the formation of various xanthate species [61]. The species that can be formed from xanthate are varied and depend upon the xanthate concentration and solution mixtures. FTIR-ATR does allow for the confirmation of the dixanthogen species based on stretching vibration peaks and comparing peak height to determine relative, non-quantitative, amounts of dixanthogen presence between mineral samples [22]. At the time of this review, there is no way to conclusively account for the xanthate species that can form during flotation. Speculations regarding the formation of intermediate xanthate species for other minerals have been made [32], as well as insoluble metal xanthates with pentlandite [61]. X-ray diffraction and infrared spectroscopy have been suggested to determine metal xanthate identification [62]. A more complete understanding of all xanthate species present could be possible with a combined array of analysis tools, but perhaps the feasibility or lack of fundamental benefit may contribute to the absence of such an investigation.

Ironically, the origin for how xanthate interaction and subsequent dixanthogen adsorption proceeds is still based upon work by Hodgson and Agar from 1989 [42]. This study has served as the source for how dixanthogen forms, with no amendments in recent years. The high uptake of xanthate on the pentlandite surface is due to the number of nickel sites naturally present in the pentlandite lattice and subsequently on the surface [22], [42]. Based on work by Hodgson and Agar, the widely accepted interaction between xanthate and the nickel sites on the pentlandite surface occurs in two steps:

1) Chemisorption of xanthate ion onto a nickel site in the pentlandite lattice:

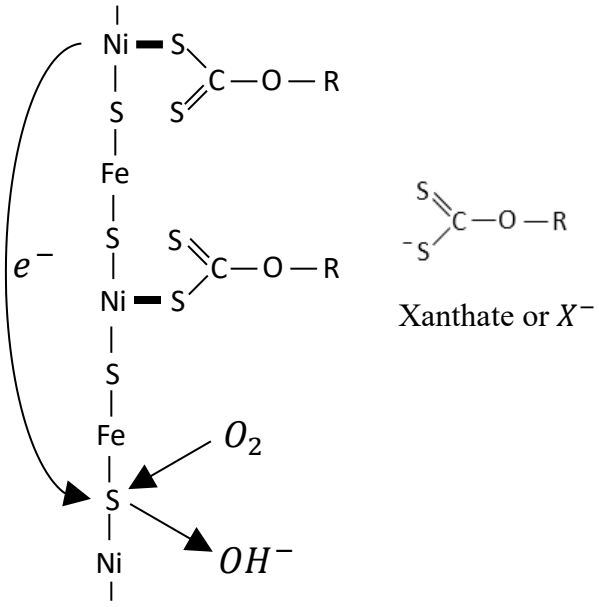

Figure 1: Representation of Xanthate Chemisorption on Pentlandite. Developed from work by various researchers [42], [63], [64]**.**

The two redox reactions for Figure 1 are below:

Anodic Reaction:

$$Ni_s + X^- = NiX + e^- \quad (3)$$

Cathodic Reaction:

$$O_2 + 2H_2O + 4e^- = 4OH^- \quad (4)$$

2) The oxidation of an additional xanthate molecule between two chemisorbed xanthate molecules, forming a xanthate bridge known as dixanthogen or bulk dixanthogen patches:

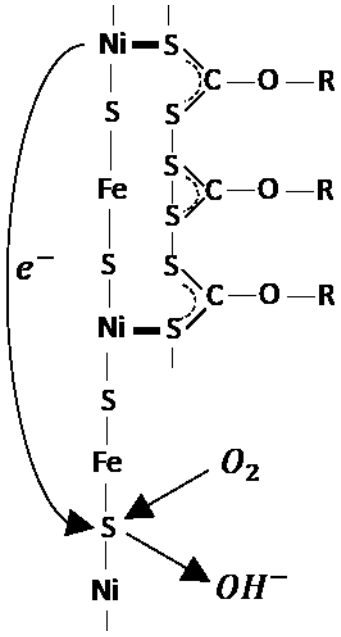

Figure 2: Representation of dixanthogen formation on pentlandite. Developed from work by various researchers [42], [63], [64]**.**

The redox reaction for the final step of bulk dixanthogen formation (Figure 2) are shown below:

Anodic Reaction

$$NiX+X^-=NiX_2+e^- \quad (5)$$

Cathodic Reaction

$$O_2+2H_2O+4e^-=4OH^- \quad (6)$$

Most studies choose to represent dixanthogen as a single molecule formed from two xanthate molecules. ATR-FTIR relies on the bulk dixanthogen formation step to identify the presence of dixanthogen. There are three characteristic xanthate peaks that have been previously measured with ATR-FTIR that provide the means of identifying the formation of bulk dixanthogen [65]–[67]. Using Figure 1 and Figure 2, the characteristic peaks can be correlated to specific bonds in Hodgson and Agar's original representation. These characteristic peaks are specific to either the xanthate molecule chemisorbed onto the pentlandite nickel site or the xanthate molecule that oxidizes between two chemisorbed molecules, forming bulk dixanthogen. Combining the commonly accepted representation of dixanthogen formation with the characteristic bond peaks

seen with ATR-FTIR shows the differing S-C-S bond peaks are for whether the xanthate is bonded to the nickel site (in the case of pentlandite) or if the xanthate is responsible for bridging two nickel-bonded xanthate molecules together and forming dixanthogen. This is made clearer in Figure 3.

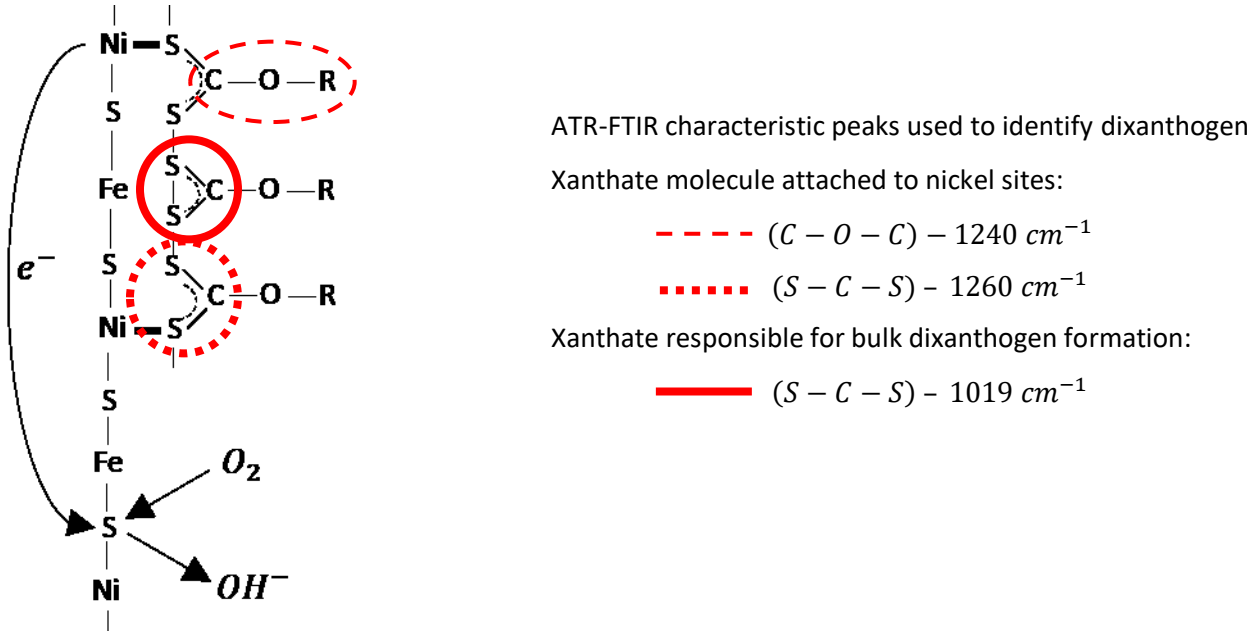

Figure 3: Representation of proposed relation between ATR-FTIR dixanthogen identification and current representation of dixanthogen formation on pentlandite. ATR-FTIR characteristic peaks from previous work by Leppinen [64], [65].

The formation of dixanthogen patches is important due to the implications on hydrophobicity. If the formation of a patch requires two closely spaced nickel-bonded xanthate molecules, then the initial uptake of xanthate onto these nickel sites is incredibly important. Furthermore, the two steps to form bulk dixanthogen are likely kinetically distinct. There is no current work that correlates hydrophobicity with dixanthogen patch surface area.

The first step of xanthate interaction with pentlandite therefore relies on the availability of nickel sites required for chemisorption. Being a sulfide mineral, pentlandite is subject to the formation of oxides that can occur, given the appropriate conditions. If an oxidation layer forms on the nickel sites, the initial chemisorption of xanthate cannot occur and therefore the formation of dixanthogen is not possible on those covered nickel sites.

2.1.4.1.1 The Relation between Pulp Potential and Xanthate Adsorption on Pentlandite

The formation of dixanthogen on pentlandite is essential to improving the hydrophobicity and subsequent flotation of pentlandite. As xanthate needs to oxidize into dixanthogen, this means that pulp potential plays a vital role in facilitating dixanthogen formation. This thesis will not focus on discussing electrochemistry basics as these fundamentals has been properly explained in other literature [17], [22], [36], [68]. The oxidation half reaction of xanthate into dixanthogen allows the calculation of the minimal potential required for oxidation into dixanthogen to proceed:

$$2X^- \leftrightarrow X_2 + 2e^- \quad (7)$$

Using the Nernst equation, this minimal potential can be calculated. At standard conditions, the Nernst equation can be reduced to:

$$E_h(V) = E_h^o(V) - 0.0591 \log[X^-] \quad (8)$$

Peres showed the dramatic effect of pulp potential using amyl xanthate. Given a standard potential (E_h^o)for amyl xanthate of -0.158V [69] with the concentration used by Peres ($X^- = 0.74 * 10^{-4}\ M$), the equilibrium potential (E_h) is 0.086 V or 86 mV. The pulp potential needs to be higher than the equilibrium potential, otherwise xanthate will not oxidize into dixanthogen. However, the pulp potential also will also serve as the driving force that affect the oxidation rate of dixanthogen [70]. The closer the pulp potential is to the equilibrium potential, the slower the oxidation rate of xanthate into dixanthogen.

When xanthate is added to a solution, the pulp potential of the slurry will reduce due to the presence of aqueous xanthate [60]. As the aqueous xanthate concentration lowers in solution, being removed due to adsorption onto pentlandite's surface, the pulp potential will eventually rise back to its original value, once all the xanthate has been consumed.

At the same time, the rest potential on the pentlandite's surface will lower as the aqueous xanthate is being adsorbed [22], [42]. These two changes in potential will occur at the same time and can be interpreted as the reduction in potential being tied to the presence of xanthate. The transfer of xanthate from solution to surface can therefore be measured in the transfer of potential reduction from the pulp potential in the solution to the reduction of the rest potential on the mineral surface. The degree which the rest potential is lowered is related to the amount of xanthate adsorbed by the sulfide surface. Comparing the change in rest potential in Figure 4with the change in pulp potential in Figure 5, this simultaneous transfer becomes more clear. This

understanding has been used to compare adsorption levels of xanthate between sulfide mineral samples.

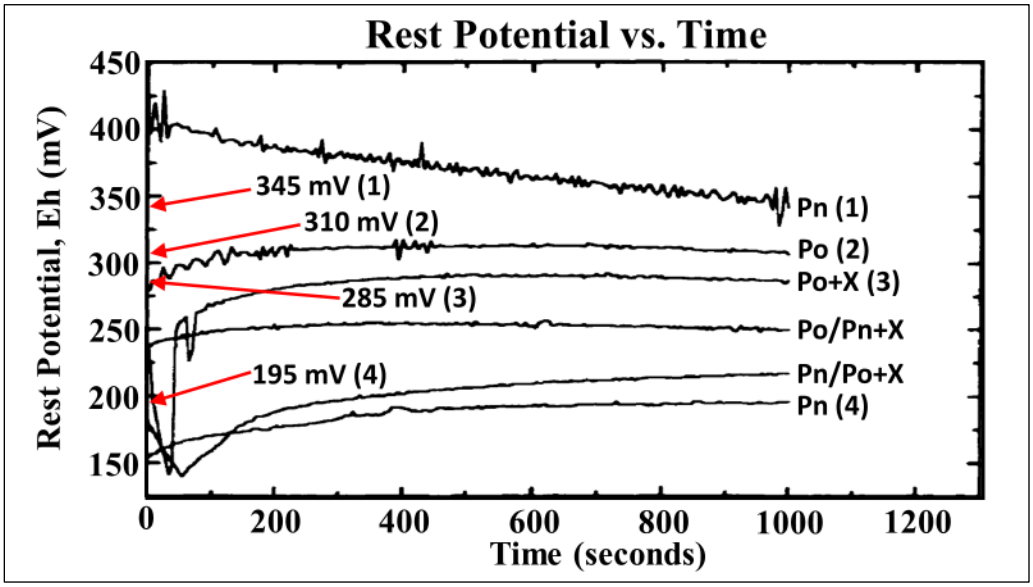

Figure 4: Rest potentials of pentlandite and pyrrhotite, before and following the adsorption of PIBX. Adapted with permission from paper by Bozkurt, 1998 [63]**.**

Peres showed the effect of pulp potential and xanthate adsorption on pentlandite by adding sulfur dioxide to lower the pulp potential before adding xanthate. The two experiments being compared used either a standard solution (Eh = 460 mV) or a solution with SO_2 addition (Eh = 285 mV). In Figure 5**,** the standard solution showed a fast adsorption of xanthate with the pulp potential rebounding within 30 seconds. Comparatively, the solution with sulfur addition had much slower xanthate adsorption with the pulp potential rebounding after 150 seconds.

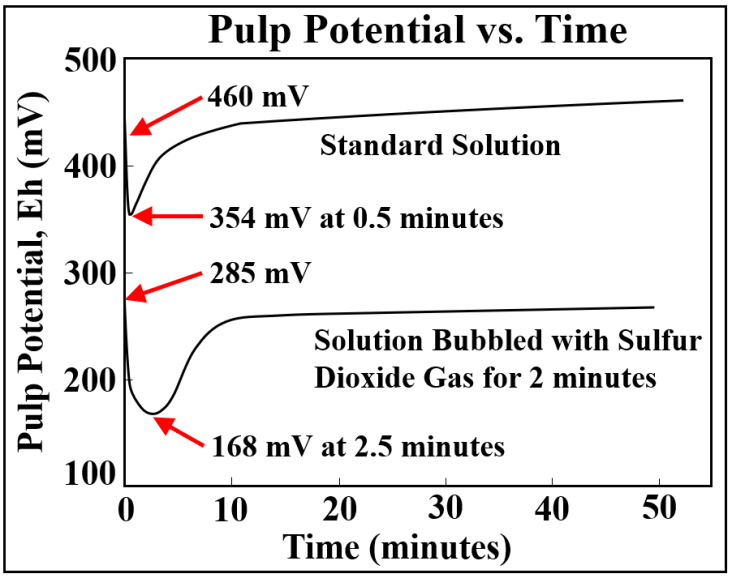

Figure 5: Pulp potential (measured through a platinum electrode) vs time for pentlandite slurry. PAX was added to a standard solution and a solution bubbled with sulfur dioxide. The figure is based on the work performed by Peres, 1979 [60].

The difference between the measured pulp potential and the equilibrium potential for amyl dixanthogen in a standard solution is shown below:

$$\Delta V_{max} = 460 \text{ mV} - 86 \text{ mV} = 374 \text{ mV} \quad (9)$$

$$\Delta V_{min} = 354 \text{ mV} - 86 \text{ mV} = 268 \text{ mV} \quad (10)$$

The next experiment used sulfur dioxide gas to lower the pulp potential and observe the impact of dixanthogen formation on pentlandite surfaces. The difference between the measured pulp potential and the equilibrium potential for amyl dixanthogen in a solution bubbled with sulfur dioxide is shown below:

$$\Delta V_{max} = 285 \text{ mV} - 86 \text{ mV} = 199 \text{ mV} \quad (11)$$

$$\Delta V_{min} = 168 \text{ mV} - 86 \text{ mV} = 82 \text{ mV} \quad (12)$$

By comparing the pulp potential fluctuations of the two tests in Figure 5, the effect is evident. Not only is the minimum pulp potential reached 5 times faster in the standard solution, but the smaller reduction in pulp potential upon xanthate addition suggests the quicker adsorption as well. This further supports that xanthate adsorption is kinetically slower at lower pulp potentials. The comparison of the pulp potential difference, between the standard solution or with the addition of sulfur dioxide, illustrates the difference in the kinetics of xanthate

adsorption. The standard solution has twice the maximum potential difference of the sulfur dioxide solution and triple the minimum potential difference. These changes can have a huge impact on pentlandite flotation, as xanthate is a reagent being competitively consumed by multiple sulfides during froth flotation. Slowing down the adsorption rate onto pentlandite can be a costly mistake in a mixed mineral environment.

2.1.4.2 Xanthate Interaction with Pyrrhotite

Pyrrhotite's ability to interact with xanthate is much more complicated than other sulfides, namely due to the different xanthate reactions based on whether pyrrhotite is activated or not by metal ions. The presence of these ions changes how xanthate adsorbs. The different xanthate interactions, based on whether activating ions are present, will be discussed. A distinction between hexagonal and monoclinic pyrrhotite xanthate interaction is still not present in current literature. However, both pyrrhotites interact with ions differently so activation will show a difference in xanthate interaction.

2.1.4.2.1 Pyrrhotite Flotation with Xanthate without Ion Activation

Prior to the interaction with xanthate, pyrrhotite needs to oxidize. The oxidation of the iron sulfide creates a positively charged iron (III) site (Equation 13) which allows the negatively charged xanthate molecule to physisorb through electrostatic attraction (Equation 14) [13], [32], [42].

$$FeS + 2H_2O = Fe(OH)[S]^+ + 2H^+ + 2e^- \quad (13)$$

$$Fe(OH)[S]^+ + X^- = Fe(OH)[S]X \quad (14)$$

Following the adsorption, the next step towards promoting hydrophobicity via collector is the oxidation of an additional xanthate molecule resulting in the formation of dixanthogen. As with pentlandite, the circumstances for dixanthogen to form are entirely electrochemical. If the pH and pulp potential are in ideal ranges, dixanthogen can form. As discussed previously, the pulp potential directly controls whether dixanthogen can occur and the rate of dixanthogen formation.

The clear difference between the formation of dixanthogen on pyrrhotite and pentlandite is that while pentlandite relies on the nickel sites in the lattice for immediate dixanthogen

formation, pyrrhotite requires a degree of oxidation before dixanthogen can form. This is the reason to why pyrrhotite is well-known as a slow floating sulfide [1], [23], [53], [71]–[73].

This behavior in pyrrhotite is expected in most sulfide separation flowsheets where the minerals are crushed followed by immediate flotation. In most processes, pyrrhotite will have the opportunity for activation of their surface via metal ions. The most common ions linked to activating pyrrhotite are copper and nickel ions.

2.1.4.2.2 Influence of Ion Activation on Pyrrhotite Flotation with Xanthate

The activation of pyrrhotite via ions in solution is a well-known phenomenon in many papers. In the early 90's, the correlation between the improved flotation of pyrrhotite and higher levels of copper and nickel ion on the pyrrhotite concentrate via LIMS analysis [3], [74]. While originally work by Nicol stated copper activation is not possible due to copper insolubility above a pH of 8, there is no doubt that the presence of copper in a solution with fresh pyrrhotite will have improved flotation [75].

2.1.4.2.2.1 Copper Ion Activation on Pyrrhotite

The mechanism attributed to copper activation of pyrrhotite is not completely understood, but there is some consensus for order of interactions. Initially, cupric ions in the solution will form a copper hydroxide on the surface of the pyrrhotite mineral (Equation 15) if the solution is above a pH value of 8 [71]. If xanthate is present in the solution, the formation of dixanthogen on a cupric ion is the next step (Equation 16). Following this, the reduction of the cupric ion to cuprous occurs based ARXPS and FTIR on pyrite studies [66], [75]. The reaction is believed to occur after dixanthogen is formed on the cupric ion (Equation 17).

$$Cu^{2+}+2OH^{-}\rightarrow Cu(OH)_2 \quad (15)$$

$$Cu(OH)_2+2X^{-}\rightarrow CuX_2+2OH^{-} \quad (16)$$

$$2CuX_2\rightarrow Cu_2X_2+X_2 \quad (17)$$

While this appears to be the most reasonable series of steps for copper activation on pyrrhotite, this is not completely confirmed. There is some work discussing the formation of a cupric sulfide, but this is not possible at a pH of 9 and therefore is not discussed [76]. There are quite a few studies that study the surface after copper activation. However, even before the current understanding of copper activation, the use of chelators such DETA or TETA and other reagents

were shown to counteract this activation [3], [13], [72], [77], [78]. Additionally, some studies have extended what is seen with pyrrhotite to potentially other minerals, such as pentlandite and feldspar [79].

The impact of copper activation is dependent upon factors usually considered during the design of a plant's flowsheet. While copper ions are essential for copper activation, too high a concentration will result in precipitation of copper hydroxide and render the pyrrhotite surface hydrophilic. As well, copper activation has the best effects on pyrrhotite with freshly ground or clean surfaces. Whether the surface already has dixanthogen patches or oxidation, the result is that copper activation has less of an impact. As copper ions naturally occur during grinding of sulfide ore in Sudbury Basin, along with a minor addition of xanthate, the copper ions not being able to interact with pyrrhotite immediately is not a situation worth discussing further.

2.1.4.2.2.2 Nickel Ion Activation on Pyrrhotite

Nickel activation is known to occur but has been much less studied. While the improvement in the flotation of pyrrhotite has been shown [3], [22], [80], the mechanism hasn't been investigated in terms of surface species. Interestingly, some work has suggested that nickel-activated pyrrhotite may form a pentlandite-like surface [7], [64], [81], [82] through the activation mechanism below:

$$Fe_7S_8+4.5Ni^{2+}+4e^-\rightarrow(Fe_{4.5},Ni_{4.5})S_8+2.5Fe^{2+} \quad (18)$$

Nickel dixanthogen (NiX_2) is found to be the oxidation product on both pentlandite and nickel-activated pyrrhotite in Mendiratta's work. It should be restated that nickel activation is known to exist through flotation experiments only [3], [53], [80], [83]. The kinetic impact of nickel activation or the difference in activation when compared to copper activation has not been studied. In a mixed mineral system, where both copper and nickel ion are present, discerning the more dominant mechanism is vital to designing optimal flotation strategies.

2.1.4.2.3 Activation Differences Between Hexagonal and Monoclinic Pyrrhotite

As with the floatability of the particle size ranges, monoclinic and hexagonal pyrrhotite react differently when interacting with ions. Hexagonal, due to its slower oxidation rate, has a stronger interaction with copper and nickel ions and results in a better flotation performance [5], [13].

However, some work has shown that monoclinic pyrrhotite is more sensitive to copper addition, although the reason for this is not known. Pyrrhotite from different regions can be varied and shows that the location and possible original formation may have an impact on copper activation [5], [84]. The underlying mechanism differentiating, the interactions have not been understood yet.

2.1.5 Galvanic Interaction between Sulfide Minerals

One of the primary challenges with studying sulfide minerals is their behavior changes drastically from a single to mixed mineral system. As sulfides are semiconductors, they can oxidize or reduce based on their surroundings and the minerals they are in contact with. In general, galvanic interaction is dependent upon the rest potential of a mineral when in contact with another mineral [22], [36]. The rest potential, also known as open-circuit potential or zero-current potential, is the potential at which no current is measured with a mineral electrode [85]. As sulfides are semiconductors, this means that sulfides at rest potential are in a state of equilibrium and are not undergoing oxidation or reduction. Rest potential is a measurement only possible under very controlled conditions and would be impossible to measure in a typical slurry. However, the rest potential does give an indication of how sulfides will interact during grinding or flotation.

Given a list of minerals, each with a specific rest potential, we can pair these minerals up and can determine whether a mineral will allow for oxidation or reduction on their surface. The mineral that has the higher rest potential will act as the cathode while the mineral with the lower rest potential acts as the anode. The oxidation reaction occurs at the anode and the reduction reaction occurs at the cathode. This is the basic understanding that drives galvanic interaction between minerals.

The electrochemical reactions are typically oxidation of the surface or reduction of water and oxygen, forming a hydroxide. However, these reactions will change based on the environment. For example, the oxidation reaction can instead be the oxidation of xanthate into dixanthogen if the conditions previously discussed for pentlandite or pyrrhotite are met. Bozkurt illustrated this perfectly (refer to Figure 4) when studying the rest potential of pentlandite and pyrrhotite, with and without xanthate addition[22]. Originally, pentlandite is measured to have a rest potential of 345 mV SHE while pyrrhotite has a rest potential of 310 mV. Based on this, pentlandite is the cathode while pyrrhotite will be the anode. However, the addition of xanthate will change their rest potentials. As discussed previously, xanthate adsorption will lower a mineral's rest potential. In this case, pentlandite can adsorb much more xanthate due to its nickel sites resulting in a new rest potential of 195 mV. Pyrrhotite has limited xanthate adsorption so its rest potential drops to 285 mV. The rest potentials have switched orders with pyrrhotite having the higher rest potential and being the anode. Since ion activation

has been discussed, xanthate adsorption on pyrrhotite can be increased resulting in a lower rest potential. It is not likely, however, that pyrrhotite's rest potential will be lower than pentlandite's rest potential in these clean surface conditions.

Before Xanthate Addition:

Pn (RP=345mV): $0.5O_2+H_2O+2e^-\rightarrow 2OH^-$ (19)

Po (RP=310mV): $Fe_{1-x}S+(2-0.5xO_2+xH_2O \rightarrow (1-x)Fe^{2+}+SO_4^{2-}+2xH^+$ (20)

After Xanthate Addition:

Po (RP=285mV): $0.5O_2+H_2O+2e^-\rightarrow 2OH^-$ (21)

Pn (RP=195mV): $2X^-\leftrightarrow X_2+2e^-$ (22)

This rest potential switch between pyrrhotite and pentlandite is quite beneficial, as it facilitates the formation of hydroxides on the pyrrhotite's surface via oxygen reduction (anodic reaction) while pentlandite can oxidize xanthate to dixanthogen, due to acting as a cathode.

Another helpful effect of galvanic interaction occurs during the grinding stage [52], [86]–[94] Steel grinding media has been documented in having the lowest rest potential when compared to all sulfides. By adding xanthate into the grinding stage, chalcopyrite and pentlandite will lower their rest potential through xanthate adsorption. Like Bozkurt's work above, pyrrhotite will likely have the highest rest potential while the grinding media will have the lowest. Therefore, we can preemptively begin forming hydroxides on the surface of pyrrhotite while preventing our sulfides from oxidizing. One of the effects on grinding with steel in a sealed drum is that the oxygen consumption lowers the pulp potential to levels that significantly inhibit xanthate oxidation. This is both beneficial and detrimental, as the sulfides surfaces do not aggressively oxidize as they would in normal conditions. However, the low pulp potentials reduce the current hydrophobicity of chalcopyrite and pentlandite, so they will not be optimally floatable until the pulp potential returns to a satisfactory value above the equilibrium potential of dixanthogen.

The complexity of galvanic interaction is that discrete particles will undergo galvanic interactions when in contact, leading to innumerable interactions in a ground slurry. Furthermore, the rest potential of the minerals is not static, but dependent upon the reactions occurring at any given time. Looking at the interactions between pyrrhotite and the grinding media gives an overly optimistic representation of what occurs, as their interactions occur between particles. The difference in the rest potentials will correlate to the speed with which a

reaction proceeds, so the largest differences will occur the fastest. However, interactions between chalcopyrite, pentlandite, pyrrhotite and the grinding media will occur simultaneously. While the galvanic interaction between chalcopyrite and pentlandite will proceed on contact, the likelihood of excessive oxidation or reduction is low due to the slower rate. While this mechanism is known to occur, there is difficulty in understanding the interactions in a complex mixture.

2.1.6 Sulfide Surface Oxidation

2.1.6.1 Pentlandite Surface Oxidation

There are two main sources of oxidation that are found to occur in pentlandite. The first is natural oxidation of pentlandite due to ore being extracted from a mine and then left out for later processing. In this case, the oxidation occurs in air and is dependent on the time from mining to processing. Ore is kept in larger pieces until being ground to the optimal particle size immediately before flotation. Grinding immediately before flotation allows for new sulfide surfaces to be created and xanthate can interact with the surface nickel sites, in the case of pentlandite. The longer the ore is left to oxidize before flotation, the worse the recovery of pentlandite will end up being [41], [88], [95]. The oxidation cannot be reversed before typical plant flotations, so there is value in processing the sulfide ore as quickly as possible once extraction from the earth has commenced.

The other source of oxidation and the one far more relevant to flotation is the electrochemical oxidation of pentlandite during froth flotation. Kinetically, this occurs much faster and is therefore of greater concern.

Richardson (1989) showed the oxidation of synthetic pentlandite in a variety of aqueous environments and used XPS, AES and CEMS for analysis [96]. All oxidants were shown to form iron sulphates, oxides and hydroxides on the surface, with an increasing ratio of ferric species as the oxidizing strength of each oxidant increased. Aqueous oxidants were shown to primarily support the formation of ferric oxy hydroxides. As the passivating oxidation layer is formed, pentlandite beneath the layer will transfer into violarite due to the diffusion of ferric ions through the ferric oxyhydroxide layer.

Buckley (1991) further supported the findings of Richardson, showing a formation of iron oxy-hydroxides on the surface, as well as the formation of violarite [97]. On pentlandite, the

oxy hydroxides were shown to be firmly attached and form in patches. It is not known if the violarite formed through ferric ion migration would function differently than pentlandite, regarding xanthate adsorption, if the oxide was eventually removed.

Characterization of pentlandite was conducted with XPS by Legrand in 1997, creating pristine pentlandite surfaces [98]. The surface was oxidized in de-ionized water and showed that the ferric oxyhydroxides formed after extensive oxidation, resulting in the inability to measure the presence of nickel with XPS. These results showed similarities with pyrrhotite.

2.1.6.2 Pyrrhotite Surface Oxidation

During the literature review, pyrrhotite oxidation has been discussed in relation to xanthate interaction and ion activation. In general, iron oxyhydroxides are attributed to rendering pyrrhotite hydrophilic during froth flotation. There have been many studies that consider the products that form on pyrrhotite through oxidation [5], [72], [99]–[102] or strive to elucidate the kinetics that govern pyrrhotite oxidation [54], [59], [109], [64], [88], [103]–[108].

2.1.7 Sulfide Recovery as a Function of Particle Size

The effective recovery of sulfide minerals requires the minerals be floated in the optimal environments, in consideration with their accompanying minerals, with the proper reagents. The sulfide minerals also need to be floated at specific particles sizes to maximize their recovery. Chalcopyrite has an excellent recovery with xanthate over all particle size ranges with recoveries above 90% from 5 to 106μm particle size. Regarding pentlandite, the optimal particle size for flotation is between 10 – 75 μm [7], [84]. Above and below this range, recovery decreases drastically. Sulfide minerals are crushed down to their ideal particle size immediately before flotation, otherwise the minerals oxidize and become much less floatable [88]. When developing a grinding procedure, increasing the degree grinding to liberate the sulfides from gangue is balanced by the energy consumption required for grinding and the creation of fine particles [11]. This understanding is reflected in many sulfide grinding procedures where the particle size of the ore after grinding is typically 56-70% passing 74 μm [58], [78], [110]

The only means to reduce the creation of fines is with controlling the grinding of ore. In an ideal case, a grinding procedure [111], [112] would be designed to create a size distribution of the ore so the majority falls into the ideal particle size range, and the distribution favors excess in

the coarse particle size range. A separate conditioning stage for the coarse particles, where extra collector is used, has shown improvement in coarse pentlandite recovery while not being as beneficial for the recovery of sulfide gangue [113]. However, the implementation of such a complex technique would require an investigation into both the grinding and conditioning stages for the orebody being processed, which is often not a feasible task in plants.

The floatable particle size range for pyrrhotite in early work has limitations due to the different crystal structures of pyrrhotite that were assumed to behave similarly during flotation, so differentiation was not a concern. Recently, the differences between monoclinic and hexagonal pyrrhotite have extended to requiring the floatable particle size range for pyrrhotite have an amendment. Originally, pyrrhotite showed poor recovery overall with a slight improvement in the 15-40 μm particle range [113]. However, in recent years, the simple truth is that monoclinic and hexagonal pyrrhotite has very different floatable ranges. The comprehensive work by Multani on these two superstructures highlights the very difference responses these minerals have during flotation[6]. Monoclinic pyrrhotite was shown to float well in the fine particle size ranges, with 50% recovery below 10 μm that drops to 30% at 40 μm. Above 60 μm, monoclinic pyrrhotite becomes nearly unrecoverable with recoveries below 20%. Conversely, hexagonal pyrrhotite has better flotation in the intermediate range with recoveries of 60% at 35 μm. Between 10-60 μm, hexagonal recovery remains consistently above 40%. Much of the work into the recovery of pyrrhotite and the truths behind how the crystal structures impact flotation has been due to XPS Consulting with Lawson et al.'s work in 2014 being largely motivated by the impact this research has on the processing of the Sudbury Basin ore. The studies emphasize the use of this knowledge for practical applications, so accuracy and reproducibility of results is paramount [84]. An extensive discussion into pyrrhotite is beyond the scope of this thesis, but the methodologies developed for pyrrhotite purification and sonication treatment, among other techniques, are extremely valuable for creating representative results. Recent studies on monoclinic and hexagonal pyrrhotite are outlined here [6], [13], [84], [114].

Understanding the impact of particle size for all minerals of interest is paramount to selective flotations while producing optimal recoveries for the minerals of interest. Prior to this work on pyrrhotite, magnetic separation of pyrrhotite was performed to reduce the magnetic pyrrhotite. However, this recent clarification illustrates the limitations of assuming pyrrhotite acts a single mineral as it explains why hexagonal pyrrhotite is easier to recover in typical

flowsheets than monoclinic pyrrhotite. The value in this information is that knowing that one type of pyrrhotite is more troublesome than another and there are specific characteristics that distinguish its recovery results in better depression strategies being developed.

2.2 High Intensity Conditioning

High intensity conditioning (HIC) refers to a technique first described by Sergei Bulatovic in 1987, where the use of high shear fields in a fluid resulted in many interesting effects [115]. Originally, the conclusions focused on cleaning the surface of fines, another interesting phenomenon noted was the improved recovery and selectivity of sulphide fines. This was later confirmed to be a mechanism known as “shear flocculation”, a technique first noted by Warren in 1975 [116]. The two main mechanism of high intensity conditioning are shear flocculation and surface cleaning. The degree of effectiveness for each mechanism depends on the minerals involved, both in the constituents and the respective amounts of each. Furthermore, the experimental design is an important factor with the tank, impeller and the speed of the impeller having a drastic effect on the overall performance[117]. Lastly, the environment the ore interacts with during high intensity conditioning will also impact these mechanisms.

Based on the variety of minerals and the investigations each performed, the literature will focus on each mechanism separately. Furthermore, the studies performed won’t be homogenized due to these differences. The phenomena that is assumed to be consistent among the studies will be discussed at the end and the general impact of high intensity conditioning on the Sudbury Basin ore will be surmised.

The experimental designs for high intensity conditioning in various publications are not consistent. This is due to the different setups used and the lack of true descriptions given in most cases. If the use of high intensity conditioning is to become widely used, the technique must be standardized so differences in investigations are not due to the difference in the equipment used. Conversely, more complete description of these setups would also be helpful in future publications.

High intensity conditioning is a term that can be interpreted as a mixing stage that utilizes a high energy dissipation directly into the pulp to create certain mechanisms. There is no clear region of mixing that can guarantee high intensity conditioning is occurring as the term itself is general at best. Rather, distinguishing the regions of power input that are conducive to the

occurrence of specific mechanisms, shear flocculation and surface cleaning, is more reasonable. Separating and contrasting the regions necessary for each mechanism, given a specific orebody, would be a more informative approach.

2.2.1 Shear Flocculation

Shear flocculation is an important phenomenon that was described by Bulatovic in 1989 but was truly first witnessed by Warren in 1975 [115], [116]. Below is Figure 6, which illustrates a simple interpretation of the steps that occur during shear flocculation within HIC:

a) Fines within a slurry will aggregate weakly due to the ionic strength of the solution when not undergoing a shear force due to the use of an impeller. These aggregates will include any minerals with fines of small enough diameter and include van der Waals and electrostatic interactions.
b) During high intensity conditioning, the shear force created by the impeller can break these aggregates up, temporarily dispersing the fines while HIC is ongoing. In this example non-sulfide gangue fines have been dispersed, releasing the pentlandite fines.
c) Following the release of pentlandite particles from these weak aggregates, xanthate adsorption on the pentlandite surface can proceed while HIC is occurring. If there are no hindering effects that would prevent the oxidation of xanthate into bulk dixanthogen, the formation of hydrophobic patches on pentlandite will occur.
d) The energy transferred into the pulp will create an environment for high energy collisions between particles. If these particles are hydrophobic, they will attach to one another and form aggregates that are strong and much more stable.
e) Once high intensity conditioning is ended, the dispersed fines will attach again due to weak forces. The main difference is the pentlandite fines will have formed aggregates with one another.
f) The shear force created during froth flotation from the impeller will disperse the fines again but will not be affect the pentlandite aggregates formed. Compared to the pentlandite fines original particle size, the aggregates are expected to have a better opportunity for attachment to a bubble and subsequent flotation [113].

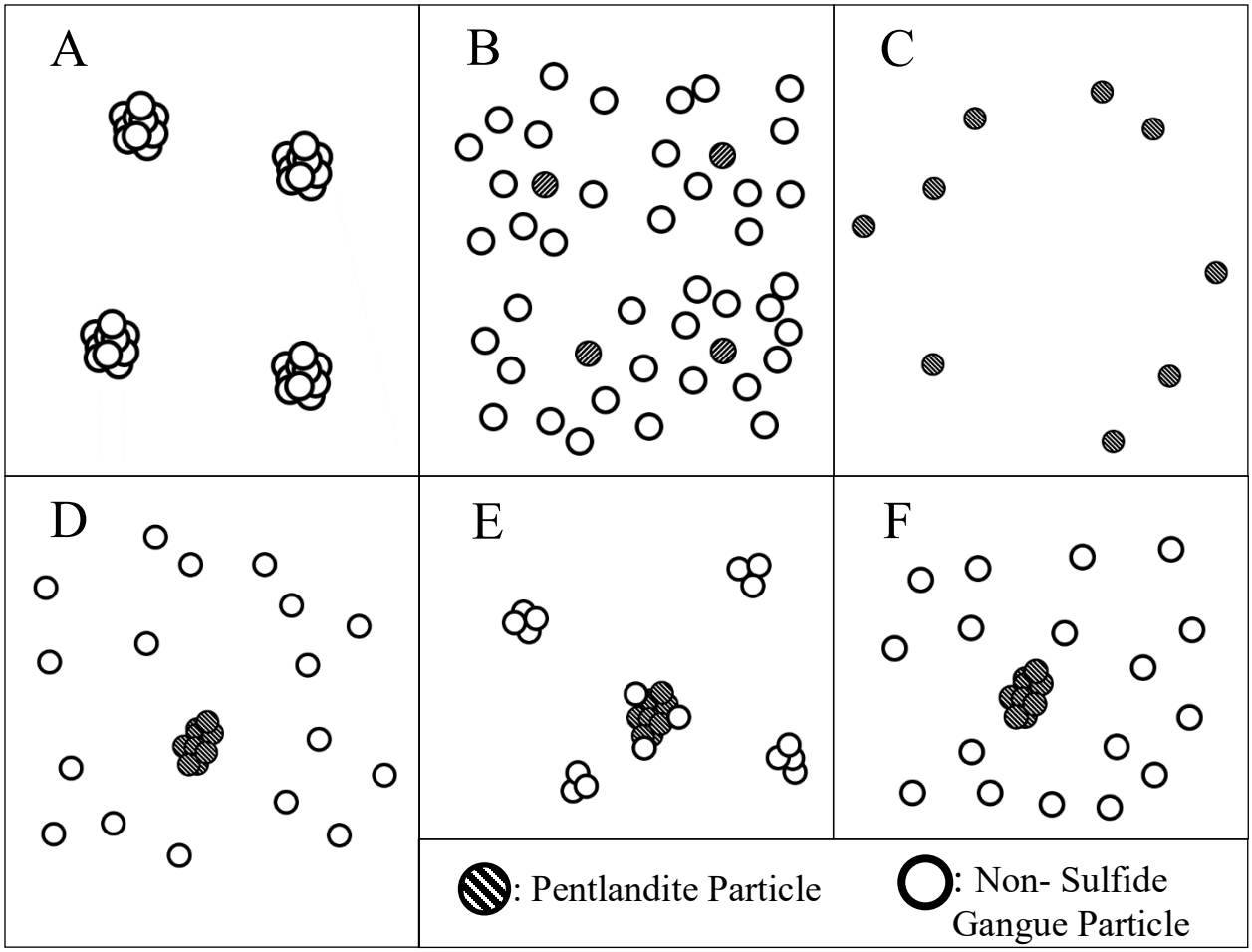

Figure 6: Shear flocculation of pentlandite and non-sulfide gangue feed illustrating autogenous carrier flotation of pentlandite fines. Created based on Figure 1-3 [48] and Figure 4 [117].

The aggregation of fines requires a few key requirements:

1) The impeller needs a high enough speed to generate the necessary mechanical energy required to overcome the energy barrier that prevents shear flocculation naturally. For aggregation to occur, the particles need to have the ability to interact with one another (collision) and this interaction needs to penetrate this energy barrier. To be clear, this does not guarantee aggregation, but dictates the minimum necessary conditions for aggregation to be possible.
2) Aggregation requires hydrophobic surfaces between particles. Warren, since his work was with scheelite, used sodium oleate to create hydrophobic surfaces. Sulfides are commonly floated with xanthates, but other collectors can also be used. However

hydrophobic surfaces are not selective, so the collector used must be not generate hydrophobic surfaces on minerals that should not be aggregated. This condition is dependent on the orebody being investigated and proper literature review is required.

3) The formation of a vortex or air entrainment has been determined to be detrimental. While previous literature failed to clearly state the reason, it is plausible that inefficient energy transfer is the reason. Due to the shear rate in the pulp being a prominent factor in the effectiveness of high intensity conditioning, air in the pulp will result in a reduction in the power input into the slurry. This reduces the effectiveness of shear flocculation overall.

While these conditions outline the required environment where shear flocculation is possible, this is only the first step. The speed of the impeller or the power input into the slurry dictates the particle interaction in the slurry. Many investigations support that an optimal impeller setting is required for the best recovery of a specific sample. The particle size distribution controls this optimal impeller setting. This will be described in the next section.

2.2.1.1 Early Work with Shear Flocculation

When Warren first discussed shear flocculation, he used a single bladed paddle stirrer in a six-baffled cylindrical beaker [116]. Using a 10^{-4} M sodium oleate solution, the rpm was varied from 850-1700 rpm. With particles around 1 μm, 1000 rpm was required to start aggregation. Particles with a diameter of 7.6-11μm aggregated well at 850 rpm, while larger particles show less aggregation with an increasing size showing worsening aggregation. Warren determined that shear flocculation occurred in the 5-20 μm range at 850 rpm, and 1-12μm at 1700 rpm. It is important to note the samples used were purified scheelite and contained no other minerals.

Another study looking at the shear flocculation of cassiterite and tourmaline was performed by Warren in 1982 [118]. This work was much better documented, in terms of experimental design. The study worked with particles in the 2-6μm range. The beaker was 63mm in diameter with 6 baffles spaced apart (6.3mm wide). The 25mm diameter paddle was placed 2mm from the bottom of the beaker, with speeds varying from 273-1200rpm. This study showed that overdosing with collector was detrimental to shear flocculation, assumedly due to the formation of opposing collector layers. One of the collectors used, styrene phosphonic acid,

showed that a good collector can be a poor choice for shear aggregation. The reason is attributed to its short hydrocarbon chain[58]. The average particle size, while dependent on the experimental conditions, showed a trend that suggested an optimal rpm is likely required. Above and below this rpm, the average particle size decreases.

The study that attracted a great deal of attention indirectly to shear flocculation was Bulatovic in 1989 [115]. The focus was on sulphide minerals and improving the recovery of fines that are notoriously difficult to float. It should be noted that the experimental method explanation was sparse at best. A variety of unspecified impellers were used, and the tank was described as a 250mm diameter with a 4L capacity. While the variety and depth of the work cements this paper as a solid foundation piece for high intensity conditioning, the lack of experimental description to reference for future work is a shame. The improved recovery of copper and nickel sulfide ores, due to high intensity conditioning, showed the best results for particles under 20 μm. As well, the power input per volume showed a detrimental effect at excessively high values, suggesting optimization is required for use in plant. The xanthate collector dosage also illustrated the dependence of the creation of hydrophobic surfaces. In contrast to Warren's work in 1982, higher collector dosages lead to improved recoveries and reverse the lower recovery seen at high power inputs (for copper at least). The work showed a close relation to the collector addition and power input. This makes most work in the high intensity field difficult to compare, due to the variety of mineral samples, collectors used and the experimental design. It is likely that an investigative study focusing on a specific ore sample is required so a less subjective interpretation of results can be achieved. Simply put, when trying to piece together the connections between high intensity conditioning and its effects on minerals, findings between different studies need a semblance of consistency to be properly linkable.

There was renewed interest in the field following the work of Bulatovic. A review paper by Bilgen in 1991 brought together the current understanding or at least the most agreed upon mechanisms at the time [119]. The main points were:

1. The dependence upon power input into a slurry and the duration the conditioning took place. In a general sense, aggregation among fines appeared to need a higher power input and longer duration while coarser particles required the opposite in both fronts. As larger particles possess more kinetic energy than smaller particles at the same speed, this does

make sense. Interestingly at lower power, fines tended to attach to coarser particles than other fines.

2. The ability of fines to aggregate stemmed from the creation of hydrophobic surfaces between attached particles. The ability to remove water layers between hydrophobic particles and allow for physical contact, comparatively fast than hydrophilic particles, plays an important role in the success of attachment to one another. Lastly, these hydrophobic surfaces have a favoured association with one another that reduces the repulsion typically felt at short distances between particles. While simply saying hydrophobic particles can aggregate together sounds logical enough, the subtle differences should be considered when applying to complex systems with more than a few minerals.

2.2.1.2 Shear Flocculation of Ultrafine Iron Ore

A study a few years later focused on the selective flocculation of ultrafine iron ore, performed by Weissenborn, Warren and Dunn[120]. The goal was to selectively flocculate ultrafine hematite from an Australian plant on Finucane Island. While the paper doesn't specifically reference shear flocculation, it relies on similar principles namely stirring rate and a surface-active reagent. In this case, the hematite was rendering hydrophilic and settled after flocculating with a starch. This is also one of the few papers the sensitivity of the experiments to a wide number of variables such as reagent concentration, pH, slurry temperature, pulp density, power input and mixing time. The conclusion was the successful flocculation of hematite from ultrafine gangue particles, but success was dependent upon finding the correct balance of conditions. This realization is also part of the challenge in developing a sound high intensity conditioning knowledge base as the optimal balance of experimental conditions can change between studies, so only general trends can be discerned.

2.2.1.3 Shear Flocculation of Fine Gold Particles

The high intensity conditioning of fine gold particles was also investigated by Valderrama in 1997, with more of a focus on the total energy transferred to the pulp[121]. Using microscopic analysis, the aggregation of gold fines was shown to change drastically in different cases of energy transfer. The degree of focus in this paper cannot be overstated, as the three

distinct regions of aggregation were shown as a function of power input. These regions consisted of either flotation without any aggregation, improved recovery of fines through attachment to coarse particles (Carrier flotation) and finally the best demonstration of recovery through gold fines aggregating with one another and being recovered (Autogenous carrier flotation). The microphotographs taken confirmed whether fines had aggregated with each other, coarser gold particles or not at all. Carrier flotation occurred at lower power input, showing an optimal region of activation. Autogenous carrier flotation occurs in a higher region. Between these two regions lie zones where aggregation did not occur effectively. The grade was the highest in the autogenous carrier flotation region. This study allowed for a clear example from the use of high intensity conditioning to success increase the recovery of the fine gold particles but required a range of total power input to see the degree of change that can occur. As the mechanisms were visually confirmed with microphotographs, the two carrier mechanisms could be successfully differentiated and compared. Below is Figure 7**,** a representation of the shear flocculation mechanism based on the work by Valderrama.

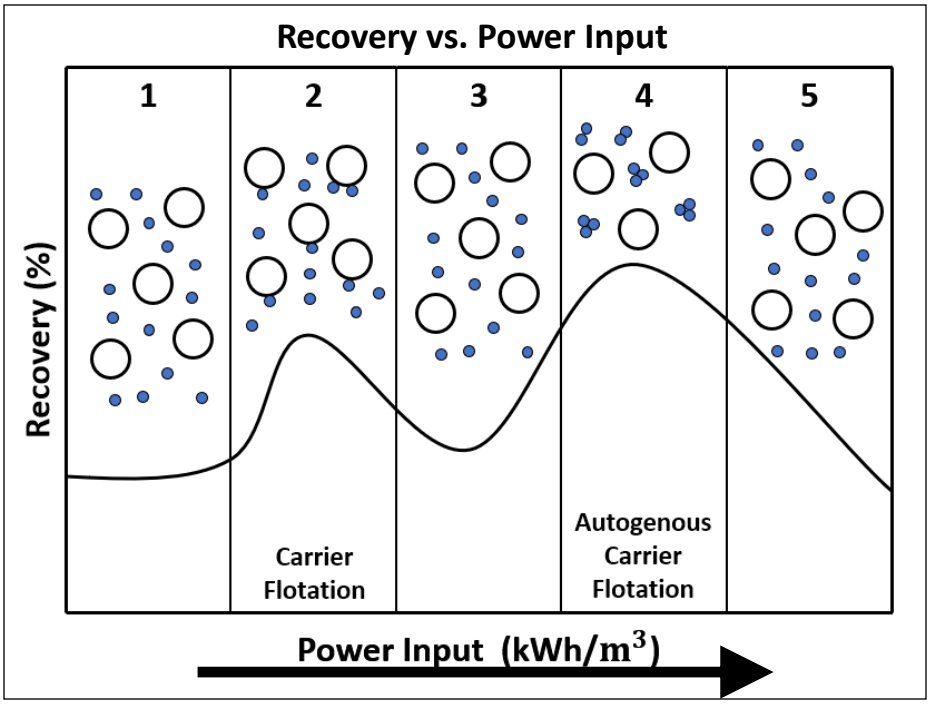

Figure 7: Relationship between power input and the change in the shear flocculation mechanism. Adapted from Valderrama [117].

In Figure 7, there are three effects of note when power input is increased:

1. Increase in particle-particle interactions
2. Increased aggregation of hydrophobic particles
3. Increased breakage of larger or coarse particles

The balance between these three effects largely determines shear flocculation. However, the trend above is only representative of gold particles. Sulfide minerals, due to redox interactions, has a changing surface that will impact shear flocculation.

2.2.1.4 Shear Flocculation of Ultrafine Pentlandite from Australian Ore

Shear flocculation of an Australian sulfide ore was investigated by Chen in 1997[50]. As ultrafine pentlandite is difficult to recover even with a collector, the possibility to aggregate these fines into a large, more floatable, particle has an obvious appeal. If this mechanism can be controlled in a plant setting, the improved recovery of pentlandite fines can lead to a great improvement in the economics of a mine.

While this study used the impeller speed as the manipulated variable, the power input is a much better measure. If 600 rpm is taken as the base speed, 800 rpm generates 2.37 times the power and 1100 rpm is 6.16 times the power of 600 rpm. The extra energy generated affects the

environment of HIC drastically and this is clearer when using power input instead of impeller speed.

2.2.1.5 Shear Flocculation of Ultrafine Pentlandite in the Absence of Collector

Without the use of a collector, pentlandite can have a degree of hydrophobicity in water with a pH of 8.5-9.0. Therefore, shear flocculation can occur. The effect of three different speeds (600, 800 and 1100 rpm) were tested. The experimental design focused on in-situ measurement of the particle size as HIC is being performed. Starting at 600 rpm, the ultrafine particles started to disappear from the particle size distribution as HIC progresses. Within 10 minutes of HIC, both the ultrafine (~2µm) and the coarser size (~14µm) ranges have disappeared, with a new size range that starts at ~9µm and gradually increases in both volume percent and particle size range (up to 10µm) as the length of HIC increases up to 30 minutes. The reason for this change is due to the shear flocculation of fines and the breakage of coarser particles due to the high energy collisions that are occurring. As the rpm is increased to 800 rpm, similar results are achieved, with a slightly higher final particle size range. This can be interpreted as the shear flocculation mechanism being more prominent[50].

At 1100 rpm, the particle size distribution was reduced when compared to the lower speeds. This is likely related to the extra energy generated which increases the energy and frequency of collisions and breaks apart coarser particles. Therefore, the speed of the impeller (or power input) needs to be chosen based on the particle size distribution that is optimal for the application.

Without using a collector, shear flocculation was rather effective at the lower speeds and in deionised water. This shows the situational ability of sulfides to be hydrophobic without a collector.

2.2.1.6 Shear Flocculation of Ultrafine Pentlandite in the Presence of Collector

The use of a xanthate collector on pentlandite will enhance the hydrophobicity of the pentlandite particles in the intermediate size range [113]. The mechanism of shear flocculation allows for the agglomeration of particles with patches of hydrophobicity to form stable aggregates of smaller particles. The work by Chen shows that the particle size distribution of pentlandite increased with the addition of xanthate at 1100 rpm. The aggregation rate constant

quadrupled from no xanthate addition to a concentration of 5.6 μM. Increasing the concentration by a factor of 10x did improve the rate constant by approx. 50%[50], but the use of excessive xanthate would be detrimental to the selective separation of sulfide minerals like pyrrhotite and pentlandite.

From the previous work with no xanthate addition, the speed of the impeller showed the best results with 800 rpm. This is assumed to be due to 800 rpm being the best balance between the aggregation of smaller particle and the breakage of coarser particles. This trend is consistent when xanthate is added with 800 rpm having a 70% higher aggregation rate constant than 1100rpm at the same xanthate concentration.

The work by Chen did not consider the type of carrier mechanism the was aggregating the fines, as Valderrama in 1997 did with his work with gold particles. Therefore, there are limitations to understanding how particles are aggregating in Chen's work, even though his results show important phenomena. As well, the use of impeller speed versus a calculated power input makes the impact of speed on power input difficult to interpret. Lastly, Mt. Keith ore had a relatively low content of ultrafine pentlandite, so any aggregation would not have resulted in a large change. This suggests that HIC of sulfide ore that includes pentlandite would be more effective when there is a larger content of fine pentlandite.

Additional Work by Tabosa looked at HIC as a pre-flotation stage for copper sulphide ore [122]. There was an improvement in the recovery of fine particles (<15μm) with HIC compared to standard methods. The improvement was related to particle aggregation being one of the mechanisms, while it was not definitively determined to be carrier or autogenous carrier flotation

2.2.2 Surface Cleaning

While shear flocculation focuses on aggregating fines that are typically challenging to float with or without a collector, surface cleaning focuses on the removal of detrimental species on sulfides surfaces that impact their floatability. Depending on the location from the ore, the surface species can be drastically different but a slime's negative impact on sulfide flotation has been well established [21], [58], [123]–[129].

2.2.2.1 Surface Cleaning of Australian Sulfide Ore using Impeller Speed

Chen also investigated the existence of a slime coating on pentlandite found in Mt. Keith's nickel ore. Following classification of these slime particles and whether HIC was able to clean the surfaces of pentlandite. The head grade of the pentlandite in the ore was only 2 wt.%. The experimental procedure developed to investigate the surface cleaning of HIC was extensive and consisted of SEM, XRD, mastersizing, and sieving. Sonication is used to remove any residual slimes, so the difference between the residual slimes after HIC and after sonication will describe the degree of cleaning. HIC was shown to clean the slimes off the surfaces when the impeller speed is 1,100 rpm but was less effective at 800 rpm and ineffective at 450 rpm, showing similar results to conditioning with no HIC. Furthermore, when an effective impeller speed is used, a longer conditioning time produced the best results with 30 minutes being optimal for surface cleaning.

It is important to truly differentiate the power input provided by the impeller, as the impeller speeds seem relatively similar. 800 rpm is only 38% of the power input when compared to 1100 rpm and 450 rpm translates to only 7% of the power input. The difference between these speeds can truly be seen when using power input instead of impeller speed.

This work showed the slime attached to the coarse particles present, with the finer slimes being more aggressive in their attachment. High intensity conditioning was able to remove these slimes, with impeller speeds at 1,100 rpm and at least 30 minutes of conditioning. The use of collector provided similar results, so collector addition was not seen to be a controlling factor.

2.2.2.2 Surface Cleaning of Australian Sulfide Ore using Power Input

The next investigation looked at total power input into a slurry. Given a different energy transfer rate from the impeller into the slurry, different rates over a different time duration will yield the same total energy transfer but show differing results[130]. Engel utilized an extensive setup focusing on varying the power input based while adjusting the impeller speed and impeller diameter. In all the tests performed, the highest power input showed the best grade and recovery of pentlandite in a low-grade ore. Longer HIC conditioning times also showed the best results, with a 3-hour conditioning time showing a minor but not insignificant improvement over a 1-hour conditioning time. However, there is not enough evidence to suggest that the drastically

longer 3-hour conditioning time would be applicable in plant designs. The cost of power and the space allocation for additional tanks may outweigh the benefit.

The comparison between power input per second during HIC and total energy input over a HIC conditioning time was also investigated. The three settings tested were 48W for 60 minutes, 144W for 20 minutes and 250 W for 11.5 minutes. Largely, there were similar results were comparing the final grade and recovery of all 3 settings. However, the test at 250 W showed consistently higher grade and recovery through the concentrates collected before eventually converging into a similar grade/recovery with the other two tests. This suggests that a higher input could allow for much shorter HIC sessions in a plant, which is obviously a benefit if plant implementation is the end goal. However, this would need to be tested with the ore of interest to ensure there are no deviances [130].

Engel highlighted another important factor to consider, the time between completing the HIC stage and froth flotation. While reducing the time between HIC and flotation will provide the best results, there is still a markedly different flotation result between a pulp that underwent HIC and was delayed for 4 hours before flotation and flotation with no HIC stage. Even with the delay, the test with HIC showed a similar grade but 15% increase in Ni recovery when compared to the no HIC test. This suggests the benefits of using HIC are not easily diminished with time. This is valuable to know, as there is some inherent forgiveness with time between HIC and flotation. While in a plant design, time delay will obviously be minimized, it is comforting to know the effects of an HIC stage cannot be diminished within minutes, but with hours and only in a slight decrease in recovery.

2.2.2.3 Surface Cleaning of Sulfide Ore in the Gansu Province

Jinchuan ore in the Gansu province has the challenge of pentlandite flotation being hindered by the serpentine slime on the surface [58]. Using high intensity conditioning, these slimes were shown to be removed which resulted in a high recovery in nickel. Various xanthate collectors of different lengths were used. When HIC was used, the shortest length was the most effective and produces the best grade and recovery. Conversely, when the reagent Calgon was used to remove these same magnesia fines through changing their surface charge, a longer xanthate chain was the most effective. As these two methods utilize different mechanisms to achieve an improvement in recovery. This difference is due to that HIC does not completely

remove all the serpentine slimes, resulting in longer xanthate chains have more difficulty adsorbing due to the higher energy barrier. While Feng describes Calgon being the most effective at dispersing the slimes, his grade/recovery curves show that there is a significant increase in recovery with HIC compared to Calgon (10% higher Ni recovery), but at the cost of grade (1% lower Ni grade). It is likely that HIC allows for other undiscussed mechanisms to improve the recovery. Based on previous literature discussed, shear flocculation of the fines is likely as well as the higher energy in the slurry assisting in overcoming the energy barrier for xanthate adsorption.

Another study on the same orebody further expanded on the interaction between HIC and the serpentine slimes covering the surfaces. The focus was on the change in various particle size fractions of the slimes and how they change with varying HIC intensity and time [123]. HIC removed all the slimes from the pentlandite surfaces that were above 40μm within 5 minutes. As the duration of HIC increases, slimes above 10μm were steadily reduced. However, slimes below 10μm were largely unaffected by HIC and appeared to have no issue with remaining attached to the pentlandite surface during HIC. This understanding can likely be applied to the previous study with Jinchuan ore [58]. The results are consistent between the two studies with the recoveries drastically increasing at the cost of a lower grade.

The power input was shown to be an important factor. At higher power inputs, the grade was improved while recovery remained the same. The power input, comparing the lowest speed to the highest, was roughly three times higher. This was offset by the duration of HIC being reduced, resulting in optimal settings being achieved with 2800 rpm for 20 minutes.

Sodium hexametaphosphate (SHMP) is known to disperse serpentine slimes in a similar way to Calgon. The effectiveness of this method is hindered by the slimes consuming this reagent in high quantities. Therefore, the use of SHMP as an initial step is likely not feasible, due to the high throughput of a plant's operation.

The use of HIC was found to be beneficial as an initial rougher step, improving the recovery of the pentlandite while being able to process large quantities of slurry. Feng found that SHMP was most effective as a final step to improve the grade of a concentrate. Utilizing the two together in an improvised flowsheet, nickel recovery was increased from 82.97% to 86.27% and serpentine weight percent was reduced from 6.91% down to 6.22%

2.2.3 Considerations for using High Intensity Conditioning on the Sudbury Basin Ore

The studies have shown that HIC is effective for a variety of minerals when the mineral that is of interest is amenable to surface cleaning and/or shear flocculation. However, none of the studies have attempted to separate pyrrhotite and pentlandite. This is likely due to the lack of focused HIC research using Sudbury ore and the studies that did look at pentlandite recovery reported negligible pyrrhotite content [50], [123]. The general variables for the use of HIC that will affect Po/Pn selectivity are shown below:

- collector addition, both in quantity and addition interval
- particle size distribution of both minerals
- impeller intensity, both in power input and the duration
- type of slime coating that will interact with the mineral's surface

2.2.3.1 Collector Addition and Interval

As said previously, many studies were not concerned with anything but maximizing the recovery and grade of the mineral of interest. In these cases, the hydrophobicity that results from the use of a collector would only impact the recovery of the valuable mineral, as gangue would exist as a slime coating[57], [123], [127], [130]–[134] and not in a major constituent like pyrrhotite. Therefore, the use of large quantities of collector had little downside. This strategy would be disastrous for Pn/Po separation as both allow xanthate adsorption and result in an increase in hydrophobicity. The addition of xanthate would need to be controlled so an excess doesn't lead to the recovery of pyrrhotite, if a preference to pentlandite adsorption can be established.

The addition of xanthate in an interval setting has not been considered but is worth considering due to the time sensitive nature of HIC. As it takes time for surface cleaning to occur, followed by subsequent xanthate adsorption, xanthate levels must be controlled to allow for preferential adsorption of xanthate on pentlandite.

Due to the need for HIC to occur without the formation of a vortex (air entrainment), reagent addition would need to be designed for use while HIC is occurring. The increase in volume would have to be considered and accounted for. As HIC would be a batch operation, the tank lid collar could be designed to account for this height difference [50].

2.2.3.2 Particle Size Distribution of Pyrrhotite and Pentlandite

Upon review of previous literature, there seems to be enough evidence to suggest shear flocculation is a mechanism that can occur during high intensity conditioning. However, this mechanism is dependant upon several requirements. Some have been mentioned previously, others have been suggested by literature:

The impeller needs to generate enough energy into the slurry that high energy collisions can occur. The type of carrier flotation should be determined [121]. The best results from previous studies have linked to fine particles aggregating with other fine particles (autogenous carrier flotation). This was shown to occur at a higher power input than which normal carrier flotation occurs (fine particles attaching to coarse particles), so these regions would need to be determined experimentally by varying power input and confirming with visual evidence.

The design of a tank that can eliminate the formation of a vortex (entrainment of gas) is required. There have been several designs that have shown promise in the laboratory [50], [122] but usually rely on the collector being added in at the beginning all at once. This will likely not be ideal for a pentlandite-pyrrhotite separation, so interval injections of collector should be considered if not to simply confirm whether it is an issue or not.

The use of a collector to form hydrophobic surfaces has been shown to be essential for the shear flocculation of sulfides. However, the shear flocculation of pentlandite without collector has been shown [50]. This leads to the expectation that there will be pyrrhotite fines that will be naturally hydrophobic and aggregate during shear flocculation. The likelihood of aggregation of pyrrhotite fines increases when xanthate has been added. Therefore, shear flocculation of a pentlandite-pyrrhotite mixture would need to be investigated. The surface cleaning of HIC should hinder xanthate adsorption on pyrrhotite, due to removal of metal oxides that serve as xanthate adsorption sites. However, the formation of hydrophobic patches on pyrrhotite is still not fully understood. The complexity of the mineral, regarding flotation with and without collector, is further compounded by the activation of ions on pyrrhotite's surface. The impact of HIC on the selective separation of a pyrrhotite-pentlandite system has not been investigated yet, which is why the results of this thesis will hopefully illuminate any challenges in the use of HIC on a Pn-Po mixture.

The reliance on shear flocculation to improve recovery of fine pentlandite is not recommended unless the stream that is being processed with HIC has a large percentage of

pentlandite fines. Chen studies showed that while fines were aggregated, the overall impact on the recovery was minimal. As discussed previously, the power input into the slurry from the impeller is a parameter that needs to be determined. The time that needs to be invested needs to be balanced by the expected benefit. The use of HIC on a feed ore from the mine is likely not feasible. This is due to the low amount of pentlandite present and even lower weight percent of fines, coupled with the high energy consumption to handle the throughput. It does make sense to use HIC as an additional step in the cleaner circuit of the Strathcona flowsheet. This is due to the higher pentlandite mass fraction (14.65 wt.% as determined by QEMSCAN) in the secondary rougher concentration at the time of sampling. Furthermore, the weight percent of pentlandite under 3μm is 7% and under 15μm is 17%. These fines are difficult to recover typically, so improving the recovery of these fines has obvious economic benefits.

2.2.3.3 Impeller Intensity, both in power input and duration

Power input from the impeller into the slurry is a parameter that is a challenge to optimize without a great deal of experimentation. All previous work in high intensity conditioning uses a paddle impeller [116], [118] or a Rushton impeller. These are also known as radial impellers which produce a high amount of shear within the slurry but will have a higher power number which is an impeller specific parameter that determines power generation. Due to unique geometry as different impellers, the shear forces an impeller can create and the direction the fluid flow will take within a slurry is dependent upon the impeller chosen. Below is Figure 8, which illustrates the difference in flow patterns with different impeller. These variations can have a notable impact on the effect caused, so impeller choice needs to be deliberate.

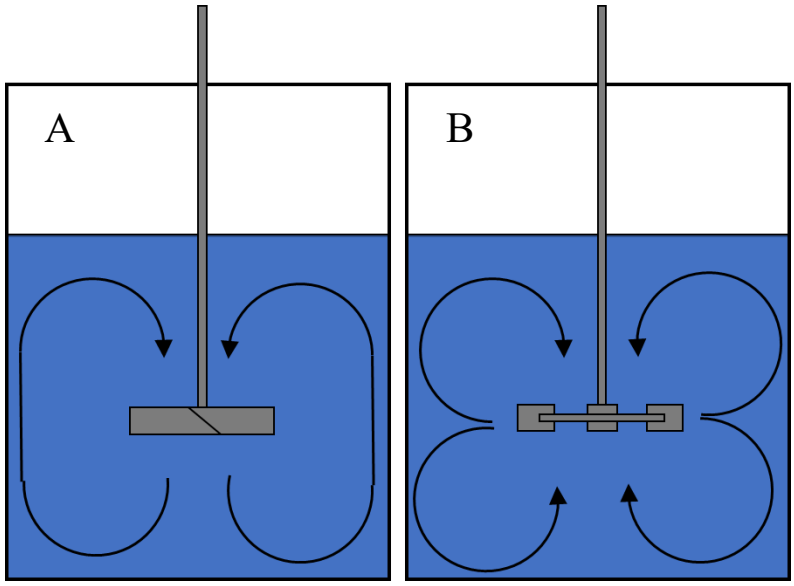

Figure 8: Representation of flow patterns of an axial, hydrofoil impeller (A) and a radial, Rushton impeller (B) [135].

As discussed earlier, power intensity and duration can be manipulated to optimize the effects desired. The power generated during shear flocculation will cause two notable effects. A higher power intensity will:

- Aggregate finer particles if these particles can be rendered hydrophobic and…
- Break down coarser particles down due to collisions

Depending on the particle size distribution of the minerals, a power input may work for one ore sample, but may not be as effective with another. Chen showed the upwards shift in particle size distribution at 800 rpm but increasing the speed to 1100rpm (roughly 2.6 times the power) increased the breakage of coarser particles and lowered the distribution. With a higher weight percent of ultrafine pentlandite, it could be argued that the higher rpm would become the more effective of the two speeds.

Valderrama shows 5 specific regions of recovery when investigating shear flocculation in Figure 7. If the shear rate is too low or too high, the recovery is low and shear flocculation is not observed. He showed that there were two optimal recovery peak that correlated to a specific power input for each. Between these peaks was a lower recovery transition zone. These two peaks were due to shear flocculation but relied on different specific mechanisms. The lower power input of the two relied on fine particles attaching to coarse particles while the higher caused fine particles to aggregate together. The latter produced the best recovery. This was only

performed on gold particles, so the impact on the sulfide ore can assumed to be similar but may require different settings.

The time that is required for high intensity conditioning is a definite downside when considering integration into a plant. However, Engel showed that similar results could be achieved with a shorter duration of HIC if a higher power input from the impeller was used. The measurement of a total power input throughout the HIC stage is a parameter that may be useful in plant implementation. Being able to reduce HIC from 60 minutes down to approx. 10 minutes by increasing the power generation proportionately means less tanks required by HIC to maintain the plant's throughput. This would need to be verified to confirm the observed effects with the Australian sulfide ore remain consistent with the Sudbury Basin ore.

2.2.3.4 Type of Slime Coating That Will Interact with the Mineral's Surface

Many of the previous HIC studies that focus on the surface cleaning of sulfide ore have slime coating [100], [132] challenges that the Sudbury Basin ore does not. This is a high magnesia-based mineral content or serpentines. This slime, due to its attractive nature towards sulfide surfaces, poses a challenge that HIC is not the most effective at solving. This is due to the ultrafine serpentine being resistant to removal with HIC [58], [123], suggesting the use of a dispersant is required for improved effectiveness.

The slimes seen in Sudbury ore are generally fine silicates that are entrained in the froth ore the formation of oxides that form naturally on the surface of sulfides due to their semiconductor nature. Based on many of the previous HIC studies improving the recovery of pentlandite, the shear force generated during high intensity conditioning can clean the surfaces of pentlandite and pyrrhotite of non-sulfide slimes and oxidation. If HIC can remove the oxidation present on the sulfides, it is logical that it should be able to continue cleaning the surfaces of oxidation. If clean sulfide surfaces can be created and maintained during HIC, then there may be new opportunities to improve the selectivity of pyrrhotite and pentlandite.

Chapter 3 Methodology

The experiments discussed in this thesis study the impact that high intensity conditioning can cause on processed slurry from the Strathcona Mill flowsheet. The slurry was sampled from the concentrate of the secondary Ni Rougher and was sent from the mill in three buckets with a volume of 2 gallons each.

3.1 Sample Preparation and Representative Testing

The slurry sent from the Strathcona Mill plant will be prepared and stored in bags of similar weight. The three buckets will be combined to provide consistent samples for flotation. The techniques used were devised with help from Manqui Xu and Ravi Multani [136], [137]. Following the completion of the sampling into bags, random bags were tested for determining the degree of representative elemental analysis.

3.1.1 Vacuum Filtering, Homogenization and Sampling

The slurry was vacuum filtered, and the cakes were homogenized together by hand. As the samples were still wet, the particles agglomerated together, and so particle size segregation was assumed to not be possible. Conic piles were made multiple times before random scoop sampling was performed to produce the samples used for flotations. Each bag had approximately 7-8 small scoops from different points of the pile and the average weight of the bags were 300g each. 3 bags were chosen for representative testing. The bags were chosen based on when they were sampled with the first bag being taken from near the beginning of the sampling, second in the middle and the last bag being the final sample taken as it was made from the remnants of the conic pile. All samples were subsequently frozen below -20 Celsius unless taken out for flotation or analysis.

3.1.2 Estimating Remaining Water Content in Sample Cakes

The 3 samples taken had smaller samples also taken to test the amount of liquid water present in the cake. This was used to estimate the true weight of solids from the slurry. Two 20g samples were taken from each bag and dried in an oven. An average of 8.86 wt.% moisture was calculated from the difference in weight, with all samples being within 0.1 wt.% of one another.

3.1.3 Elemental Analysis of Sample Bags

XRF analysis was used to test the representativity of the samples. The samples were dried in an oven overnight at 50 Celsius. Samples were then finely ground with a mortar and pestle, then a Quantachrome rotary riffler was used to split the samples into 2-3 grams representative powder samples. These samples were weighed, and boric acid powder was added to the powder sample at 0.3g Boric acid: 1g powder sample ratio. The mixture was then homogenized with a mortar and pestle until the boric acid powder was no longer visible. This powder was then pressed into a pellet with a 3mm boric acid layer base. These samples were covered with an Etnom film, 1.5-micron thickness, to reduce the effect of the film. XRF analysis showed the samples had Cu, Ni and Fe values within 0.1 wt.% of one another. Therefore, the homogenization of the filtered cake is assumed to be effective and the samples are representative.

3.1.4 EDTA Extraction of Oxide on Sample Surfaces and Metal Analysis in Solution

EDTA or Ethylenediaminetetraacetic acid is used to dissolve metal oxides from sulfide minerals. The procedure used in this work followed procedures outlined by previous studies by was largely influenced by Rumball's work [75], [128], [138]. Nitrogen purging was used during EDTA extraction to limit additional oxidation of the samples. Each sample was mixed in 250 ml of a 3% w/w Na_2EDTA solution for 30 minutes. All solutions were batch made 1L at a time, were sealed with parafilm and bubbled with nitrogen for 30 minutes before use. Standard flowrate of nitrogen into the batch beaker and the extraction beakers was 1 lpm each. The pH of the EDTA solution was adjusted to 9.00 with sodium hydroxide after all EDTA powder was dissolved (being visually confirmed through the solution clarity changing from cloudy to crystal clear after dissolution was complete). Sample sizes ranged from 4 to 14 grams due to the different concentrate weights gathered, but the EDTA solution was always assumed to be in excess due to Rumball's work and our own work to check the impact of EDTA concentration.

Following EDTA extraction, a 25 ml filtered solution sample was extracted and send for testing with either atomic absorption spectroscopy (AAS) or Inductively coupled plasma mass spectrometry (ICP-MS). Iron, copper and nickel concentrations were measured from the solutions. From these concentrations, metal oxidation levels can be calculated. Refer to Rumball's work for a clear calculation procedure [128].

3.2 QEMSCAN of the Secondary Rougher Concentrate

A sample of the homogenized filter cake was sent to Expert Process Solutions for analysis. Mineralogy, deportment, liberation and locking were determined. The sample was analyzed by Scott Brindle and Elizabeth Whiteman.

3.2.1 Mineralogy of Secondary Rougher Concentrate

Table 1: Mineral Mass wt.% for individual size fractions. Mineralogy was performed by XPS in Sudbury, Ontario and provided for use in this thesis.

		CS7	CS6	CS3-5	CS1-2	-106/+53	+106
Min Size (µm)		0	3	18	18	53	106
Max Size (µm)		3	15	38	53	106	425
Size Distribution (%)		11.84	9.41	19.08	24.41	20.39	14.86
	Mineral Distribution for Size Ranges (%)						
	Mineral Dist. (wt.%)	CS7	CS6	CS3-5	CS1-2	-106/+53	+106
Pentlandite	14.65	7.33	9.85	17.92	24.44	29.48	10.97
Chalcopyrite	10.86	18.02	10.81	6.39	4.95	14.19	45.64
Pyrrhotite	54.10	7.21	6.24	22.62	33.26	21.18	9.49
Misc. Sulfides	3.03	-	-	-	-	-	-
Non-Sulfide Gangue	17.36	27.45	19.00	18.04	8.24	12.41	14.87
	Mineral Assay for Size Ranges (%)						
	Mineral Dist. (wt.%)	CS7	CS6	CS3-5	CS1-2	-106/+53	+106
Pentlandite	14.65	9.07	9.85	17.92	24.44	29.48	10.97
Chalcopyrite	10.86	16.52	12.47	3.64	2.20	7.56	33.35
Pyrrhotite	54.10	32.93	35.85	64.14	73.71	56.20	34.53
Misc. Sulfides	3.03	-	-	-	-	-	-
Non-Sulfide Gangue	17.36	40.24	35.05	16.41	5.86	10.57	17.37

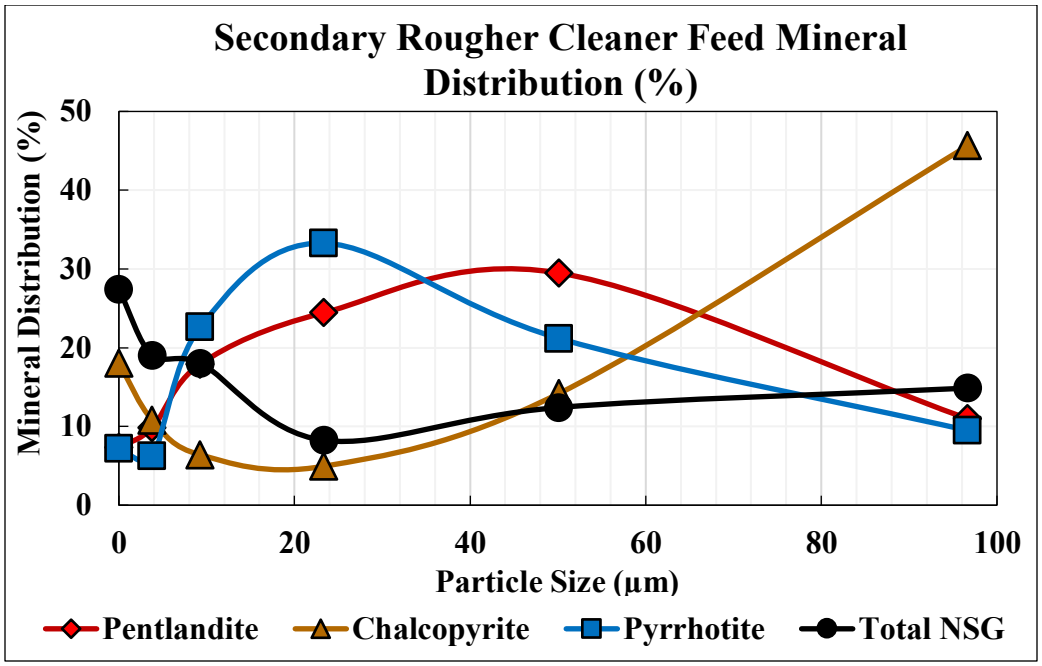

Figure 9: Mineral Distribution of Secondary Rougher Cleaner Feed. Mineralogy was performed by XPS in Sudbury, Ontario and provided for use in this thesis

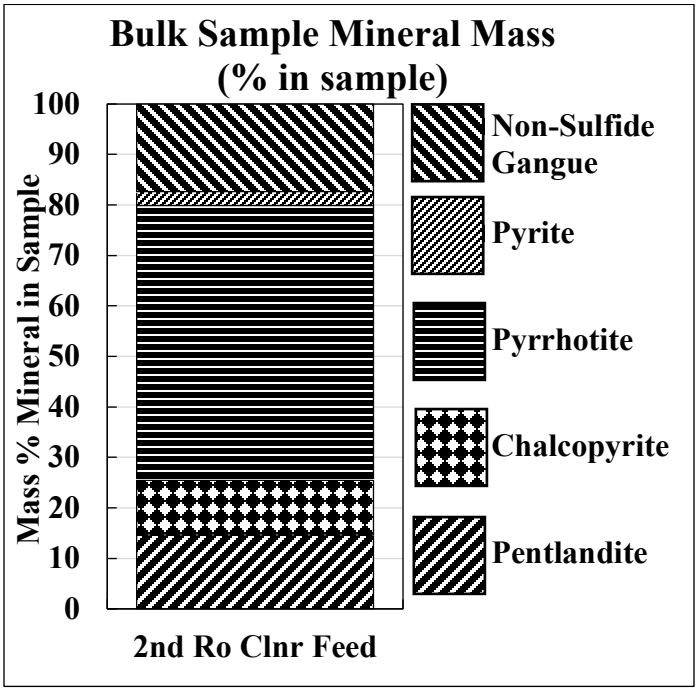

Figure 10: Bulk Sample Mineral Mass (% in sample). Mineralogy was performed by XPS in Sudbury, Ontario and provided for use in this thesis.

The mineralogy (available in Table 1, Figure 9 and Figure 10) of the sample analyzed through QEMSCAN shows over half of the sample is pyrrhotite, with 14.65% pentlandite and 10.86% chalcopyrite. The remaining 20% was primarily non-sulfide gangue with some minor amounts of cubanite, bornite, sphalerite and other sulfides.

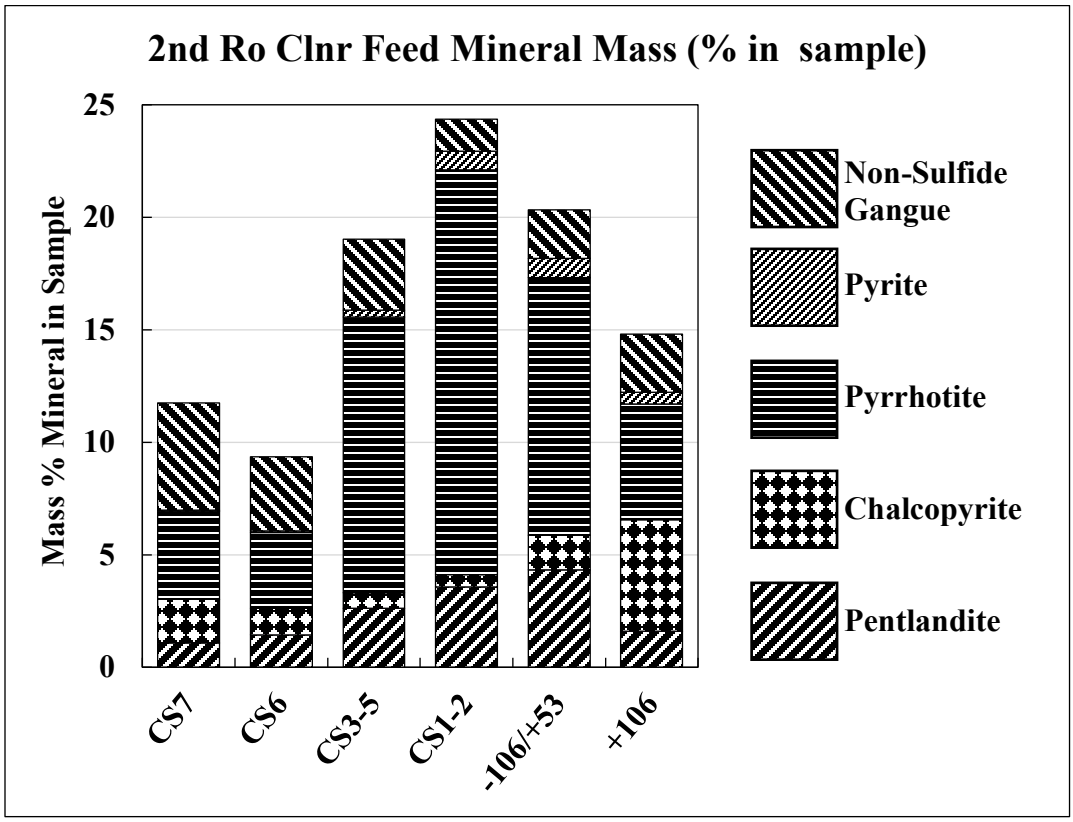

Figure 11: Secondary Rougher Cleaner Feed Mineral Mass (% in sample). Mineralogy was performed by XPS in Sudbury, Ontario and provided for use in this thesis.

As shown in Figure 11 above, chalcopyrite, pyrrhotite and pentlandite are accompanied by several non-sulfide minerals in smaller quantities. Chalcopyrite is present generally as coarse particle with the remaining chalcopyrite being found in the fines. The non-sulfide gangue is largely present as fines in the sample. Since pyrrhotite is over half of the sample, it is well represented in all size fractions, but is largely found in the intermediate size ranges. Pentlandite shows increasing amounts as the size fraction increases, with the coarse size fraction having a relatively lower amount.

3.2.2 Elemental Deportments for Nickel and Copper in Secondary Rougher Concentrate Sample

The elemental deportment of Ni and Cu in Figure 12 shows the minerals that encompass these elements. While pentlandite is the primary source of nickel at 91.5%, the minor Ni present in the pyrrhotite lattice accounts for 8.28% of the total Ni content in the sample. The copper content is primarily chalcopyrite (98.00%) with under 2% being accounted for in cubanite and negligible amounts in bornite and sphalerite.

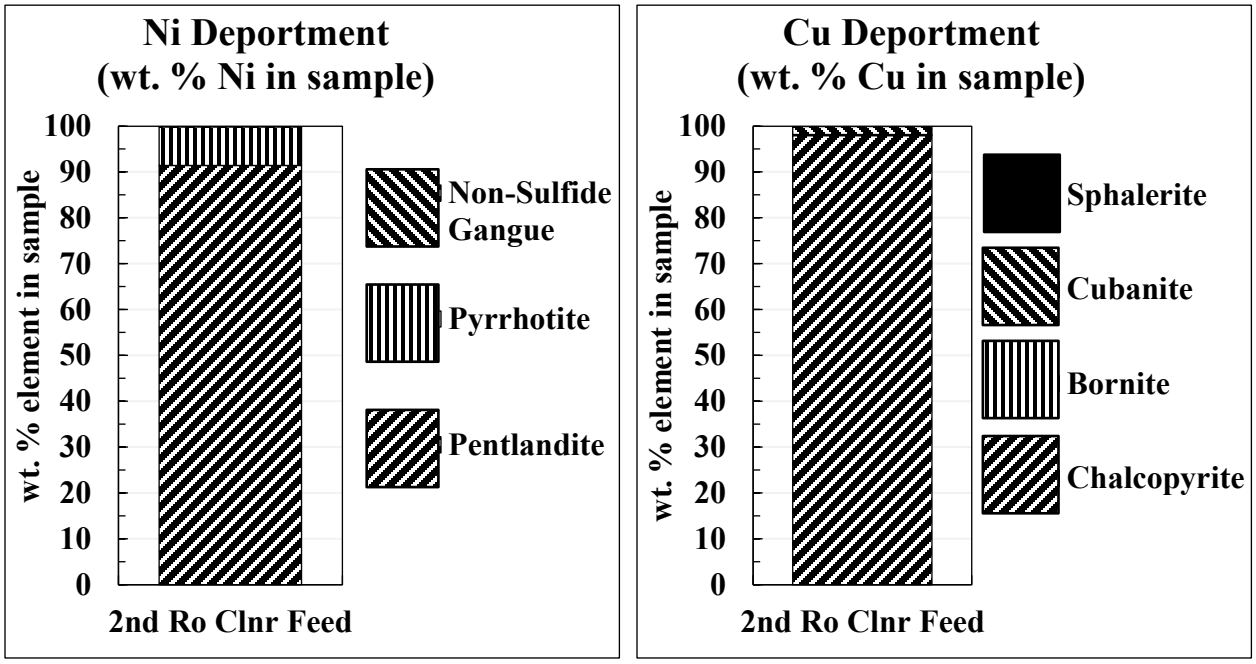

Figure 12: Nickel (left) and Copper (right) deportment of secondary rougher concentrate. Deportment was performed by XPS in Sudbury, Ontario and provided for use in this thesis.

3.2.3 Degree of Liberation for Minerals in Secondary Rougher Concentrate Sample

The creation of fines from grinding improve the degree of liberation of minerals from one another but the presence of fines negatively impacts the flotation. Pentlandite has a large degree of liberation with over 85% of the pentlandite particles being over 95% pentlandite. Pyrrhotite is also well liberated with 90% of particles having a 95% purity. Chalcopyrite has a lower degree of liberation with 75% of particles being over 95% pure.

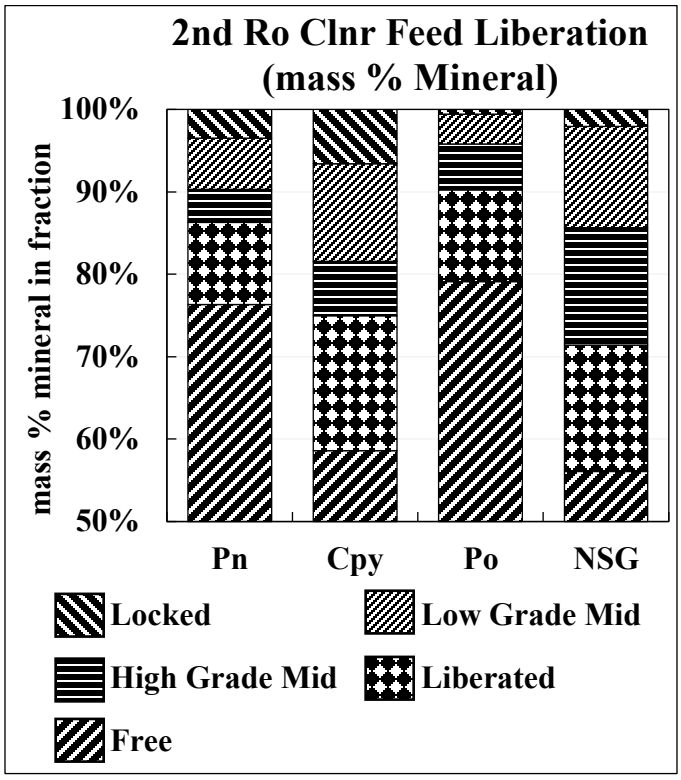

Liberation Category	% of particle is mineral of interest
Free	100%
Liberated	>95%
High Grade Middling	80-95%
Low Grade Middling	30-80%
Locked	<30%

Figure 13: Degree of liberation for secondary rougher concentrate sample. Liberation was performed by XPS in Sudbury, Ontario and provided for use in this thesis.

3.2.4 Degree of Locking for Minerals in Secondary Rougher Concentrate Sample

The particles that have less than 95% purity of a single mineral can be analyzed for the minerals they lock with. Figure 14 describes what may affect the flotation of a specific mineral due to the particle sharing surface area with multiple minerals. Pentlandite and pyrrhotite are largely liberated with most of the binary associations being with each other. Chalcopyrite shares a great deal of non-sulfide gangue association and some pyrrhotite association.

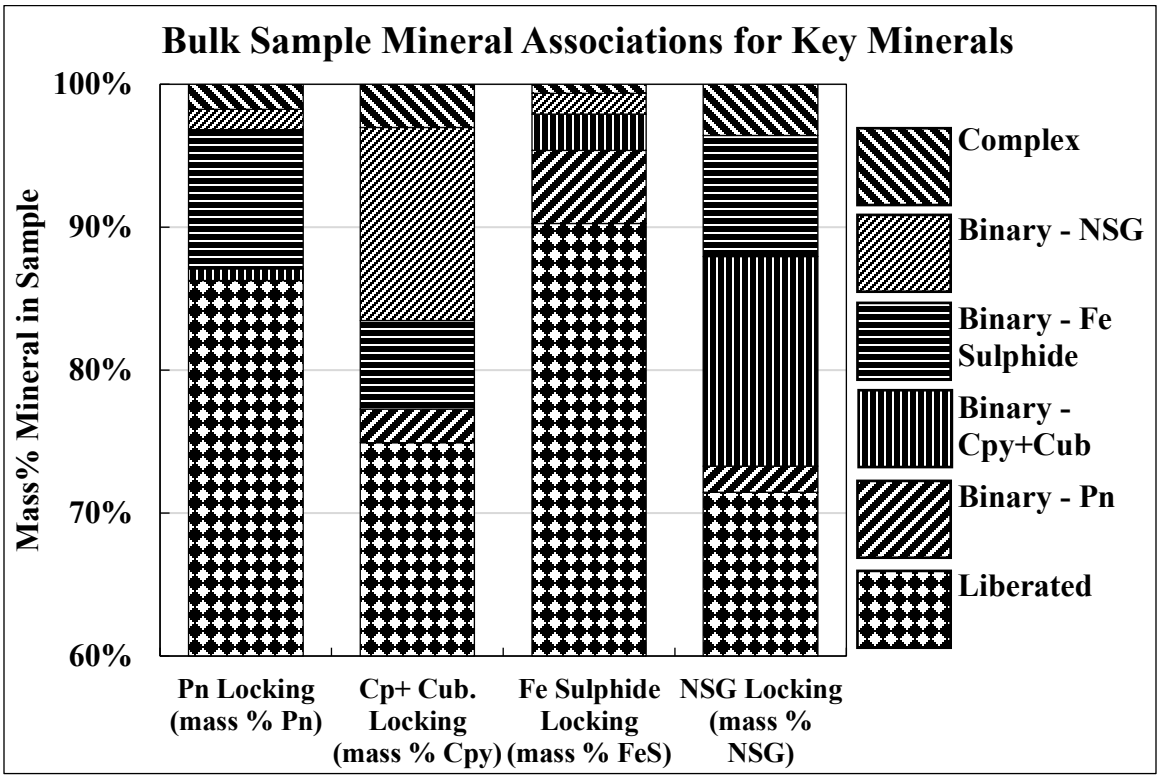

Figure 14: Mineral associations for each of the key minerals in sample. Locking mineral analysis was performed by XPS in Sudbury, Ontario and provided for use in this thesis.

The binary association between pentlandite and pyrrhotite appears over a largely particle size range (18-106 microns) as seen in Figure 15. Pentlandite was largely liberated in the fines. Conversely, chalcopyrite and non-sulfide gangue largely associated in the coarse particle size (see Figure 16) with slight pyrrhotite association in the finest particle size range.

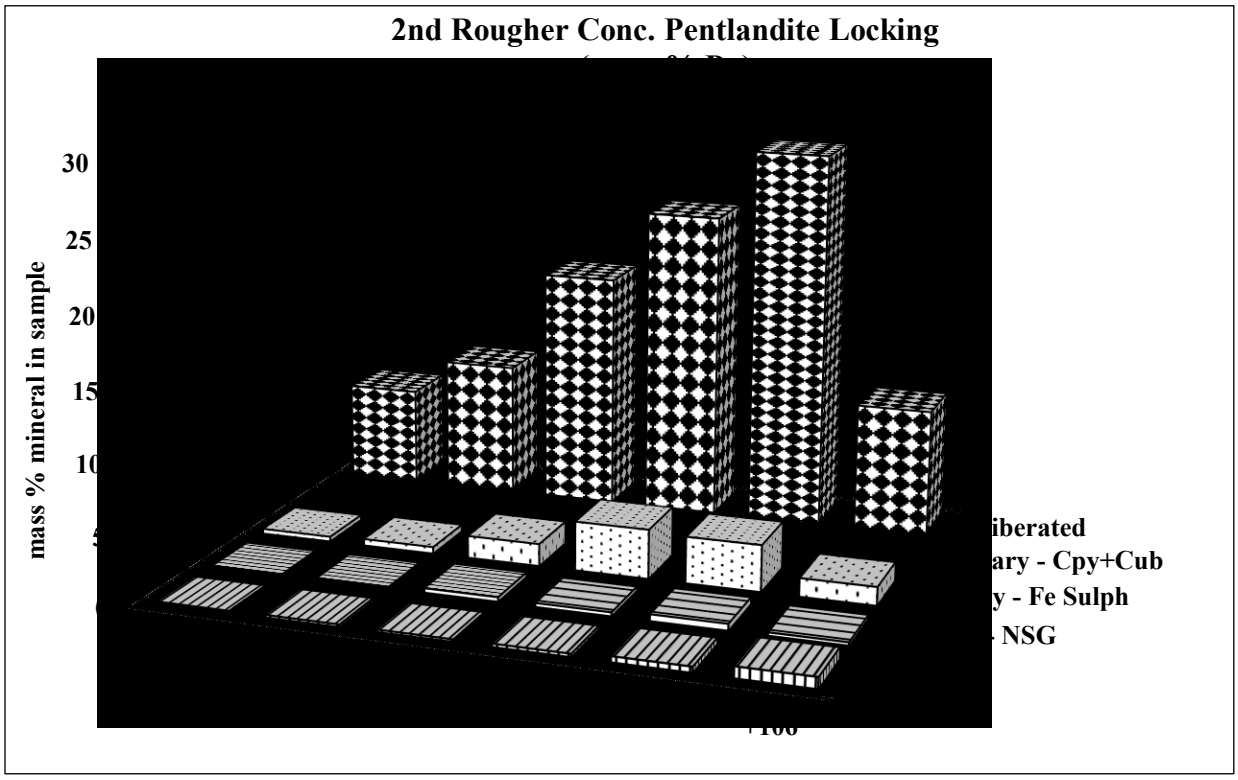

Figure 15: Mineral associations for pentlandite size fractions. Mineral analysis was performed by XPS in Sudbury, Ontario and provided for use in this thesis.

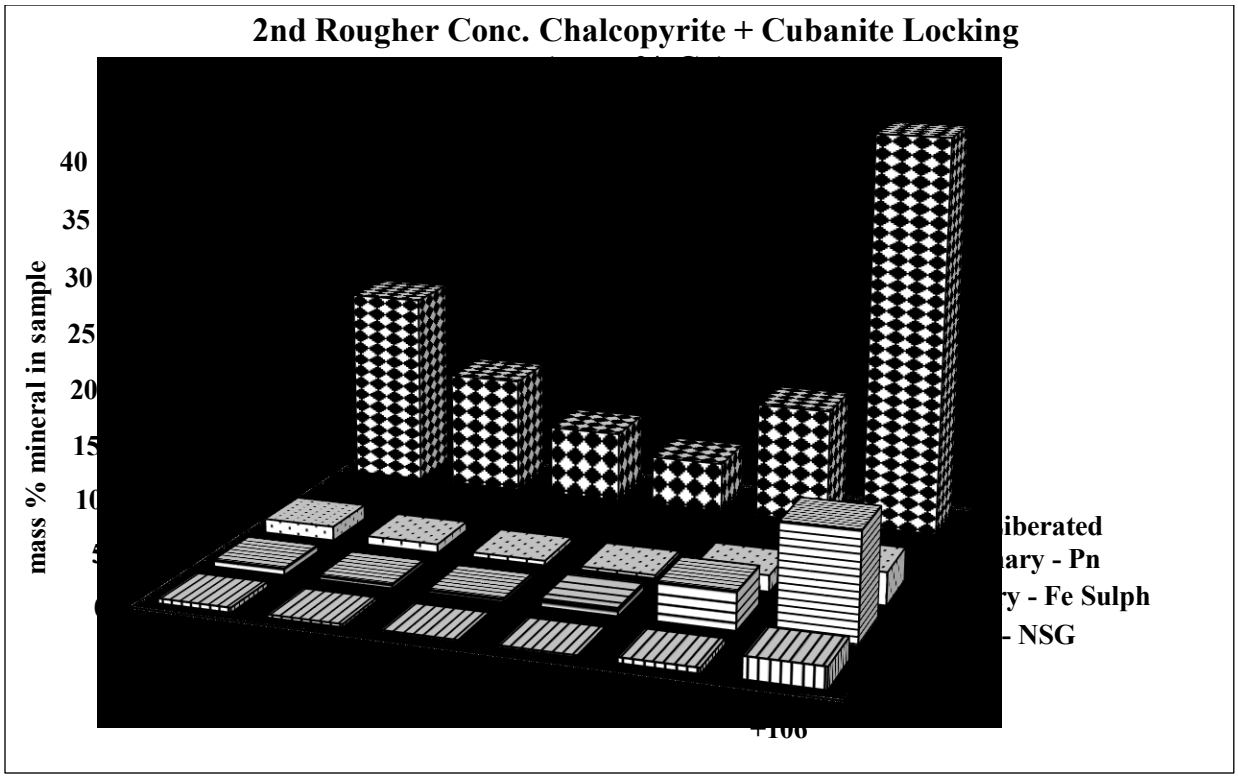

Figure 16: Mineral associations for chalcopyrite size fractions. Mineral analysis was performed by XPS in Sudbury, Ontario and provided for use in this thesis.

Chapter 4 High Intensity Conditioning using a Hydrofoil Impeller

Considered a low shear impeller, a hydrofoil impeller produces an axial circulation pattern within the tank. Common benefits for this flow pattern include excellent tank cleaning resulting in solid particles not settling under proper placement.

Experimental Procedure for Hydrofoil Impeller HIC

The high intensity conditioning stage using a hydrofoil impeller consists of adding the mineral to deionized water and adjusting the pH to 9.2 with lime. Once adjusted, the rpm of the impeller is increased to the speed to 1,100 rpm. The sides of the Denver tank are checked for particle settling. The impeller was positioned in the center of a Denver tank, approx. 1cm from the bottom of the tank. This height was determined to assist in tanking cleaning so particles could not accumulate in the corners of the square tank.

The HIC stage commences for 30 minutes. Once complete, the hydrofoil impeller is cleaned, and the Denver tank is transferred to a Denver flotation cell. The pH was readjusted to 9.2 and then MIBC is added. As xanthate was added during HIC stage (5% of total dosage every minute for 20 minutes).

Modified Flotation Rate Constants

Earlier work by Manqui Xu [139] explained the calculation of a modified rate constant through fitting a recovery-time plot with the specific trendline show below:

$$y=a(1-\exp(-bx)) \tag{23}$$

This trendline can be fit to the following first-order model [139], [140]:

$$R=R_{\infty}(1-\exp(-kt)) \tag{24}$$

A modified rate constant (MRC), K_M, is the product of $R_\infty * k$ from the first-order model or $a * b$ from the trendline can be calculated. This modified rate constant is unitless and allows for a reasonable comparison between flotations. The cited works can be reviewed for a more in-depth understanding [139], [140]. The trendline was fitted with Origin software with the line was referred to as “BoxLucas1”.

Table 2: Modified Rate Constants (MRCs) for Hydrofoil HIC and No HIC Tests

	Modified Rate Constant, Km		
Flotation Tests	Cp	Pn	Po
0/No HIC	20.6	9.5	7.9
10/No HIC	27.7	29.2	18.7
20/No HIC	58.3	58.3	35.7
0/1100 HF	17.9	1.9	3.1
10/1100 HF	23.4	8.2	7.5
20/1100 HF	29.8	14.7	11.6

4.1 Effect of Xanthate Dosage with and without High Intensity Conditioning using a hydrofoil impeller

Chalcopyrite Recovery

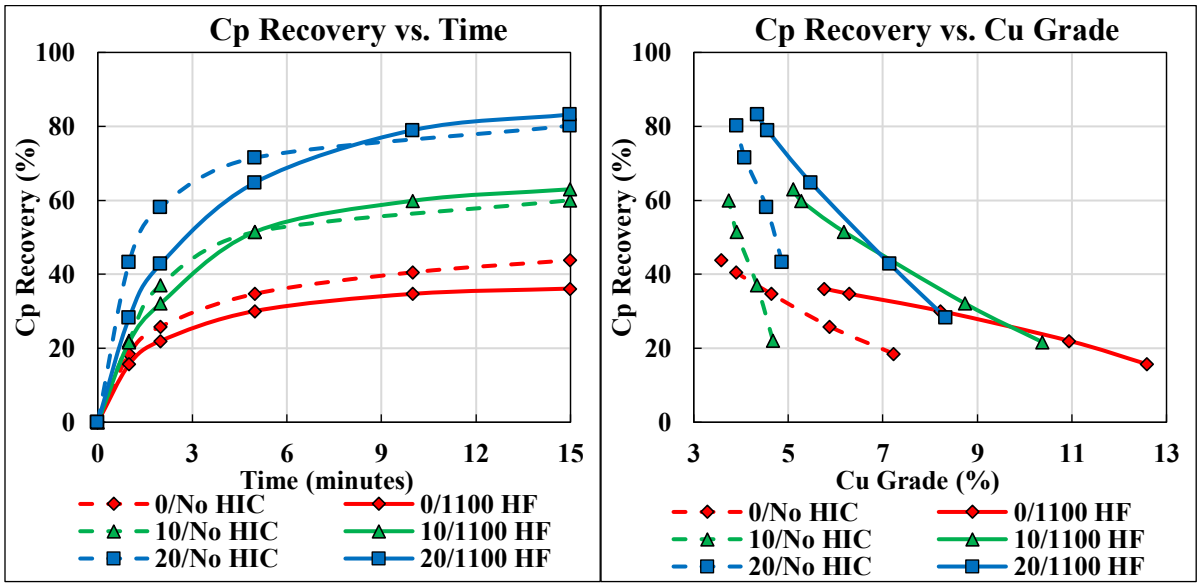

Figure 17: Chalcopyrite recovery over Time (left) and Chalcopyrite Recovery vs. Cu Grade (right) comparing No HIC vs. Hydrofoil HIC (with RPM) at various xanthate dosages (g/ton).

The effect of HIC on the recovery of chalcopyrite is shown in Figure 17 above. The measured recovery varies based on whether additional xanthate was added. Without xanthate, the recovery of chalcopyrite is reduced when compared to immediate flotation of the ore sample. Similarly poor flotation behaviour without xanthate was noted by Bulatovic [115]. As the

sample was originally a concentrate, there will be hydrophobic species present. HF HIC does appear to reduce the hydrophobicity of chalcopyrite by a small degree. However, when xanthate is added, chalcopyrite recovery with HF HIC is higher than a standard conditioning prior to Denver cell flotation (No HIC stage is used). The improvement is only minor. The MRCs for chalcopyrite in Table 2 show that while similar recoveries were achieved by the 15 minute mark with HF HIC and the No HIC tests, the HF HIC showed a much slower flotation rate with nearly half the rate of the No HIC tests. The higher grade shown in Figure 17 is likely related to the lower recovery of both pentlandite and pyrrhotite with HF HIC.

Pentlandite Recovery

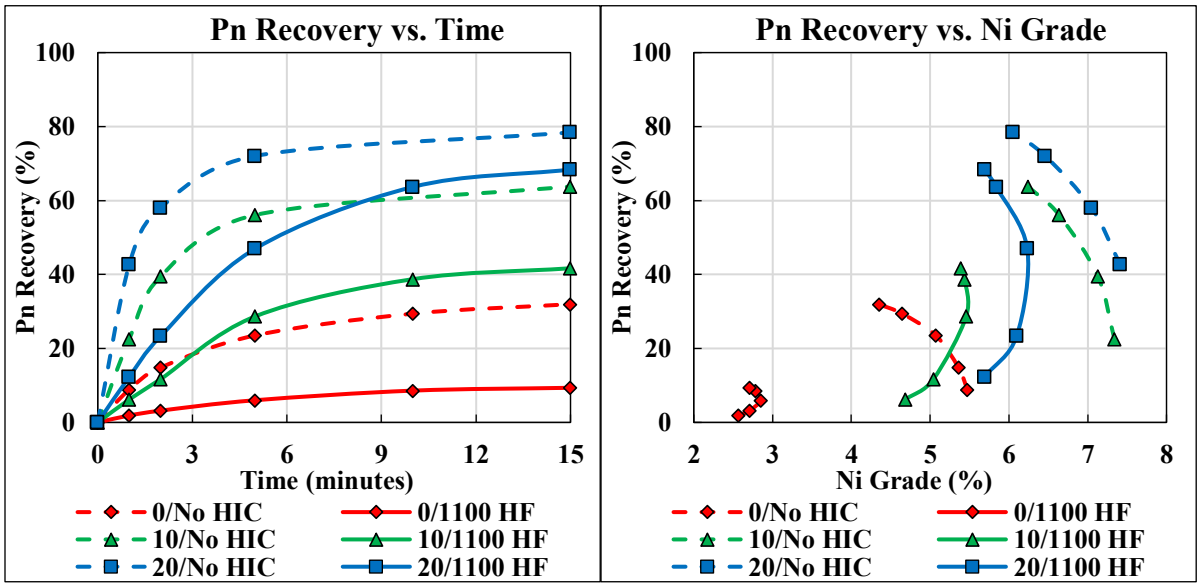

Figure 18: Pentlandite recovery (left) and Pentlandite Recovery vs. Ni Grade (right) comparing No HIC vs. Hydrofoil HIC (with RPM) at various xanthate dosages (g/ton).

The recovery of pentlandite is greatly hindered by HF HIC as seen in Figure 18. With no xanthate added, pentlandite recovery drops to below 10% which suggests a drastic reduction in pentlandite hydrophobicity. When xanthate is added, the recovery is improved but does not reach the recovery of pentlandite without HIC. The MRCs for pentlandite show that the No HIC tests have nearly a 3.5-4 times higher flotation rate than with the HF HIC.

Pyrrhotite Recovery

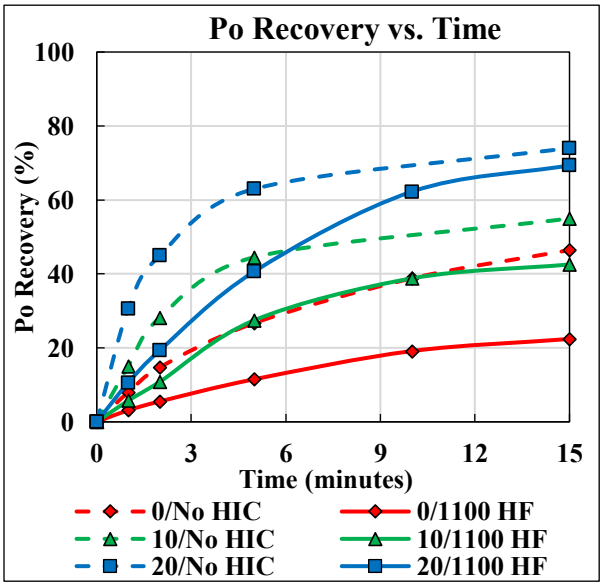

Figure 19: Pyrrhotite recovery comparing No HIC vs. Hydrofoil HIC (with RPM) at various xanthate dosages (g/ton).

Similarly, pyrrhotite shows a similar trend in floatability with and without HIC to pentlandite. The differences in recovery are smaller than pentlandite. The MRCs for pyrrhotite show that No HIC rate constants 2.5-3 times faster than the HF HIC.

Selectivity of Pyrrhotite with Pentlandite and Chalcopyrite

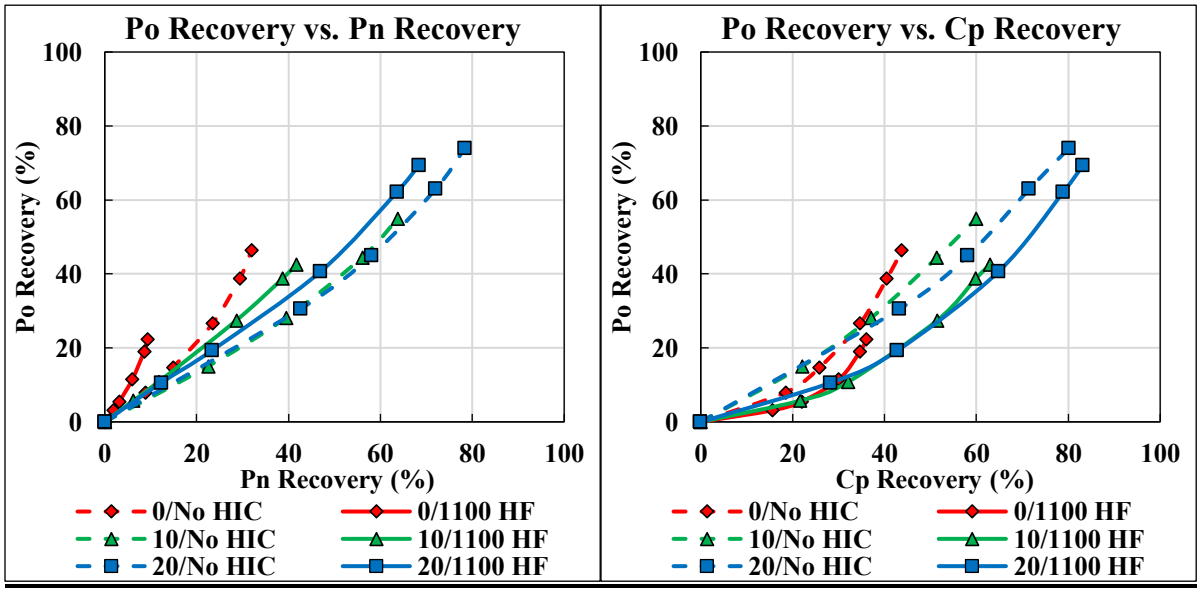

Figure 20: Pyrrhotite-pentlandite (left) and pyrrhotite-chalcopyrite (right) selectivity curves comparing No HIC vs. Hydrofoil HIC (with RPM) at various xanthate dosages (g/ton).

The selectivity curves for the initial experiments (shown above in Figure 20) with the hydrofoil HIC stage is quite poor. Pentlandite showed a drastic reduction in floatability that was not fully understood. Pyrrhotite showed similar trends but not nearly as detrimental as pentlandite which resulted in the selectivity between the two being worse with HIC. Chalcopyrite did show slight improvements with HIC, but the selectivity was still not promising.

4.2 Comparing Different Xanthate Addition Dosages with HIC with a Hydrofoil Impeller

From the various tests with the hydrofoil impeller, there appeared to be an inherent detrimental effect on the recovery of pentlandite that could not be fully understood. As the hydrofoil impeller is a choice that differed from previous HIC literature, there may be an unintended effect that is either removing hydrophobic species (dixanthogen) or creating hydrophilic species due to oxidation. As HIC literature states the presence of a collector is required for HIC to function, the slow xanthate addition may be the reason for poor results. As only 5% of the total xanthate is added per minute, the relative xanthate concentration remains low throughout the experiment. This was used to emulate starvation conditions, but faster xanthate additions may yield more information about the effects of HIC with a hydrofoil impeller.

The following experiments will test the effect of using a higher xanthate concentration (4x the typical amount). Comparatively, the previous experiments saw complete xanthate addition at 19 minutes (first addition at start of experiment or t = 0), these experiments will have complete xanthate addition at 4 minutes.

Table 3: Modified Rate Constants (MRCs) for Hydrofoil HIC and different xanthate addition speeds.

	Modified Rate Constant, Km		
Flotation Tests	Cp	Pn	Po
20/No HIC	58.3	58.3	35.7
20/1100 (5%) HF	29.8	14.7	11.6
20/1100 (20%) HF	33.2	9.8	15.4

Chalcopyrite Recovery

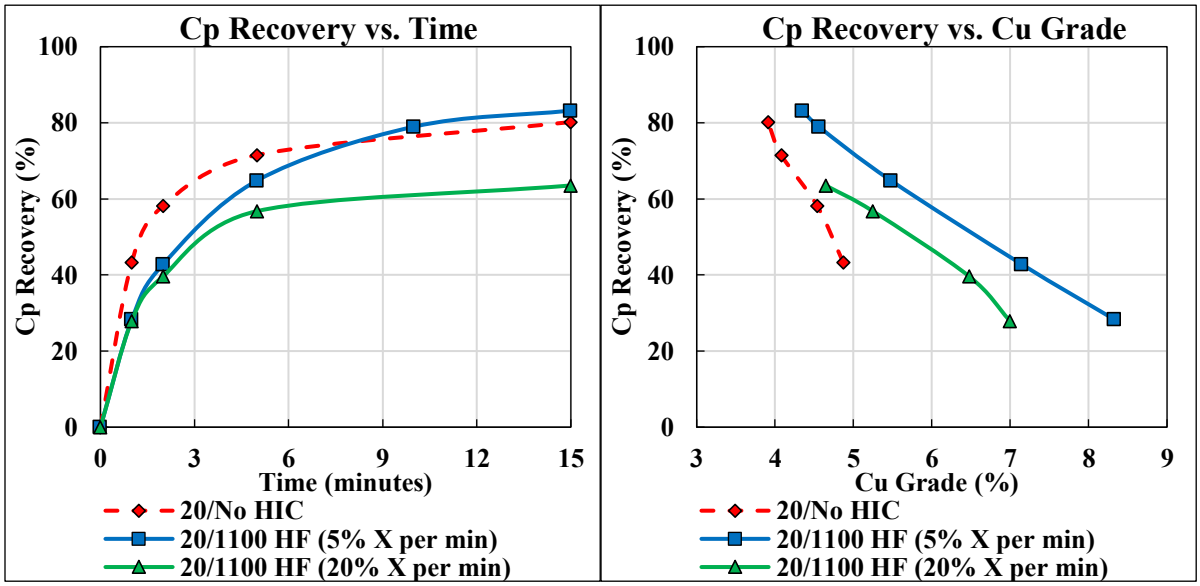

Figure 21: Chalcopyrite recovery over Time (left) and Chalcopyrite Recovery vs. Cu Grade (right) comparing No HIC vs. Hydrofoil HIC (with RPM) with an overall xanthate dosage of 20 g/ton. The HIC tests have a fast or slow xanthate addition speed.

When the xanthate is added faster, the recovery of chalcopyrite is shown to be worse compared to adding the xanthate slower. This suggests that there is a negative effect being produced by the HIC with the hydrofoil impeller. Ironically, the MRC value in Table 2 for the fast addition was slightly higher (33.2 vs. 29.8), but still resulted in a lower recovery.

Pentlandite Recovery

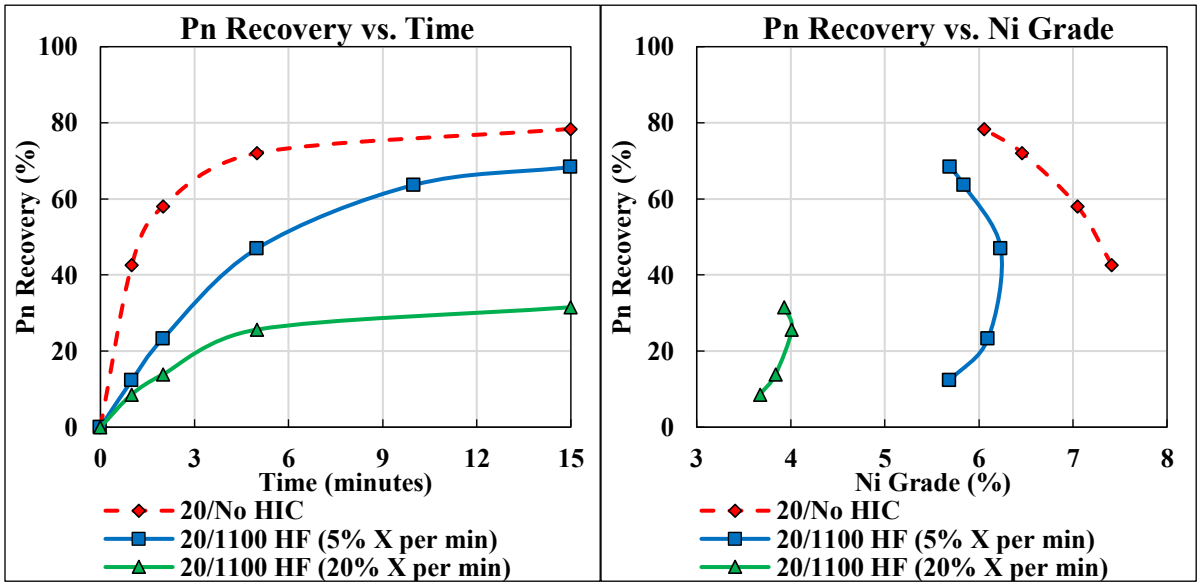

Figure 22: Pentlandite recovery (left) and Pentlandite Recovery vs. Ni Grade (right) comparing No HIC vs. Hydrofoil HIC (with RPM) with an overall xanthate dosage of 20 g/ton. The HIC tests have a fast or slow xanthate addition speed.

The adjusted use of xanthate has a drastic effect on the recovery of pentlandite. The recovery of pentlandite drops to less than half of the same amount of xanthate added over a longer interval. The recovery of this is unacceptably low and shows there is a constant effect of the current HIC setup that is inconsistent with other HIC setups. The MRC at the higher addition drops from 14.7 to 9.8 which shows the pentlandite was less floatable and floated more slowly.

Pyrrhotite Recovery

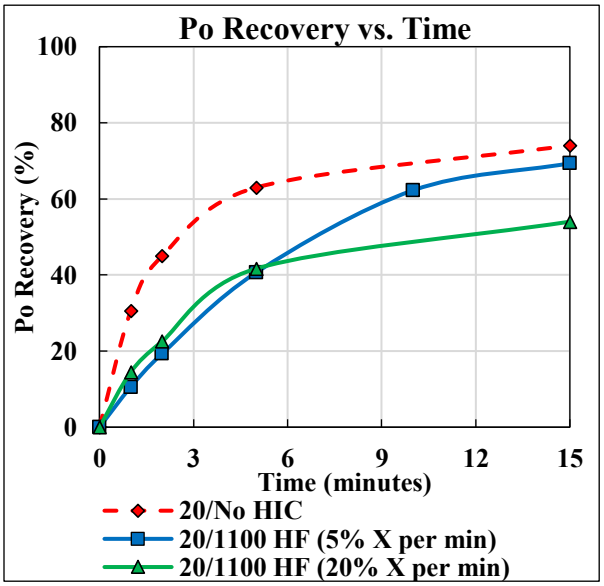

Figure 23: Pyrrhotite recovery comparing No HIC vs. Hydrofoil HIC (with RPM) with an overall xanthate dosage of 20 g/ton. The HIC tests have a fast or slow xanthate addition speed.

Like the other minerals, pyrrhotite shows a recovery loss when the xanthate is added faster. The flotation rate of pyrrhotite increased from 11.6 to 15.4 which showed the pyrrhotite floated much faster

Thoughts on The Results from HIC with A Hydrofoil Impeller

In other studies, xanthate is added all at once at the beginning and then HIC commences. This has shown increased recoveries of pentlandite. While the recovery of sulfide minerals was shown to worsen without the addition of xanthate, the results seen with the hydrofoil impeller are not representative of previous studies. The main differences are the use of the axial hydrofoil impeller compared to the widely used radial Rushton turbine. The power number of a Rushton turbine ($N_P = 6.75$) is approx. 19 times higher than the hydrofoil impeller ($N_P = 0.35$) meaning the energy input into the slurry is 19x more with the Rushton impeller.

The use of the hydrofoil shows that the impeller was not suited for HIC and was detrimental to the recovery of sulfides. The increased concentration of xanthate at the beginning of the HIC stage in fast addition tests should have resulted in an increased flotation of the minerals but led to

drastically lower recoveries of all minerals. Therefore, it is plausible to say there is a negative influence on the flotation from the HIC setup with the hydrofoil impeller that affects the recovery of the mineral over the course of the 30 minutes HIC stage. The higher recoveries seen with the lower concentration addition shows that creating the hydrophobic surfaces later in the HIC stage lead to the overall hydrophobicity of each mineral at the end of the HIC being higher. As the purpose of this thesis is not to investigate the explicit reason for this poor response but to evaluate the use of the HIC stage, the hydrofoil impeller was replaced with a Rushton turbine to mimic other HIC studies previously performed.

Chapter 5 High Intensity Conditioning using a Rushton Impeller

High intensity conditioning was performed with a Rushton turbine. Three different impeller speeds (900, 1,100 and 1,400 rpm) were chosen. When converted to power input, 1,100 was taken as the median speed. 900 rpm was calculated to be 55% of the power generated by 1,100 rpm while 1,400 rpm calculated to be 206% of 1,100 rpm.

Xanthate addition was controlled with xanthate being added every minute from the start of HIC (time = 0 minutes) to the 19th minute mark of HIC, which would correspond to the 20th xanthate addition. Therefore, each addition of xanthate was approx. 5% of the total xanthate added. For the remaining 11 minutes of high intensity conditioning, no more xanthate was added.

Following the high intensity conditioning stage, the slurry was transferred from the HIC cell to a standard stainless-steel Denver cell. There are several steps during the transfer where the slurry is not agitated and where the slurry would be oxygenated from pouring. The time between the end of the HIC stage and the beginning of the froth flotation stage was measured to be approx. 5 minutes for all experiments.

Once the flotation stage commenced, 4 concentrates were taken over a 15-minute flotation. Table 4 describes the time duration for each concentrate.

Table 4: Concentrate collection outlining individual collection time and overall duration

Concentrate #	Time (min.)	Length of collection time (min.)
1	1	1
2	2	1
3	5	3
4	15	10

The concentrates were vacuum filtered, and ethanol was used to further dry the cakes. The minerals were dried in an oven at 30 Celsius for 2 hours and then sampled the next day. The slurry cakes were largely in a discrete powder form with a few agglomerates. A pestle was used to gently breakage apart these agglomerates. The powders were split into a rotary micro riffler and samples were created, weighed and stored for analysis.

The samples taken from the Rushton experiments underwent EDTA extraction to dissolve the surface oxidation and analyze the metals that are removed through atomic absorption spectroscopy (AAS) or Inductively coupled plasma mass spectrometry (ICP-MS). The procedure followed the method provided by oxidation studies performed by Rumball and Richmond. [128]. The copper, nickel and iron metals were analyzed due to the sulfides being composed of iron, copper and nickel primarily.

5.1 Effect of Xanthate Dosage with and without High Intensity Conditioning using a Rushton Impeller

Four xanthate doses were used during HIC experiments, where the Rushton impeller speed was kept at a constant 1,100 rpm. Xanthate doses were calculated based on the standard g/ton dosage.

Table 5: Modified Rate Constants (MRCs) for Rushton HIC and No HIC Tests.

	Modified Rate Constant, Km		
Flotation Tests	Cp	Pn	Po
0/No HIC	20.6	9.5	7.9
10/No HIC	27.7	29.2	18.7
20/No HIC	58.3	58.3	35.7
0/1100 RT	6.0	5.0	6.3
5/1100 RT	27.7	34.7	33.6
10/1100 RT	47.2	57.7	48.4
20/1100 RT	65.4	70.0	50.4

Chalcopyrite Recovery

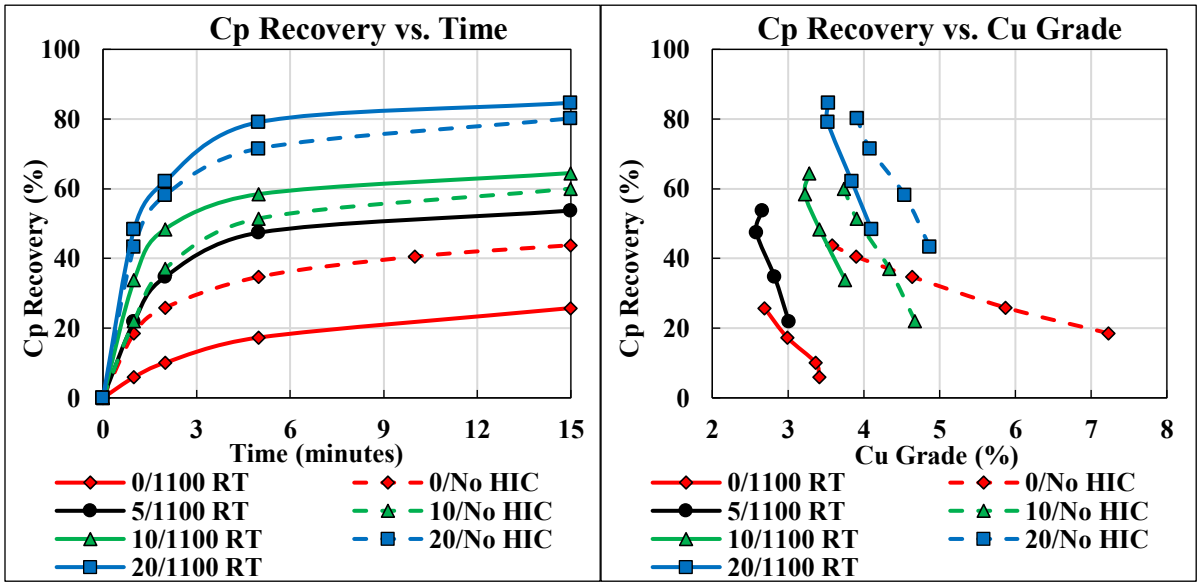

Figure 24: Chalcopyrite recovery over Time (left) and Chalcopyrite Recovery vs. Cu Grade (right) comparing No HIC vs. Rushton HIC (with RPM) at various xanthate dosages (g/ton).

The recovery of chalcopyrite, when xanthate is added, shows improvement when HIC is used. When no xanthate is added, HIC lowers the recovery of chalcopyrite compared to simply floating the mineral. The addition of 5 g/ton of xanthate with HIC showed a drastic improvement in the recovery of chalcopyrite, showing a cumulative recovery slightly less the 10 g/ton of xanthate with no HIC stage. The MRC for chalcopyrite with 10 g/ton of xanthate for Rushton HIC was 70% higher than No HIC tests. Increasing the xanthate dosage to 20 g/ton showed an MRC increase of 35% for RT HIC and this rate constant for HIC was 12% higher than No HIC.

Pentlandite Recovery

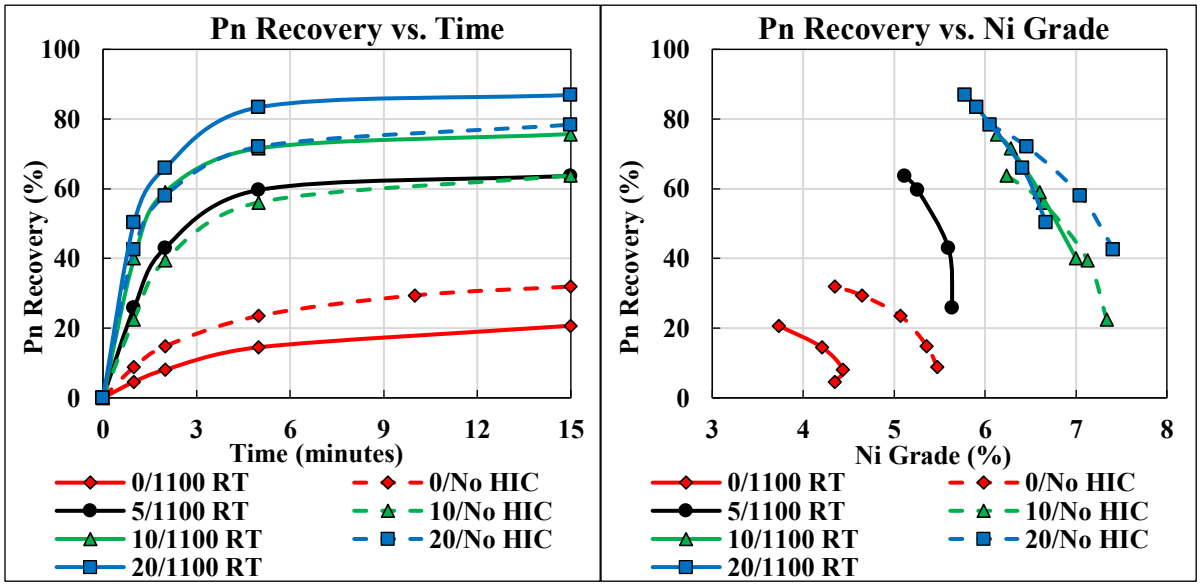

Figure 25: Pentlandite recovery (left) and Pentlandite Recovery vs. Ni Grade (right) comparing No HIC vs. Rushton HIC (with RPM) at various xanthate dosages (g/ton).

Pentlandite recovery, similar to chalcopyrite recovery, shows a drastic improvement in recovery when HIC is used with xanthate when compared to similar xanthate additions without HIC. Similarily, the recovery of pentlandite with HIC, but without xanthate (0/1100) is reduced. When 5 g/ton of xanthate is added during HIC, the recovery pentlandite increases by 40% and matching the recovery of double the xanthate with no HIC stage (10/No HIC). Similarily, 10 g/ton with HIC improves the recovery of pentlandite further, resulting in similar recovery when using 20 g/ton of xanthate with no HIC (20/No HIC).

The modified flotation rate constants for pentlandite also correlated the higher recovery with faster flotation speeds. With Rushton HIC, 5 g/ton of xanthate allowed pentlandite to float 20% faster than 10 g/ton of xanthate without HIC. Similar trends were seen when comparing the 10/1100 RT MRC (57.7) and 20/No HIC (58.3).

Difference between Pentlandite and Chalcopyrite Recoveries under HIC with a Rushton Turbine

When comparing the impact of HIC on chalcopyrite and pentlandite, their sensitivies to HIC appear to be quite different. With no xanthate, both minerals have an expected reduction in recovery when compared to the test without HIC. Upon adding xanthate during HIC, pentlandite shows a massive improvement over the no HIC test. Comparatively, chalcopyrite improves but not as dramatically as pentlandite with HIC. Chalcopyrite and pentlandite recovery were 4.5% and 9% higher, respectively, with Rushton HIC than the no HIC tests when using xanthate showing pentlandite responded better than chalcopyrite.

Comparing Pentlandite and Chalcopyrite recovery based on HIC impeller (Hydrofoil vs. Rushton)

Table 6: Modified Rate Constants (MRCs) for Rushton HIC and Hydrofoil HIC Tests.

	Modified Rate Constant, Km		
Flotation Tests	Cp	Pn	Po
0/1100 HF	17.9	1.9	3.1
10/1100 HF	23.4	8.2	7.5
20/1100 HF	29.8	14.7	11.6
0/1100 RT	6.0	5.0	6.3
10/1100 RT	47.2	57.7	48.4
20/1100 RT	65.4	70.0	50.4

Chalcopyrite Recovery

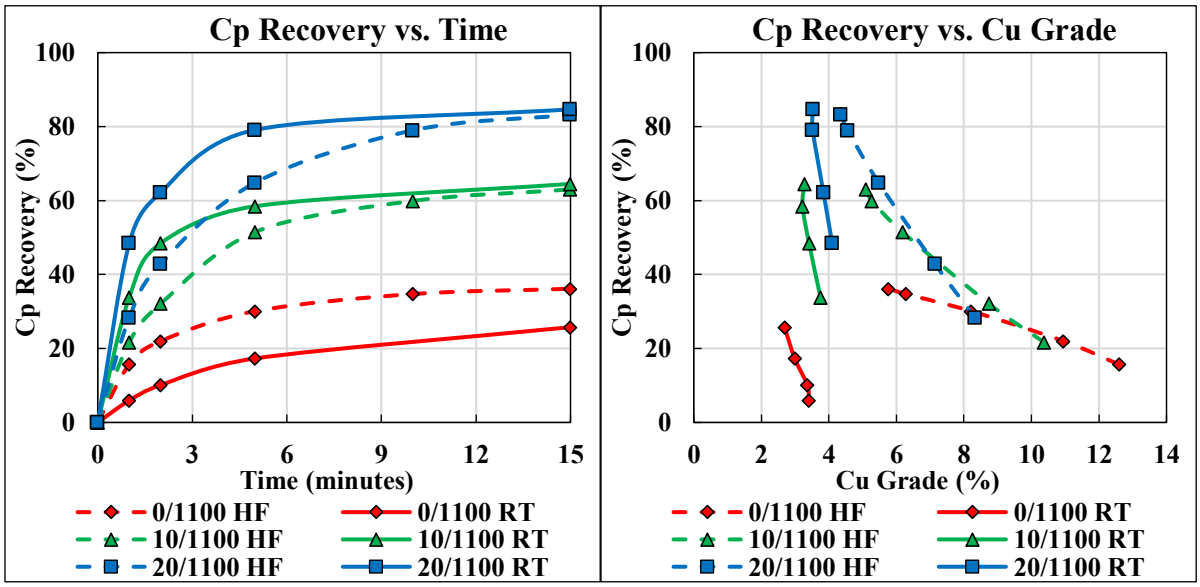

Figure 26: Chalcopyrite recovery over Time (left) and Chalcopyrite Recovery vs. Cu Grade (right) comparing Hydrofoil HIC vs. Rushton HIC (with RPM) at various xanthate dosages (g/ton).

The change from the hydrofoil impeller to the Rushton turbine shows so interesting trends as well. Chalcopyrite showed nearly identical total recovery between the two impellers but showed more chalcopyrite floated earlier. Specifically, it took 6 minutes of flotation following the hydrofoil HIC to yield the same recovery with Rushton HIC after only 2 minutes when either

10 or 20 g/ton of xanthate was used. With 10 minutes of hydrofoil HIC, it only took 5 minutes of Rushton HIC to result in the same recovery. So, while the end results were the same for a 15-minute test, chalcopyrite floated with Rushton HIC was much faster. A comparison of the MRCs show that the use of xanthate and Rushton HIC resulted in rate constants double the constants of Hydrofoil HIC with identical xanthate dosages.

Pentlandite Recovery

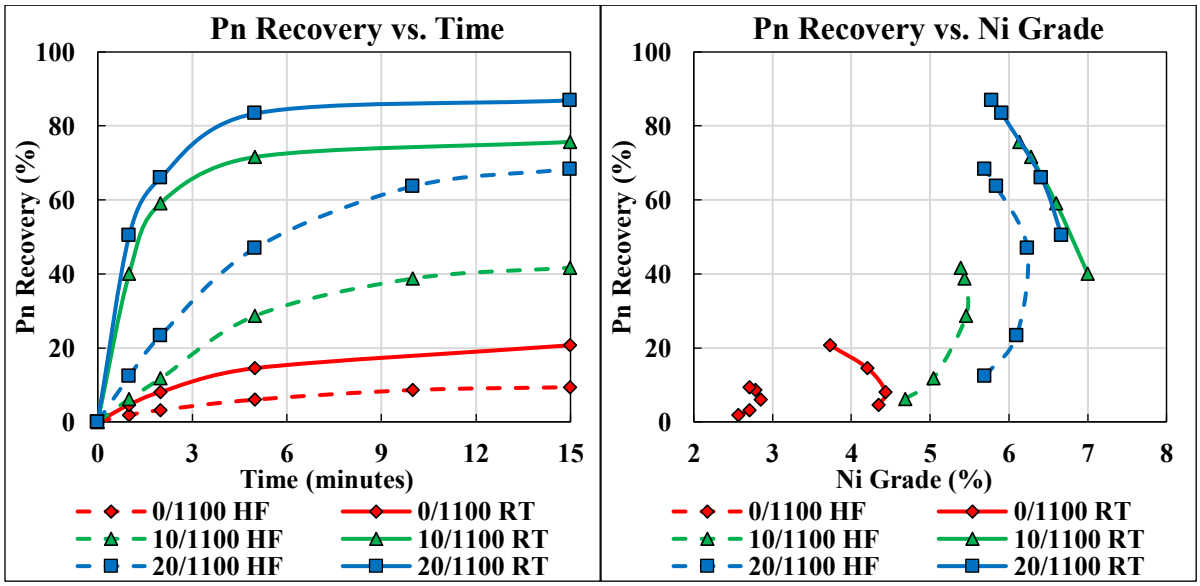

Figure 27: Pentlandite recovery (left) and Pentlandite Recovery vs. Ni Grade (right) comparing Hydrofoil HIC vs. Rushton HIC (with RPM) at various xanthate dosages (g/ton).

Pentlandite's recovery with Rushton HIC were much higher than with hydrofoil. Using a xanthate dosage of 10 and 20 g/ton, Rushton HIC recovery was 34% and 18.5% higher, respectively than with hydrofoil HIC. Pentlandite floated much faster with Rushton HIC. When xanthate was not used, the minerals responded differently with each HIC impeller. While pentlandite floated poorly with the hydrofoil when compared to the Rushton, chalcopyrite floated worse with the Rushton vs. the hydrofoil. Due to the Rushton generating 19 times more energy than the hydrofoil impeller (based on similar size/speed), chalcopyrite may respond better to lower power inputs than pentlandite. This will be explored further when the Rushton turbine speeds are adjusted. As the improved recovery of pentlandite is extremely important in this thesis, further HIC work with the hydrofoil impeller was not performed and all future HIC tests

used a Rushton Turbine. The recovery of pentlandite is greatly improved with Rushton HIC, with MRCs 7.1 and 4.7 times higher than Hydrofoil HIC with 10 and 20 g/ton respectively.

Pyrrhotite Recovery

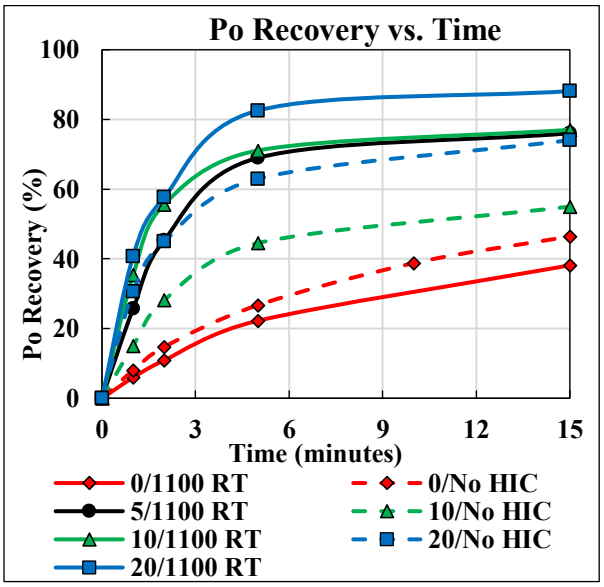

Figure 28: Pyrrhotite recovery comparing No HIC vs. Rushton HIC (with RPM) at various xanthate dosages (g/ton).

The recovery of pyrrhotite was greatly enhanced using Rushton HIC. Even with 5 g/ton of xanthate, pyrrhotite recovery with HIC reaches 75% easily. The recovery with 5 g/ton with HIC was higher than 20 g/ton of xanthate without HIC. Based on the analysis of oxide found in the concentrates (see Figure 30), copper and nickel activation are assumed to be responsible for the excessive flotation of pyrrhotite.

Based on the surface cleaning the RT HIC is providing, the surface of pyrrhotite would be clean throughout HIC. During this HIC period, the surface will be continually oxidized and cleaned. This will result in higher concentration of ions being present in the solution. This phenomenon is seen in EDTA extraction with sulfides [128] where Rumball noted the metal concentration is the solution was much higher if nitrogen was not bubbled during EDTA extraction. This is likely what is occurring during HIC. Once HIC is stopped, the copper ions immediately interact and activate the pyrrhotite.

Selectivity of Pyrrhotite with Pentlandite and Chalcopyrite

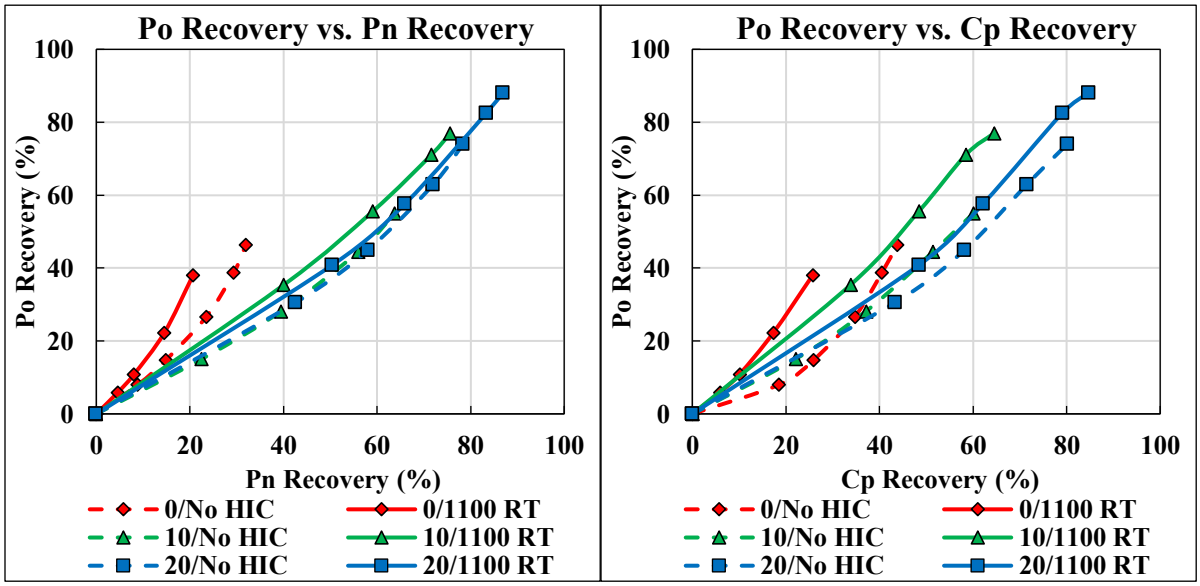

Figure 29: Pyrrhotite-pentlandite (left) and pyrrhotite-chalcopyrite (right) selectivity curves comparing No HIC vs. Rushton HIC (with RPM) at various xanthate dosages (g/ton).

As xanthate dosage increases, the selectivity improves. With no xanthate, the selectivity is better without high intensity conditioning. In general, the selectivity is better for chalcopyrite with no HIC while the maximum chalcopyrite recovery is seen with Rushton HIC. Regarding pentlandite, the selectivity with xanthate doses is very similar. At 20 g/ton, the selectivity with and without HIC was nearly identical. With HIC, the selectivity curve stayed consistent but reached higher levels of recovery for both pentlandite and pyrrhotite.

Copper, Nickel and Iron Oxidation on the Concentrate Surface

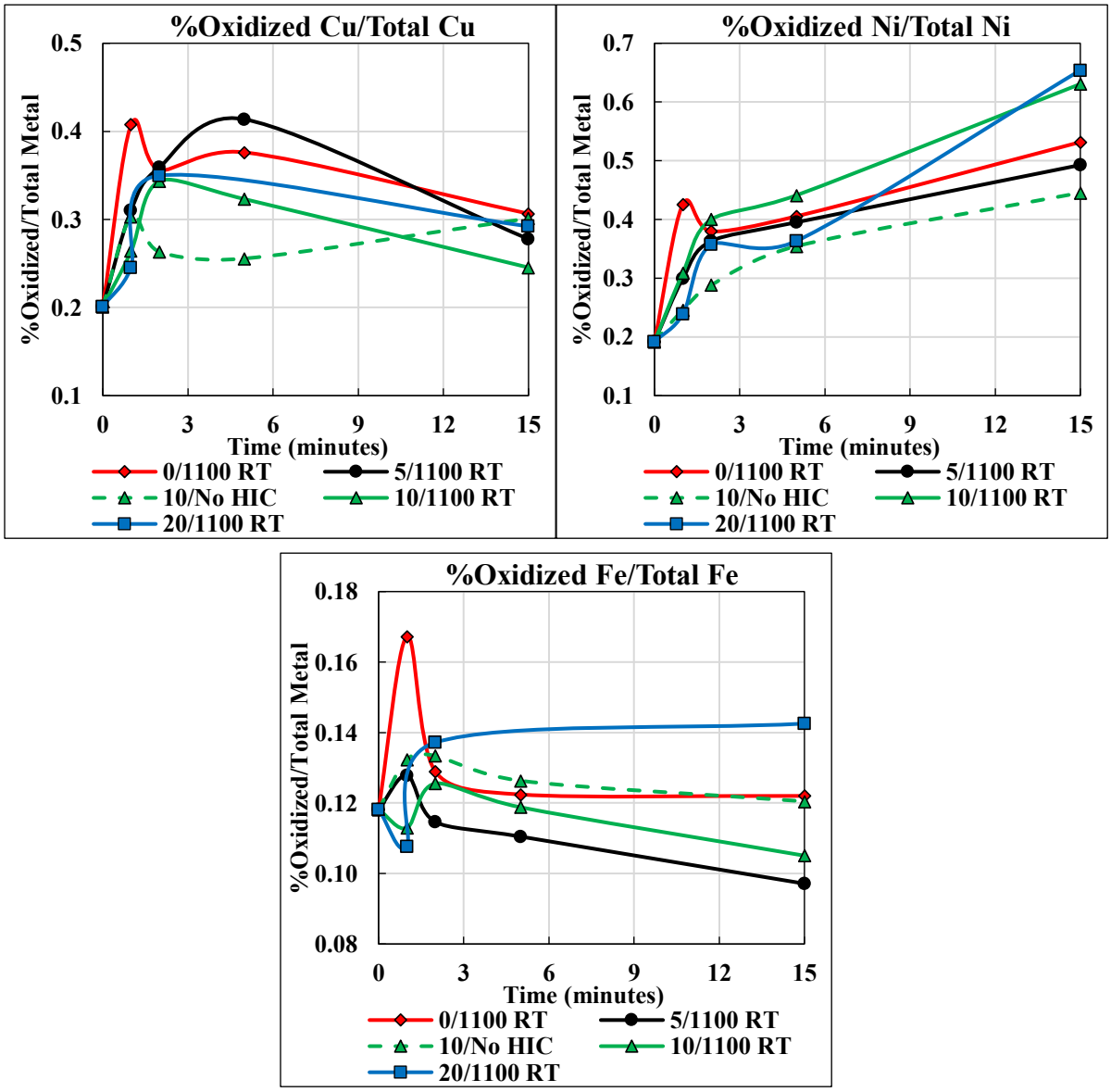

Figure 30: Copper Oxidation Levels (Top-Left), Nickel Oxidation Levels (Top-right) and Iron Oxidation Levels (Bottom-Left) for various flotation experiments. Oxidation levels were attained through EDTA extraction and AAS.

The effect of Rushton HIC and the formation of a metal oxide show that, in general, the addition of xanthate reduces the oxidation on the early concentrates. When comparing the copper, nickel and iron oxidation in Figure 30, higher levels of xanthate correlates to less metal oxides on the surfaces initially. The highest degree of oxidation with Rushton HIC is seen when no xanthate is added which supports the poor recovery that is noted following flotation.

Each metal shows a different trend that is dependent on time and concentration. Nickel oxidation shows increasing oxidation levels throughout the flotation. Nickel oxidation was higher with Rushton HIC at any xanthate addition that No HIC, showing that Rushton HIC resulted in more nickel oxidation when the concentrates were gathered. Copper oxidation was interesting, showing initially increasing levels in the first few minutes and then decreased as the flotation continued. Like nickel oxidation, Rushton HIC resulted in more copper oxide being found on the surfaces of the concentrates when compared to No HIC. Iron oxidation was relatively stable levels for each flotation, but xanthate addition was an important factor. When comparing the 5, 10 and 20 g/ton of xanthate with Rushton HIC, the first concentrate showed that more xanthate reduced the initial iron oxidation, but quickly reversed with 20 g/ton of xanthate having the highest iron oxidation in the final concentrate. When comparing the No HIC test, iron oxidation was higher than the Rushton HIC test with similar xanthate addition.

The considerably higher recoveries of the sulfides with Rushton HIC is related to four points concerning oxidation:

1. Copper and nickel oxidation were higher with Rushton HIC than without No HIC.
2. Iron oxidation was higher with No HIC than with Rushton HIC.
3. Rushton HIC reduced the initial iron oxidation than what is found on the feed. This reduction increased with xanthate addition.
4. The xanthate dosage has a direct impact on the impact of Rushton HIC effectiveness.

The use of HIC without xanthate showed that chalcopyrite responded differently than pentlandite and pyrrhotite. Hydrofoil HIC (0/1100 HF) showed that chalcopyrite was only slightly reduced when compared to No HIC (0/No HIC) in Figure 17, but pentlandite was severely depressed (refer to Figure 18). Rushton HIC without xanthate (0/1100 RT) showed that chalcopyrite was greatly depressed in Figure 24, but pentlandite minor reductions in recovery (refer to Figure 25). Since Rushton HIC has a much higher shear than Hydrofoil HIC (19 times more based of impeller power number), this suggests each mineral has an optimal power input for the flotation. The next series of tests vary the impeller speeds of the Rushton HIC to see if this observation is consistent.

5.2 Effect of impeller speed during HIC with 5 g/ton xanthate dose

When the impeller speed is adjusted, the power that is generated in the slurry is drastically affected. By using levels of xanthate during HIC, the effect of power input is tested. Three speeds were chosen. The power generated by an impeller can be calculated:

$$P=N_p\rho N^3D^5 \quad (25)$$

As all parameters except for impeller speed remain consistent, the power generated can be related to the speed. If 1,100 rpm is used as a base, the impact on power input from decreasing or increasing the impeller speed can be calculated:

Table 7: Relation between impeller speed (RPM) and power input.

RPM	Power Input (%) of 1,100 RPM
900	55%
1,100	100%
1,400	206%

Table 8: Modified Rate Constants (MRCs) for Rushton HIC (5 g/ton X) with various impeller speeds.

	Modified Rate Constant, Km		
Flotation Tests	Cp	Pn	Po
5/900 RT	33.3	20.9	25.7
5/1100 RT	27.7	34.7	33.6
5/1400 RT	27.0	32.4	33.9

Chalcopyrite Recovery

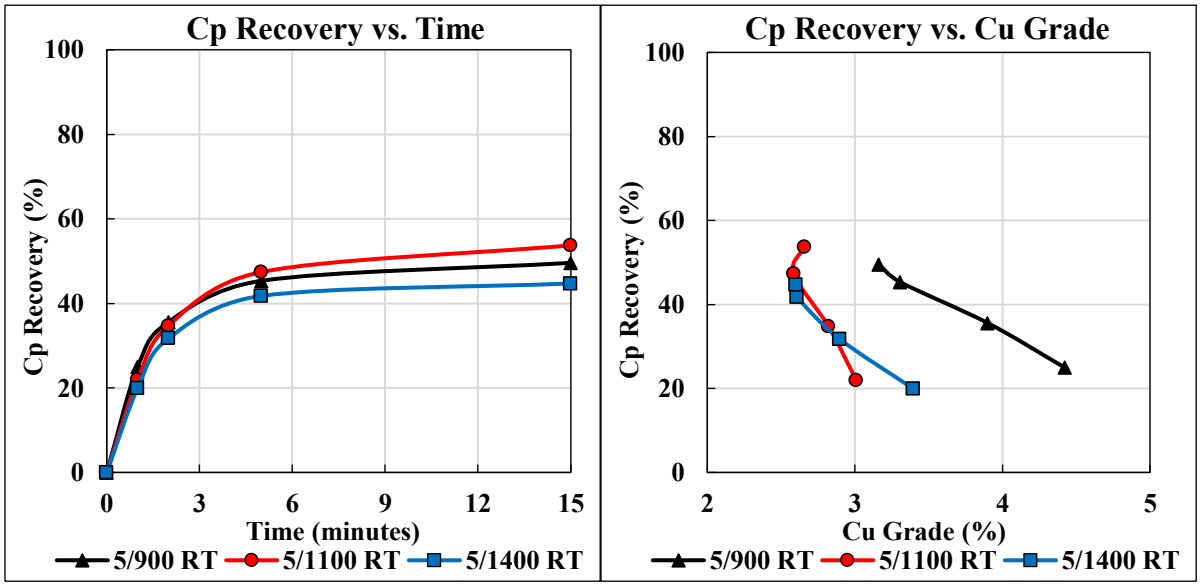

Figure 31: Chalcopyrite recovery over Time (left) and Chalcopyrite Recovery vs. Cu Grade (right) comparing Rushton HIC tests with various impeller speeds (RPM) at a 5 g/ton xanthate dosage.

The recovery of chalcopyrite shows a preference for lower impeller speeds. At double the power input (1,400 RPM), the recovery is lower. Given the slight amount of xanthate used, the manipulation of the impeller speed decreases the recovery by 10% from 1,100 to 1,400 rpm. The MRCs in Table 8 show that chalcopyrite had the fastest rate constant at the lowest rpm tested (900 rpm) and decreased at higher impeller speeds.

Pentlandite Recovery

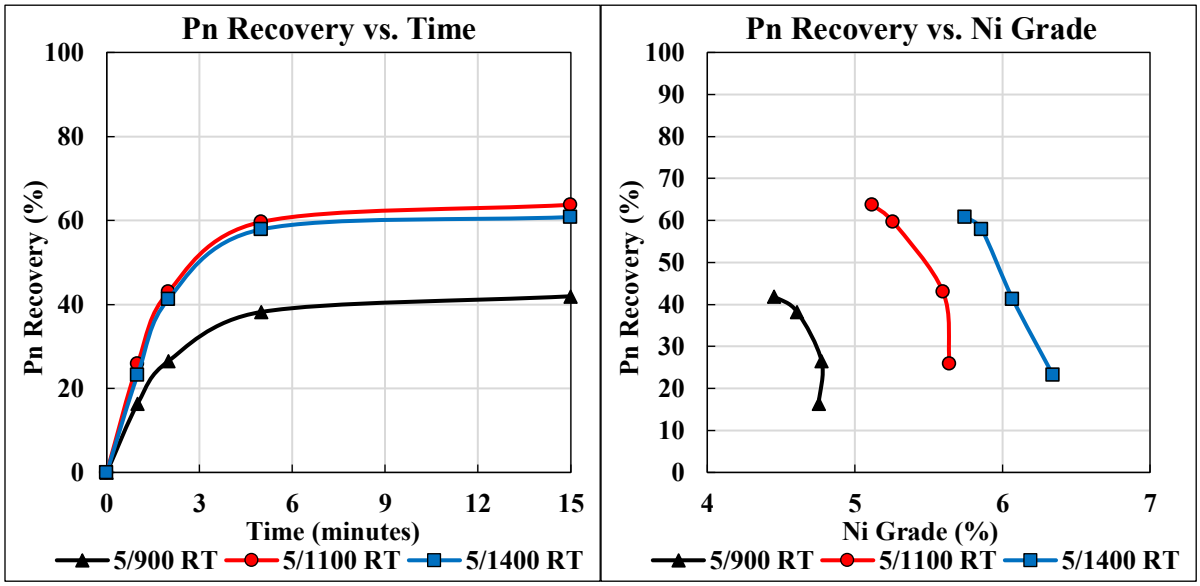

Figure 32: Pentlandite recovery (left) and Pentlandite Recovery vs. Ni Grade (right) comparing Rushton HIC tests with various impeller speeds (RPM) at a 5 g/ton xanthate dosage.

Pentlandite exhibit a notably higher recovery at higher impeller speeds, with both 1,100 and 1,400 rpm having approx. 20% more recovery than 900 rpm. The MRCs for pentlandite showed that pentlandite had the lowest rate constant at 900 rpm and floated much faster at higher speeds.

Pyrrhotite Recovery

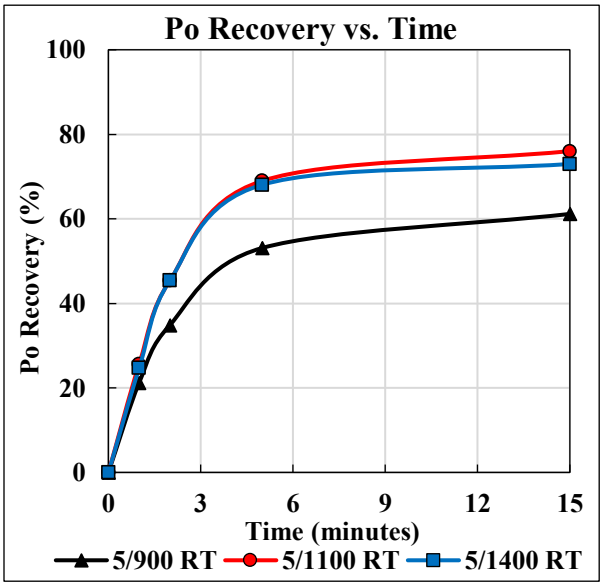

Figure 33: (left) Pyrrhotite recovery comparing Rushton HIC tests with various impeller speeds (RPM) at a 5 g/ton xanthate dosage.

The recovery of pyrrhotite is very similar to the recovery of pentlandite at 5 g/ton of xanthate. Higher impeller speeds showed the best recovery. An increase in speed from 1,100 to 1,400 rpm (2 times increase in power generation) resulted in a slightly lower recovery. A comparison of the MRCs showed that pyrrhotite had the highest rate constant at 1,400 rpm and as the impeller speed decreased, the rate constant decreased.

Sulfide Selectivity

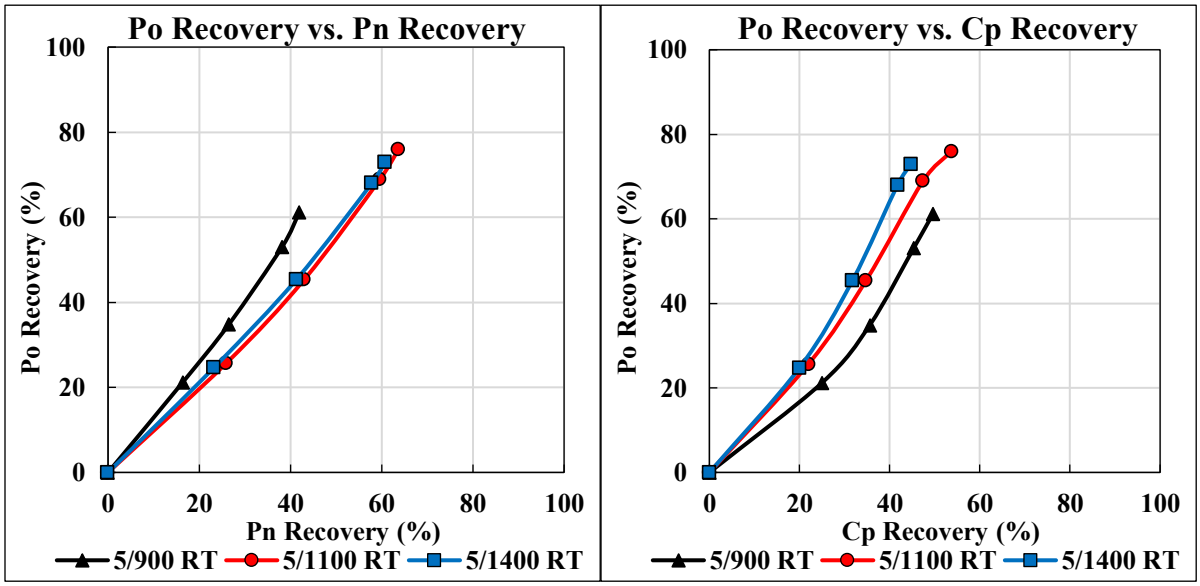

Figure 34: Pyrrhotite-pentlandite (left) and pyrrhotite-chalcopyrite (right) selectivity curves comparing Rushton HIC tests with various impeller speeds (RPM) at a 5 g/ton xanthate dosage.

The selectivity between chalcopyrite and pyrrhotite shows a great deal of variance. At the lower impeller speeds, chalcopyrite is more easily recovered while pyrrhotite is more floatable at the higher speeds. It is in the intermediate speed of 1,100 rpm that chalcopyrite is the most floatable. However, pyrrhotite is also the most floatable with this speed as well. Pentlandite and pyrrhotite are affected by the impeller speeds in very similar ways as both show similar recoveries at higher speeds. The lowest speed of 900 rpm shows an approximate drop of 20% for both minerals.

With a low xanthate dose, the selectivities are poor. Chalcopyrite and pentlandite benefit from different impeller speeds, so finding an optimal power speed for both is likely not feasible. From the EDTA extraction of the oxides, chalcopyrite recovery is best when there is a lower amount of chalcopyrite oxidation. Pentlandite was also the most floatable in the test with the lowest amount of pentlandite oxidation. The best recovery of both minerals is with 1,100 rpm.

Copper, Nickel and Iron Oxidation on the Concentrate Surface

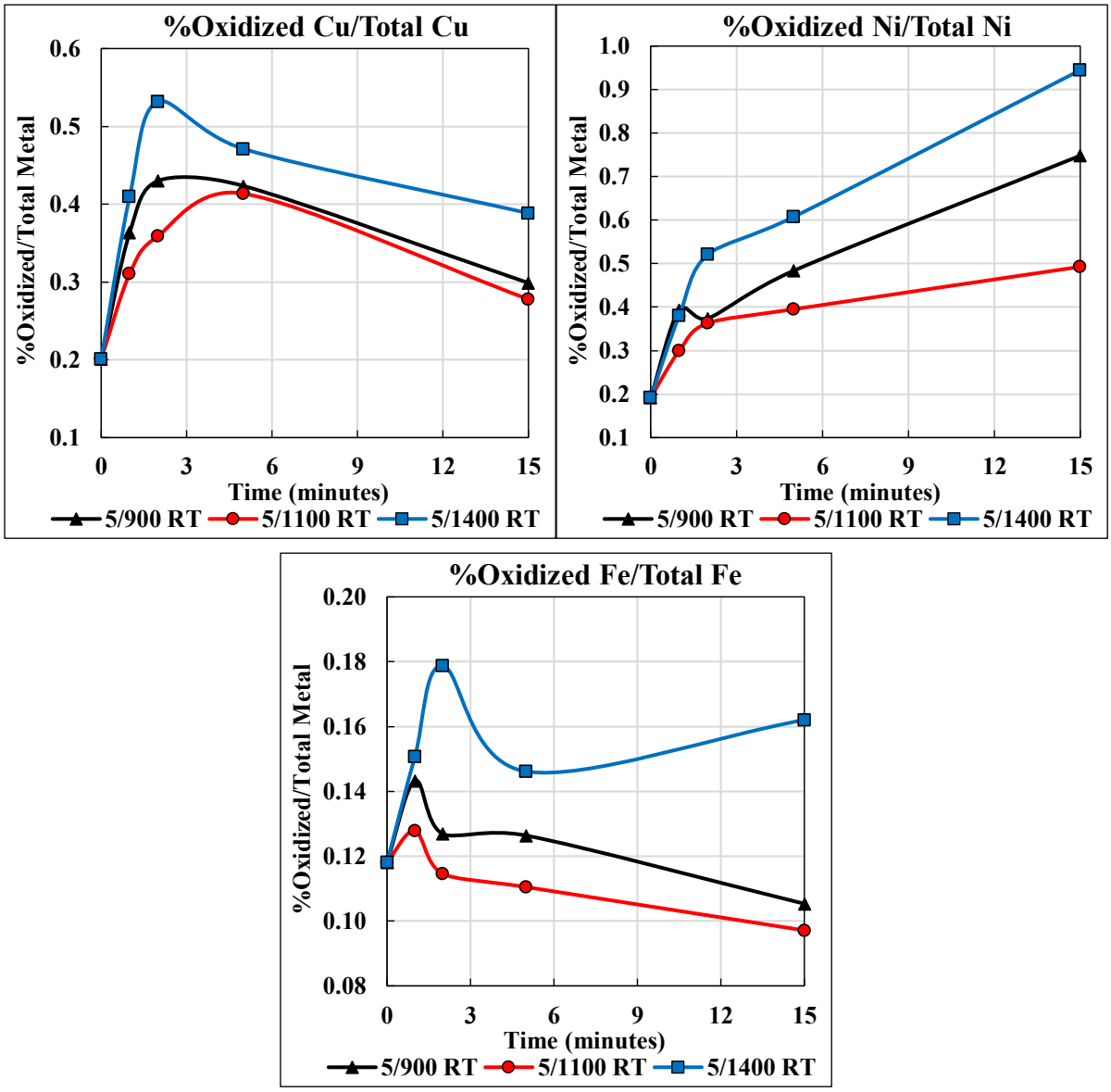

Figure 35: Copper Oxidation Levels (Top-Left), Nickel Oxidation Levels (Top-right) and Iron Oxidation Levels (Bottom-Left) for various flotation experiments. Oxidation levels were attained through EDTA extraction and AAS.

Based on the results from the EDTA extraction, increasing the impeller speed (and therefore the power input) appears to increase the degree of oxidation for copper, nickel and iron oxidation. Copper oxidation was the highest around 5 minutes at 900 RPM but as the impeller speed increased to 1,400 RPM, the maximum oxidation level shifted to 2 minutes. Nickel oxidation showed ascending oxidation levels as time progressed with the slopes increasing as

impeller speed increased. Iron oxidation showed similar trends with the degree of oxidation increasing as the impeller speed increases.

5.3 Effect of impeller speed during HIC with 10 g/ton xanthate dose

Previous work with high intensity conditioning shows a close relation between the effectiveness of HIC and the xanthate adsorption. Testing the effect of additional xanthate will help gauge the impact HIC can has on the sulfide ore.

Table 9: Modified Rate Constants (MRCs) for Rushton HIC (10 g/ton X) with various impeller speeds.

	Modified Rate Constant, Km		
Flotation Tests	Cp	Pn	Po
10/No HIC	27.7	29.2	18.7
10/900 RT	46.3	46.8	39.0
10/1100 RT	47.2	57.7	48.4
10/1400 RT	37.5	59.7	47.4

Chalcopyrite Recovery

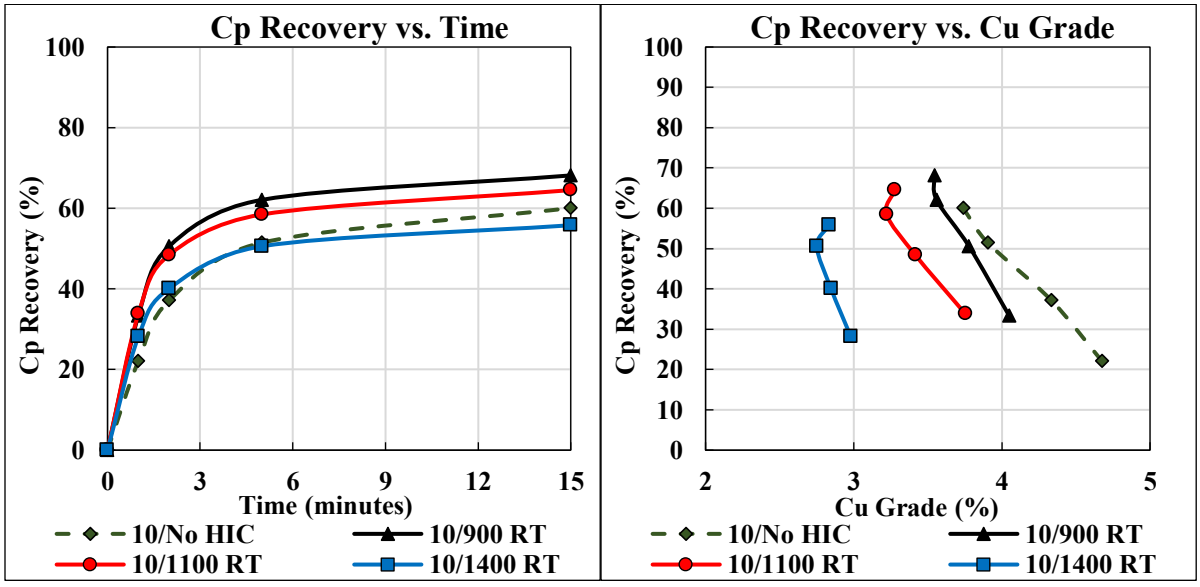

Figure 36: Chalcopyrite recovery over Time (left) and Chalcopyrite Recovery vs. Cu Grade (right) comparing No HIC and Rushton HIC tests (with various impeller speeds in RPM) at a 10 g/ton xanthate dosage.

Chalcopyrite recovery appears to show the best results at the lowest speeds used in HIC. As the speed of the impeller increases, the recovery decreases. The overall drop in recovery from 900rpm to 1,400 rpm is approx. 15%. Based on the MRCs from Table 9, the lower impeller speed correlated with a higher flotation constant for chalcopyrite.

Pentlandite Recovery

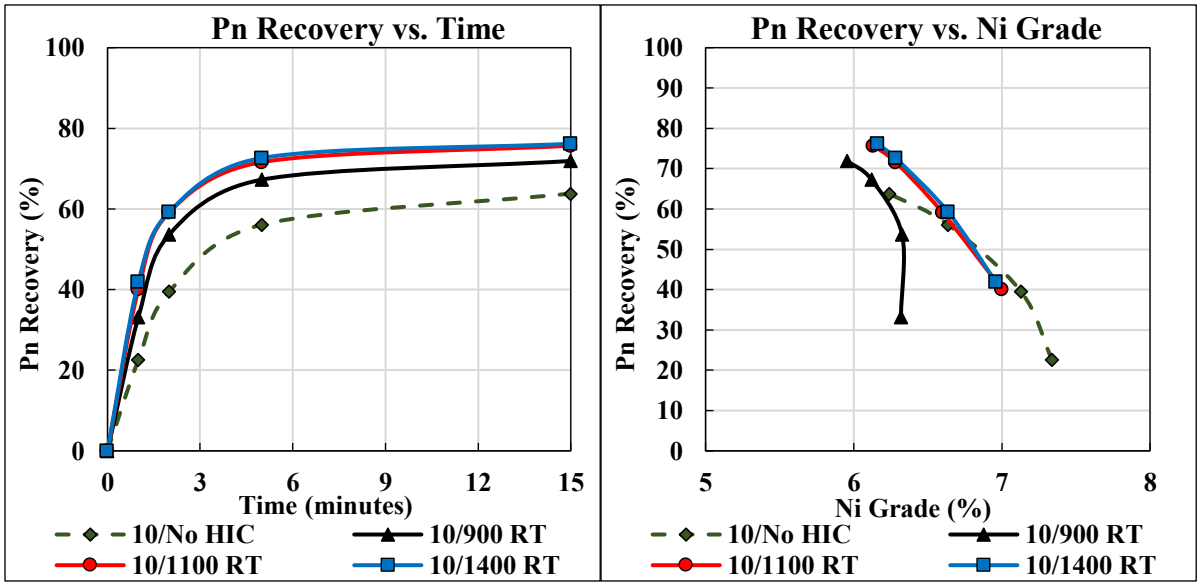

Figure 37: Pentlandite recovery (left) and Pentlandite Recovery vs. Ni Grade (right) comparing No HIC and Rushton HIC tests (with various impeller speeds in RPM) at a 10 g/ton xanthate dosage.

Like previous tests, the recovery of pentlandite shows the highest results with the highest impeller speeds. The lower speed of 900 rpm showed a slightly lower recovery although the results were close. The recovery of pentlandite at the highest speeds were nearly identical.

Pyrrhotite Recovery

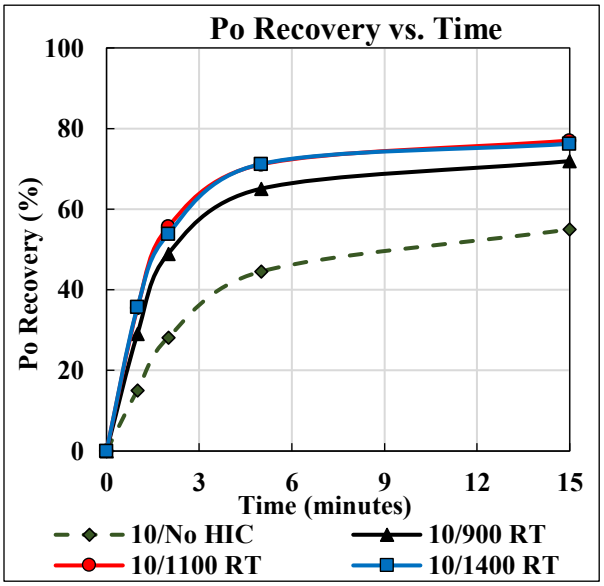

Figure 38: Pyrrhotite recovery comparing No HIC and Rushton HIC tests (with various impeller speeds in RPM) at a 10 g/ton xanthate dosage.

The recovery of pyrrhotite is quite like pentlandite with the highest impeller speeds showing the best recovery. Similarly, the lower speed had a slightly worse result. As with previous results, the recovery of pyrrhotite is related degree of copper oxidation found on the surface.

Sulfide Selectivity

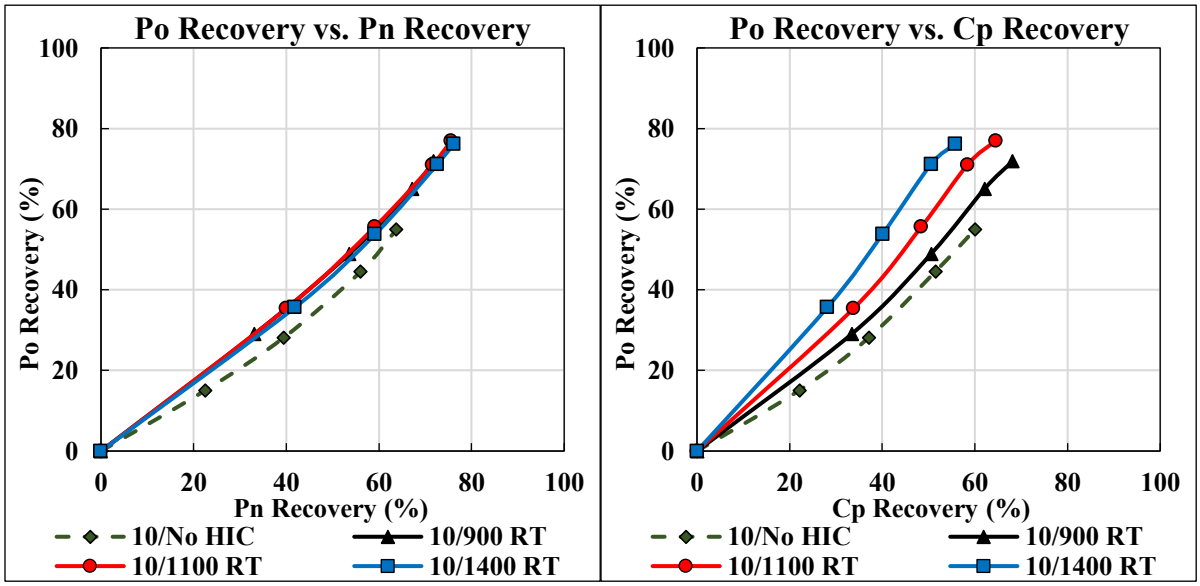

Figure 39: Pyrrhotite-pentlandite (left) and pyrrhotite-chalcopyrite (right) selectivity curves comparing No HIC and Rushton HIC tests (with various impeller speeds in RPM) at a 10 g/ton xanthate dosage.

The selectivities of chalcopyrite and pentlandite against pyrrhotite are very different. Chalcopyrite shows a drastic reliance on impeller speed. When using HIC, the selectivity of chalcopyrite shows improvement as the impeller speed decreases. While the recovery of pyrrhotite shows a decrease as the speed decreases, the improved recovery of chalcopyrite is the main reason for the improved selectivity with slower impeller speeds.

Regarding the selectivity of pentlandite and pyrrhotite, all the tests follow the same selectivity curve. The 900-rpm impeller speed reduced the recovery of both minerals but followed the selectivity curve trend regardless.

Copper, Nickel and Iron Oxidation on the Concentrate Surface

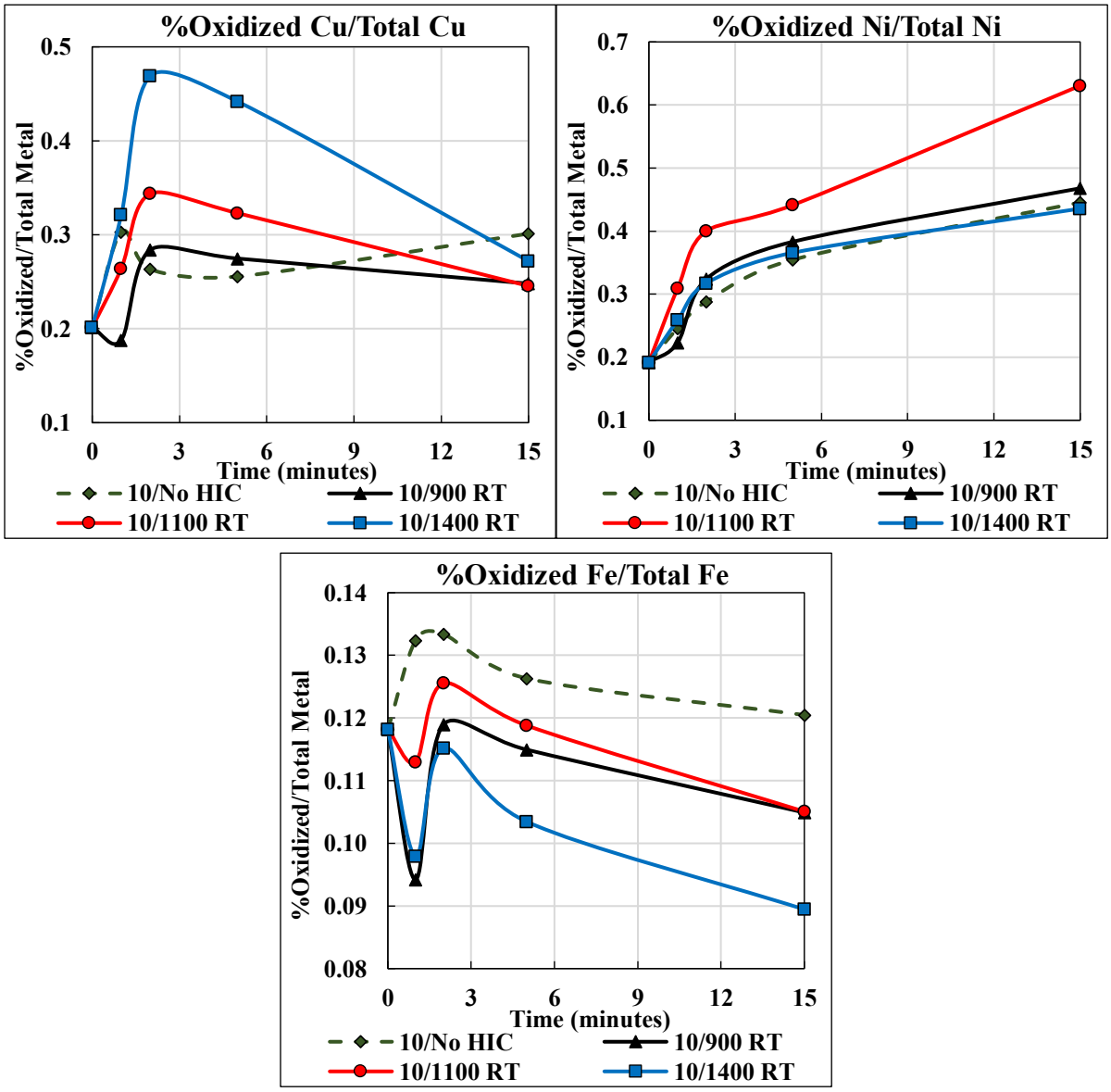

Figure 40: Copper Oxidation Levels (Top-Left), Nickel Oxidation Levels (Top-right) and Iron Oxidation Levels (Bottom-Left) for various flotation experiments. Oxidation levels were attained through EDTA extraction and AAS.

At the higher xanthate dosage, the oxidation of the various metal (see Figure 40) proceeds quite differently. This difference is likely due to the formation of more dixanthogen patches on the surface of the minerals, affecting which metal oxide preferentially formed first.

Copper oxidation showed a direct increase when the impeller speed was increased. The difference in copper oxidation level was quite dramatic, with 1,400 RPM having nearly 70%

more copper oxidation than with 900 RPM. As well, the three different speeds testing showed the maximum copper oxidation occurred at the 2-minute mark in the flotation and then steadily decreased after. The increase in copper oxidation on the surface seems to coincide with lower chalcopyrite recovery. The increase in xanthate dosage from 5 to 10 g/ton decreased the levels of copper oxidation consistently form all impeller speeds with the highest copper oxidation typically occurring at the 2-minute mark (Figure 41).

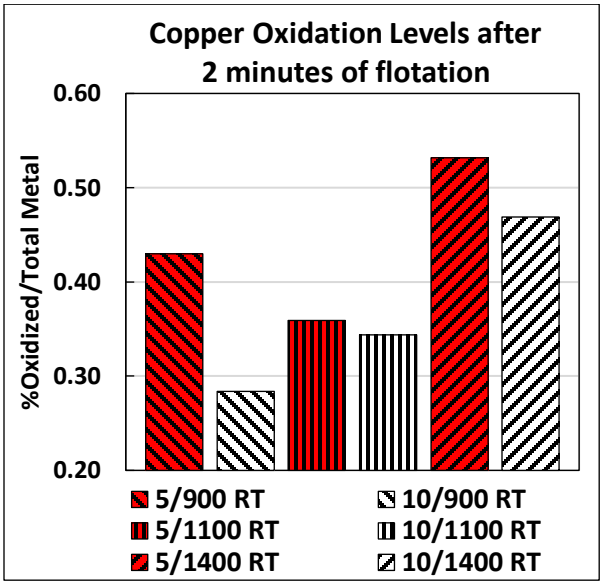

Figure 41: Copper Oxidation Levels for various Rushton HIC Tests after 2 minutes of Flotation.

Nickel oxidation shows increasing levels of oxidation that were seen in the other tests. The level of nickel oxidation was the highest with 1,100 RPM and the lowest levels were with 1,400 RPM.

Iron oxidation levels are initially reduced with the higher xanthate dosage of 10 g/ton (see Figure 40) suggested that the Rushton HIC was able to clean the surface of iron oxide (Figure 42). When comparing the 10/No HIC test, all Rushton HIC test had lower iron oxidation overall which likely contributed to the better sulfide seen in the Denver cell flotation. This reduction in iron oxidation did not occur in the 5 g/ton Rushton HIC tests (Figure 35) which reinforces that the effective cleaning of the surface is dependent upon xanthate dosage. The removal of iron oxide was likely followed by the formation of dixanthogen, resulting in the blocking of the site for further oxidation. The higher iron oxidation level at the 2-minute mark for all three speeds suggests this state quickly changes but is still clearly prevalent. Furthermore, reviewing iron

oxidation as a function of xanthate addition (see Figure 30) shows that this decrease in iron oxidation in the first minute of flotation is inversely related to xanthate dosage, but the rise in the level of iron oxidation at the 2-minute mark rises with xanthate addition.

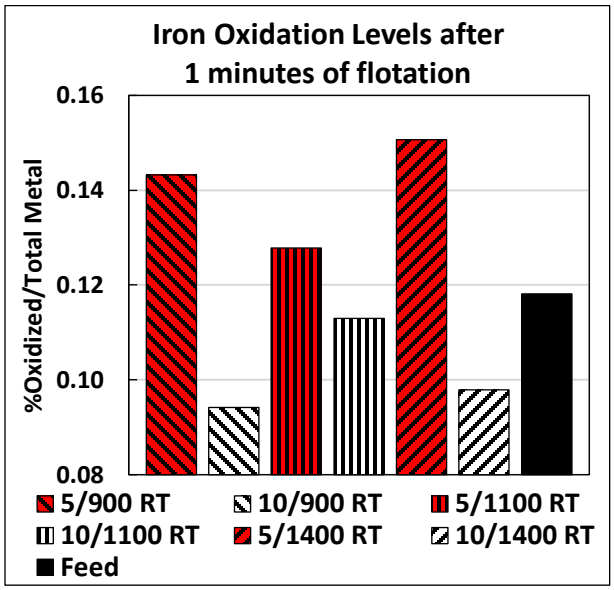

Figure 42: Iron Oxidation Levels for various Rushton HIC Tests after 1 minute of Flotation.

The final observation from this work is based on the trends that are not seen in the 10/1400 RT oxidation results that are prevalent in the 5 g/ton xanthate tests (Figure 35). Typically, the faster the impeller speed, the more oxidation of copper, nickel and iron was seen on the surfaces. However, this was not the case at higher xanthate dosages. When considering the results, the additional xanthate will form more dixanthogen patches on the mineral surfaces and lead to a more competitive environment between copper, nickel and iron oxidation. The reduction in iron oxidation with higher xanthate dosages supports this shift in surface availability. Based on the idea of reduced surface availability, the higher degree of copper oxidation still present and the markedly lower levels of nickel and iron oxidation, it is plausible to say that copper oxidation is more preferential than the other two and a larger proportion of the surface will be covered with a copper oxidation species than nickel or iron oxidation if a scarcity of surface area is present. As the recovery of pyrrhotite coincided with this phenomenon, copper activation can be assumed to be primarily responsible for the immediate flotation of pyrrhotite. Figure 43 shows the increase in pyrrhotite recovery as copper oxidation increases once there is competition for the surface of the minerals.

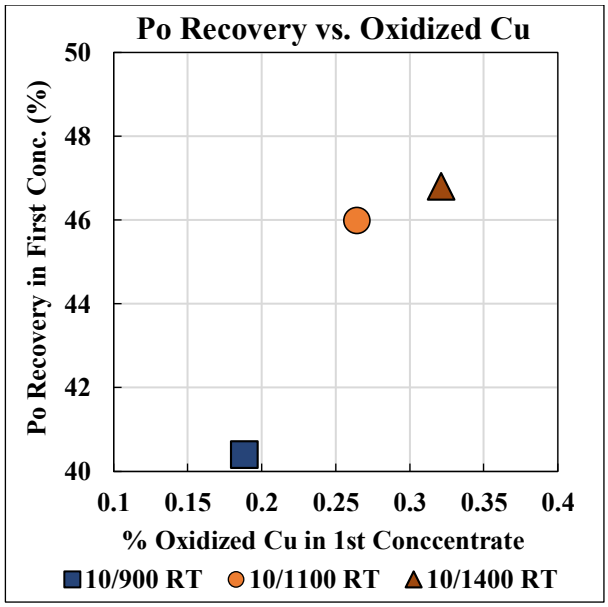

Figure 43: Pyrrhotite Recovery as a function of Oxidized Copper Levels in the First Concentrate.

However, as increased levels of nickel oxidation were not related to poorer sulfide recovery, there is still merit is suggesting nickel activation may play an important role in overall pyrrhotite recovery, specifically slow floating pyrrhotite.

While the results cannot provide a comprehensive picture, there are some generalizations that can be state based on the work:

- Increased levels of copper oxidation occur with decreased chalcopyrite recovery and higher impeller speeds/power input from the impeller. Higher levels of oxidized copper correlated with higher pyrrhotite and pentlandite recovery.
- Increased levels of nickel oxidation do not corelate to a lower recovery of all 3 sulfides.
- Decreased levels of initial iron oxidation (within 1 minute) correlate to higher recovery of all 3 sulfides.
- Increasing the xanthate dosage from 5 g/ton to 10 g/ton resulted in a reduction of the iron oxidation found on the immediately floatable mineral (collected within the first minute of flotation).
- Copper oxidation appears to be preferential to nickel and iron oxidation at 10 g/ton of xanthate where a competition for available surface area is present.

5.4 Effect of DETA/SMBS on the Recovery of Sulfide Mineral

The use of DETA/SMBS in this thesis was chosen due to the perceived negative impact of ion activation on pyrrhotite. As these reagents are renowned for their success in depressing pyrrhotite, their effects would allow for further understanding of Rushton HIC. The concentrations of DETA/SMBS were chosen based on the work by Ravi Multani where this dosage were effective in depressing both monoclinic and hexagonal pyrrhotite [6].

The DETA and SMBS is added at the beginning of the HIC stage before the minerals are added and not incrementally like xanthate. In the No HIC tests, DETA/SMBS is added before xanthate into the Denver cell during the conditioning stage.

Table 10: Modified Rate Constants (MRCs) for No HIC and Rushton HIC tests with DETA/SMBS (150/300 g/ton).

	Modified Rate Constant, Km		
Flotation Tests	Cp	Pn	Po
10/No HIC (D/S)	17.0	3.6	2.7
20/No HIC (D/S)	21.5	6.4	4.6
10/1100 RT (D/S)	44.0	18.8	11.5
20/1100 RT (D/S)	38.2	15.3	9.8

5.4.1 DETA/SMBS Tests Comparing HIC and No HIC Tests

Chalcopyrite Recovery for DETA/SMBS Tests

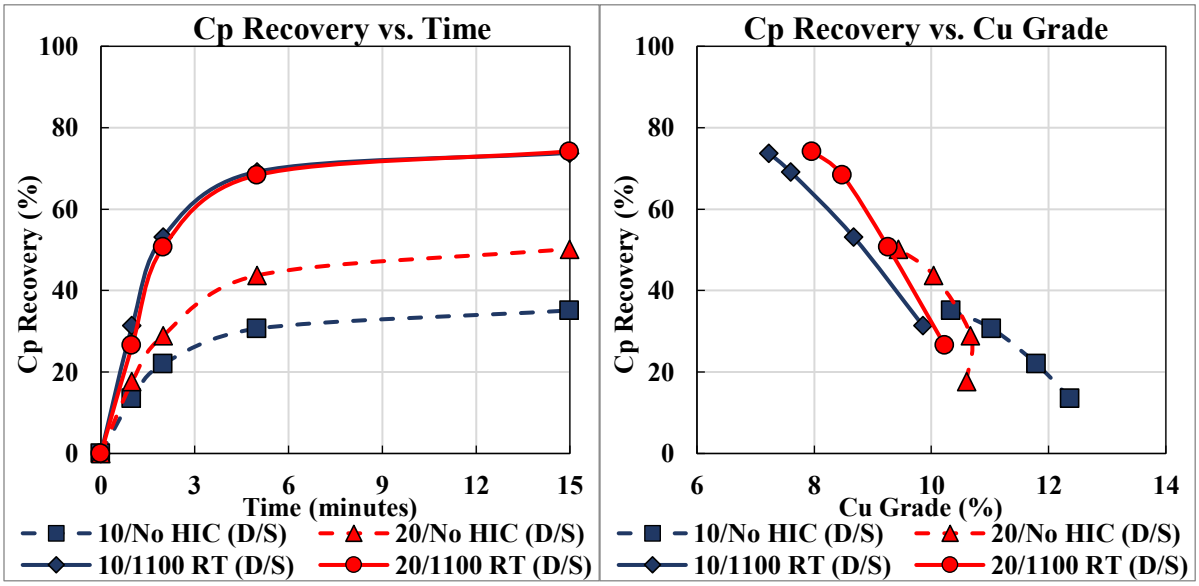

Figure 44: Chalcopyrite recovery over Time (left) and Chalcopyrite Recovery vs. Cu Grade (right) comparing No HIC and Rushton HIC tests using DETA/SMBS (150/300 g/ton respectively) at various xanthate dosages.

When DETA and SMBS are added as reagents, HIC shows better recovery over the conventional conditioning period, followed by froth flotation. Chalcopyrite recovery shows relatively similar values with Rushton HIC, with double the xanthate dosage not yielding any improvement.

Comparing the MRC values in Table 10 show that the lower recovery of chalcopyrite in the No HIC tests also correlated to a much lower rate constant with Rushton HIC showing a 2.5 times larger constant than the No HIC at 10 g/ton.

Pentlandite Recovery for DETA/SMBS Tests

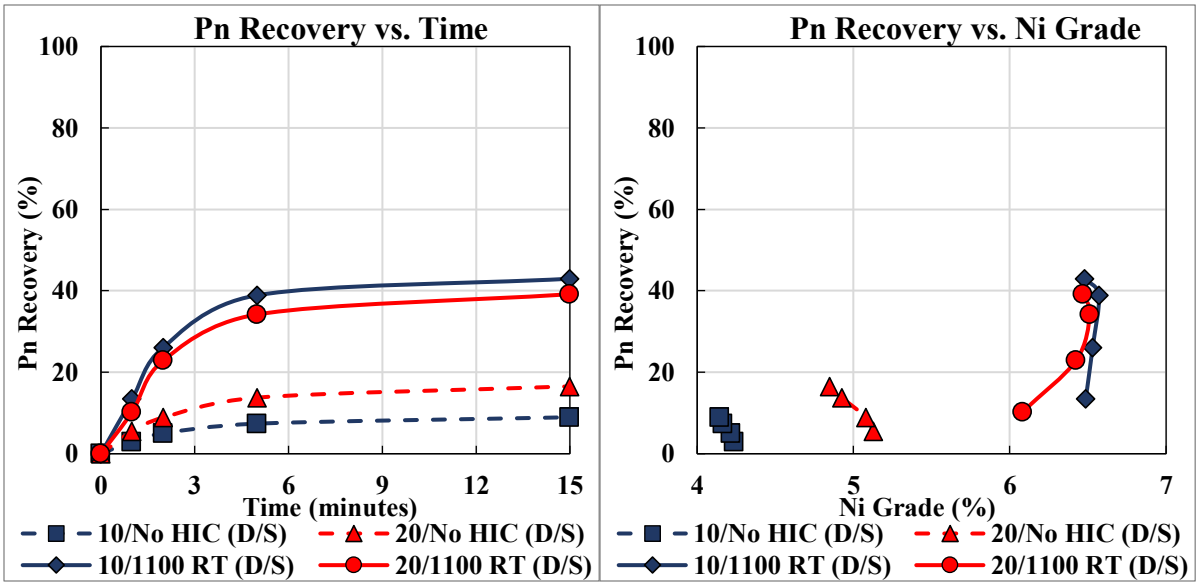

Figure 45: Pentlandite recovery (left) and Pentlandite Recovery vs. Ni Grade (right) comparing No HIC and Rushton HIC tests using DETA/SMBS (150/300 g/ton respectively) at various xanthate dosages.

The pentlandite recovery of the no HIC tests showed low pentlandite recovery even with higher xanthate dosages. When the HIC stage is added, the recovery doubles but is still quite low. When comparing the MRC values, the No HIC values are only a fraction of the Rushton HIC rate constants, with 10 g/ton having a 5.3 times higher value showed that pentlandite floated much slower in the No HIC tests when DETA/SMBS was used. At higher xanthate doses, this difference is diminished but pentlandite floats much slower in the No HIC tests overall.

Pyrrhotite Recovery for DETA/SMBS Tests

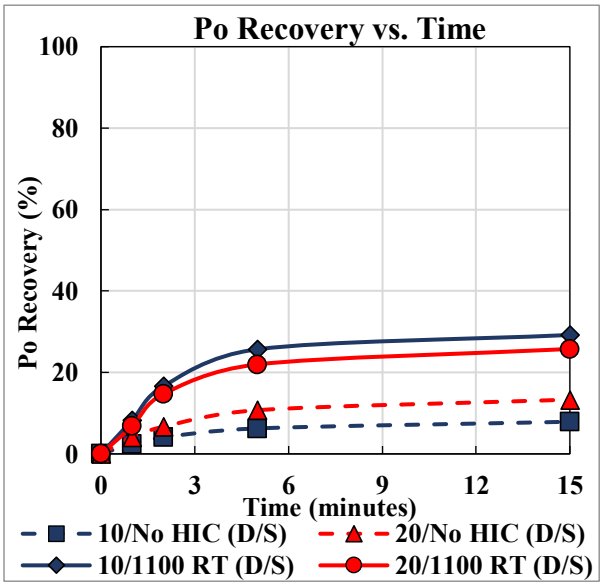

Figure 46: Pyrrhotite recovery comparing No HIC and Rushton HIC tests using DETA/SMBS (150/300 g/ton respectively) at various xanthate dosages.

Pyrrhotite recovery was greatly diminished with the use of DETA and SMBS. Like with chalcopyrite and pentlandite, the lowest recoveries of pyrrhotite were seen with the no HIC tests. However the recovery of pyrrhotite did not improve with HIC to the degree of the other two sulfide minerals. When comparing the MRC values, pyrrhotite rate constants with Rushton HIC were 4.2 and 2.1 times faster than the No HIC tests at 10 and 20 g/ton xanthate, respectively.

Sulfide Selectivity during the DETA/SMBS tests

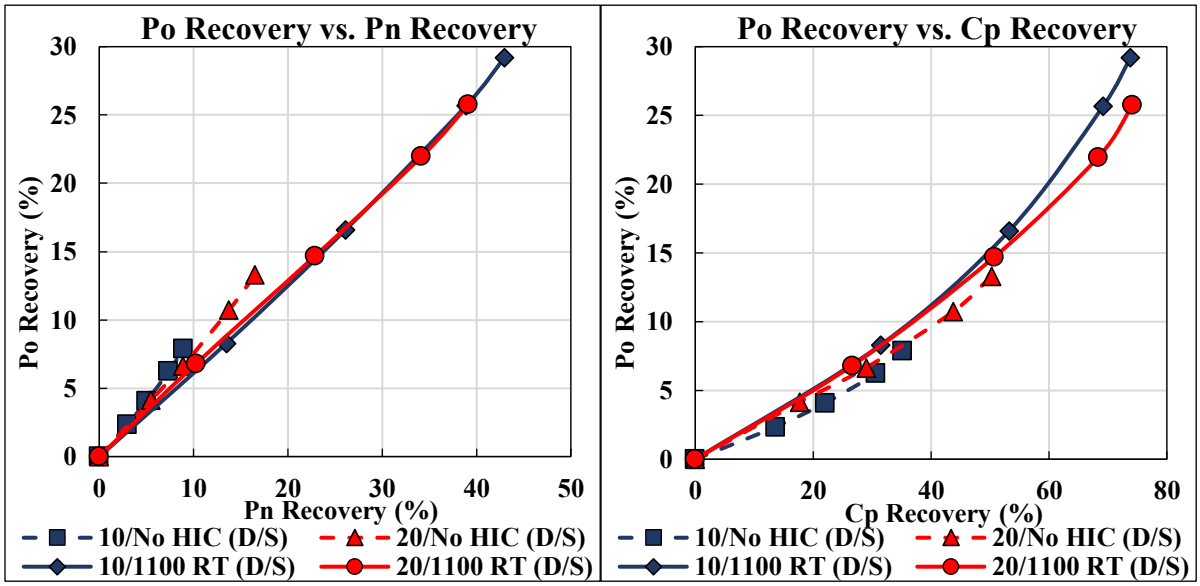

Figure 47: Pyrrhotite-pentlandite (left) and pyrrhotite-chalcopyrite (right) selectivity curves comparing No HIC and Rushton HIC tests using DETA/SMBS (150/300 g/ton respectively) at various xanthate dosages.

The selectivity curves for the DETA/SMBS experiments overall are quite similar. The HIC Po-Pn selectivities are slightly better than those of the no HIC tests, but the difference is nearly indistinguishable. The Po-Cp selectivities are identical for all tests, with the HIC tests simply following the curve further due to higher recoveries seen with HIC.

Copper, Nickel and Iron Oxidation on the Concentrate Surface for DETA/SMBS Tests

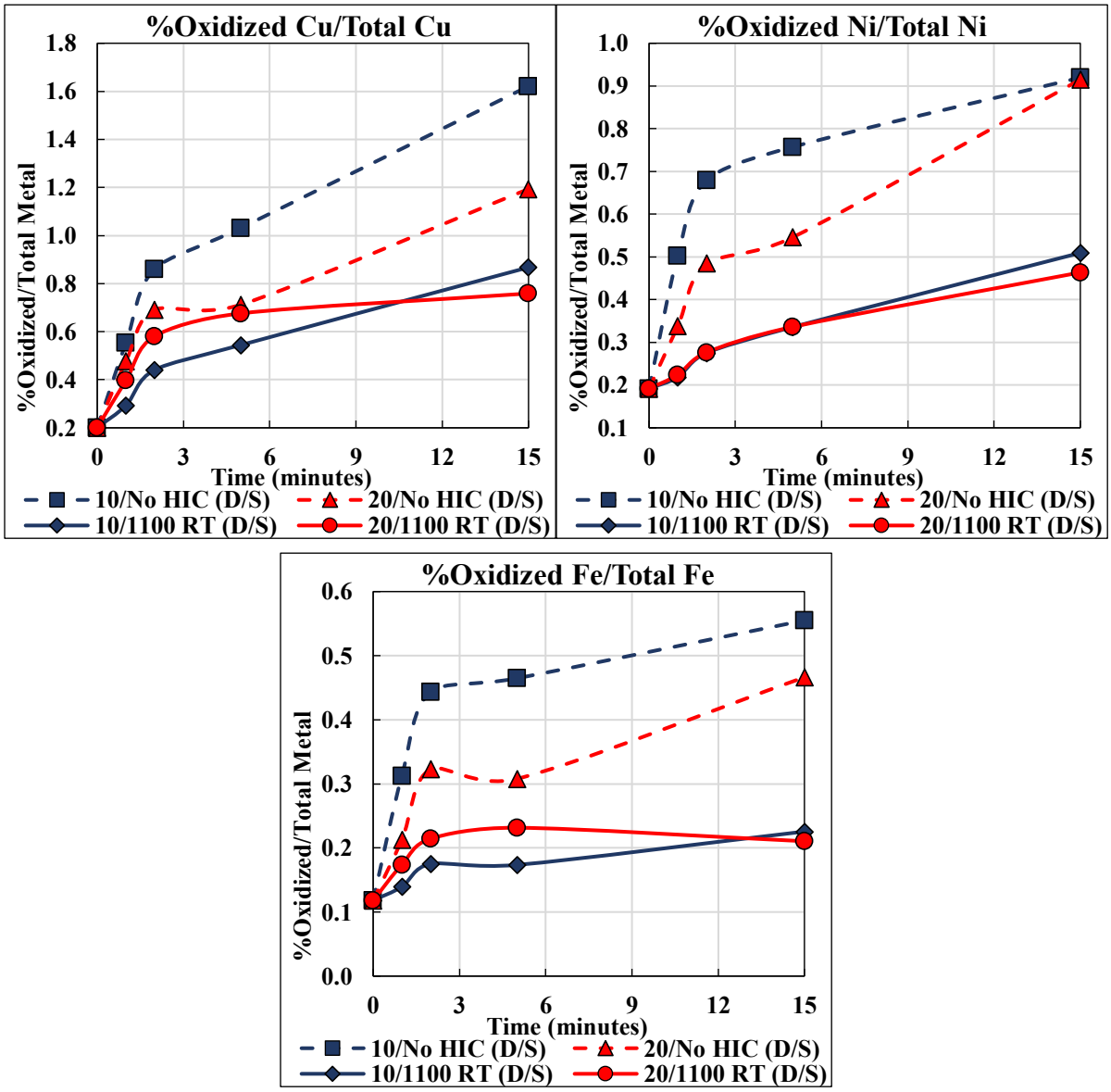

Figure 48: Copper Oxidation Levels (Top-Left), Nickel Oxidation Levels (Top-right) and Iron Oxidation Levels (Bottom-Left) for RT HIC and No HIC tests with and without DETA/SMBS Addition. Oxidation levels were attained through EDTA extraction and AAS.

The levels of oxidized metals on the surface of the concentrates were drastically higher on the No HIC tests than the Rushton HIC tests, suggesting that the addition of DETA/SMBS resulted in greater oxidation of the surface.

The change in copper oxidation trends was interesting, as all previous Rushton HIC tests show that copper oxidation diminished after the second or third concentrate while nickel oxidation steadily increased. With the addition of DETA/SMBS, copper oxidation slowly increases over time. This trend is seen with nickel oxidation as well.

The much higher degree of oxidized metals on the No HIC tests are likely the reason for the greatly reduced recovery of the minerals. While copper oxidation can be related to metal sites for activation on pyrrhotite, iron oxidation is clearly detrimental to flotation. While previous iron oxidation typically decreases overall in other tests (Figure 30, Figure 35 and Figure 40), the increasing amount of iron oxides over the flotation show that DETA/SMBS changes this trend and greatly increases iron oxidation.

The lower recovery of the Rushton HIC at 20 g/ton xanthate, when compared to the 10 g/ton xanthate dosage, is likely linked to the higher degree of initial iron oxidation. This could have occurred due to experimental error (possibly more time was needed to bleed air from HIC cell). However, as standard Rushton HIC at 20 g/ton xanthate had higher iron oxidation when compared to 10 g/ton xanthate (see Figure 58), the addition of DETA/SMBS could have increased the impact of this difference in iron oxidation, resulting in poor recovery at the higher xanthate dosage.

Copper, Nickel and Iron Oxidation on the Concentrate Surface for 10 g/ton Xanthate dosage tests comparing RT HIC or No HIC with/without DETA/SMBS

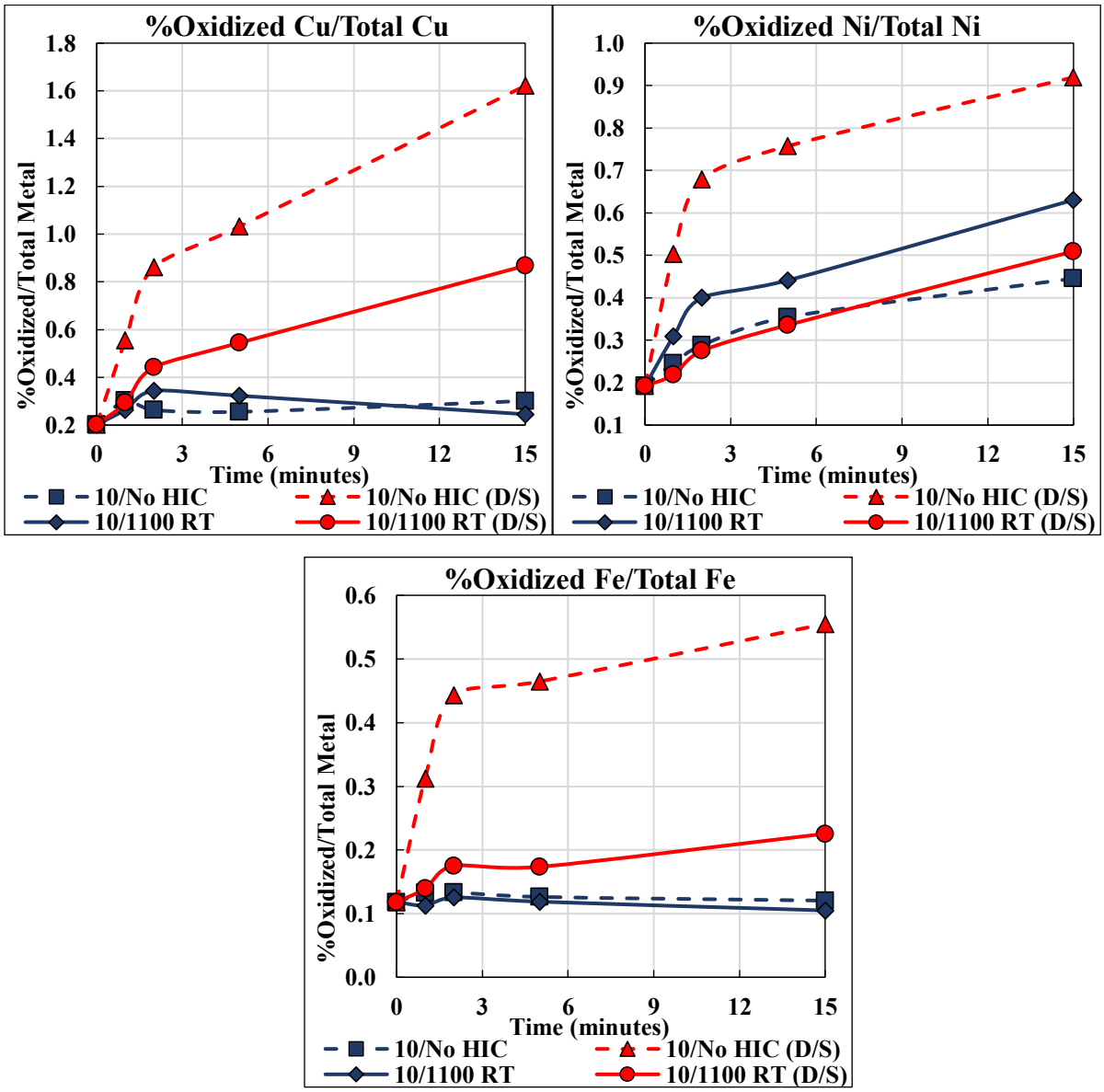

Figure 49: Copper Oxidation Levels (Top-Left), Nickel Oxidation Levels (Top-right) and Iron Oxidation Levels (Bottom-Left) for No HIC tests with and without DETA/SMBS Addition. Oxidation levels were attained through EDTA extraction and AAS.

The comparison of the oxidized metals at the same xanthate concentration truly shows the difference when DETA/SMBS is introduced. When comparing the copper, nickel and iron

oxidation, the degree of oxidation for the No HIC test with DETA/SMBS was 3-4 times higher than the other tests. Nickel oxidation shows relatively similar slopes for all tests after 5 minutes. The largest increase is in the first 3 minutes, where the initial oxidation changes drastically between tests. At the first few minutes also account for most of the concentrate recovery, the relation between oxidation and recovery is obvious. Aside from the nickel oxidation, Rushton HIC with DETA/SMBS addition shows higher oxidation. The degree of oxidation in the first three minutes is still considerably higher than tests without using DETA/SMBS, but the fact that copper and iron oxidation switches from a decreasing trend without DETA/SMBS (Figure 49) to a sharply increasing trend shows that DETA/SMBS increases the oxidation rate dramatically.

Table 11: Modified Rate Constants (MRCs) for No HIC and Rushton HIC tests with/without DETA/SMBS (150/300 g/ton) and 10 g/ton of xanthate.

	Modified Rate Constant, Km		
Flotation Tests	Cp	Pn	Po
10/No HIC	27.7	29.2	18.7
10/No HIC (D/S)	17.0	3.6	2.7
10/1100	47.2	57.7	48.4
10/1100 (D/S)	44.0	18.8	11.5

5.4.2 No HIC Tests with and without DETA/SMBS Addition

Table 12: Modified Rate Constants (MRCs) for No HIC tests with/without DETA/SMBS (150/300 g/ton)

	Modified Rate Constant, Km		
Flotation Tests	Cp	Pn	Po
10/No HIC	27.7	29.2	18.7
20/No HIC	58.3	58.3	35.7
10/No HIC (D/S)	17.0	3.6	2.7
20/No HIC (D/S)	21.5	6.4	4.6

Chalcopyrite Recovery for No HIC Tests with and without DETA/SMBS Addition

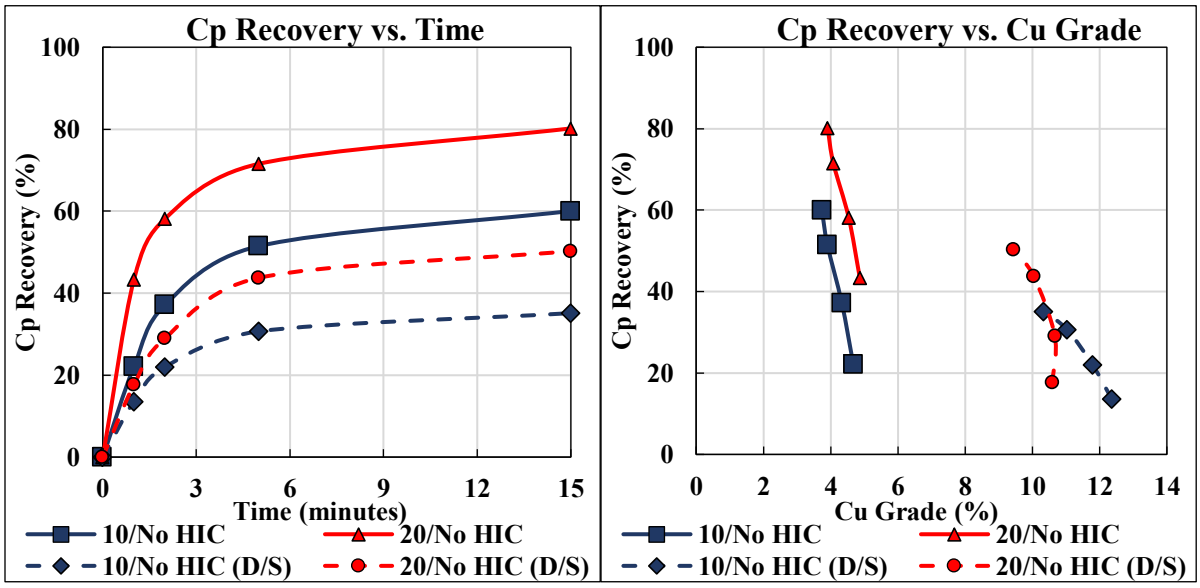

Figure 50: Chalcopyrite recovery over Time (left) and Chalcopyrite Recovery vs. Cu Grade (right) comparing No HIC tests with and without DETA/SMBS (150/300 g/ton respectively) at various xanthate dosages.

The recovery of chalcopyrite with DETA/SMBS was greatly reduced, with recovery with 20 g/ton of xanthate and DETA/SMBS being less than 10 g/ton of xanthate without DETA/SMBS. The grades were much higher with DETA/SMBS, but this is due to the depression of everything else in the slurry.

Pentlandite Recovery for No HIC Tests with and without DETA/SMBS Addition

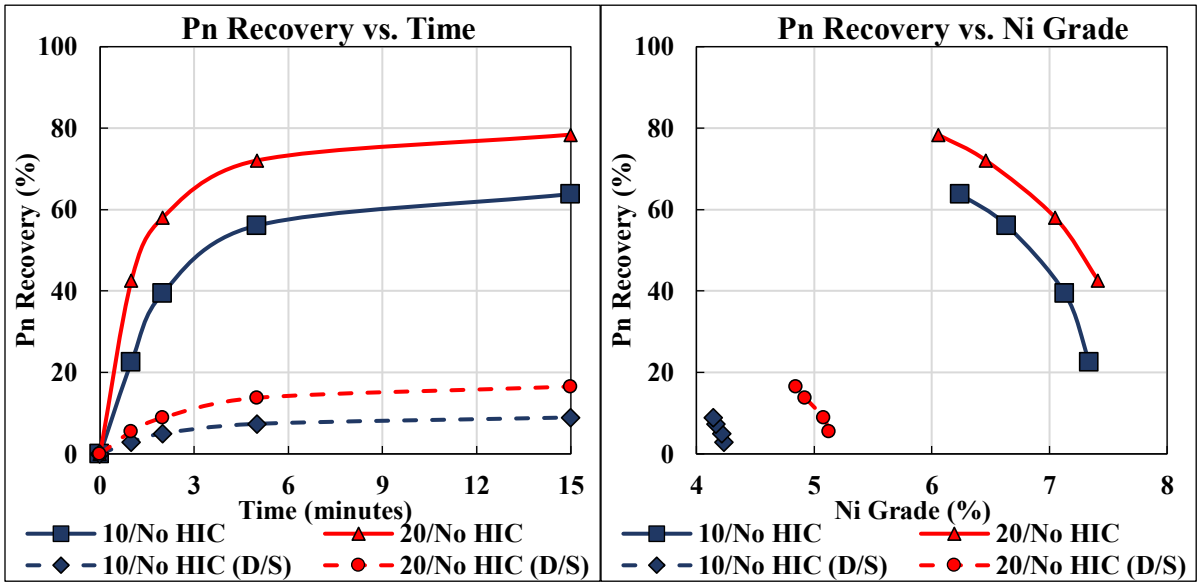

Figure 51: Pentlandite recovery (left) and Pentlandite Recovery vs. Ni Grade (right) comparing No HIC tests with and without DETA/SMBS (150/300 g/ton respectively) at various xanthate dosages.

Pentlandite recovery was completely halted using DETA/SMBS. The MRCs for pentlandite were nearly reduced to 10% of their original values without DETA/SMBS.

Pyrrhotite Recovery for No HIC Tests with and without DETA/SMBS Addition

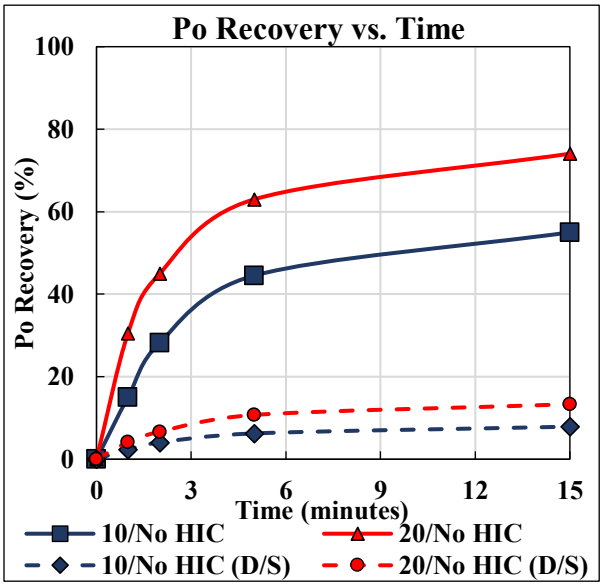

Figure 52: Pyrrhotite recovery comparing No HIC tests with and without DETA/SMBS (150/300 g/ton respectively) at various xanthate dosages.

Like pentlandite, pyrrhotite saw complete depression with DETA/SMBS. The addition of additional xanthate did not improve recovery.

Sulfide Selectivity for No HIC Tests with and without DETA/SMBS Addition

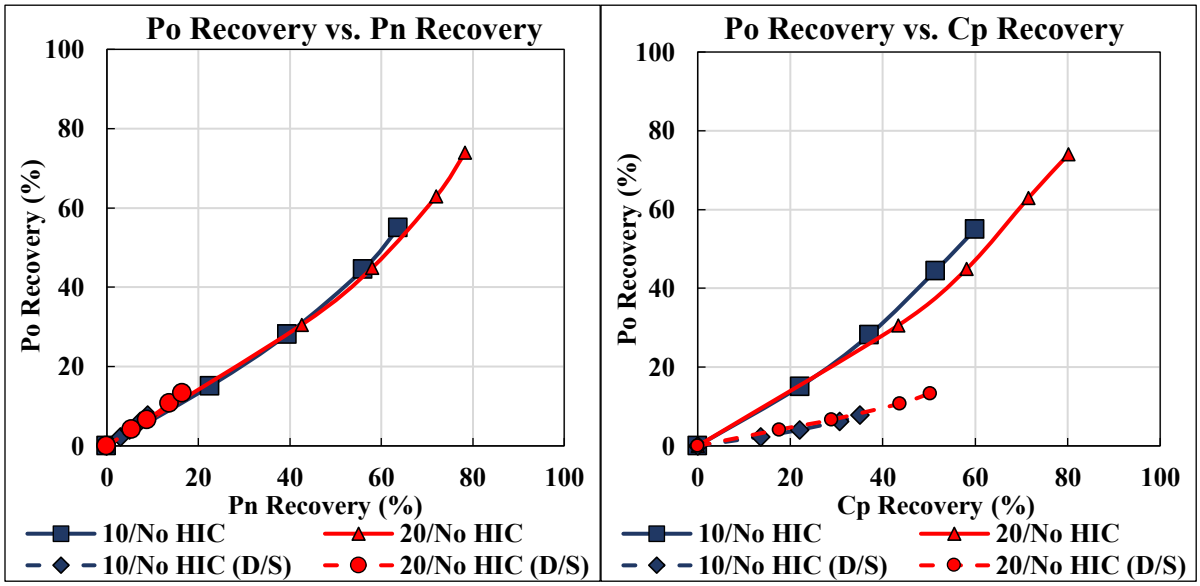

Figure 53: Pyrrhotite-pentlandite (left) and pyrrhotite-chalcopyrite (right) selectivity curves comparing No HIC tests with and without DETA/SMBS (150/300 g/ton respectively) at various xanthate dosages.

The use of DETA/SMBS improved the selectivity between Cp and Po quite well. However, the Pn-Po selectivity curve largely remained unchanged.

5.4.3 Rushton HIC with and without DETA/SMBS Addition

Table 13: Modified Rate Constants (MRCs) for Rushton HIC tests with/without DETA/SMBS (150/300 g/ton)

	Modified Rate Constant, Km		
Flotation Tests	Cp	Pn	Po
10/1100 RT	47.2	57.7	48.4
20/1100 RT	65.4	70.0	50.4
10/1100 RT (D/S)	44.0	18.8	11.5
20/1100 RT (D/S)	38.2	15.3	9.8

Chalcopyrite Recovery for HIC with and without DETA/SMBS Addition

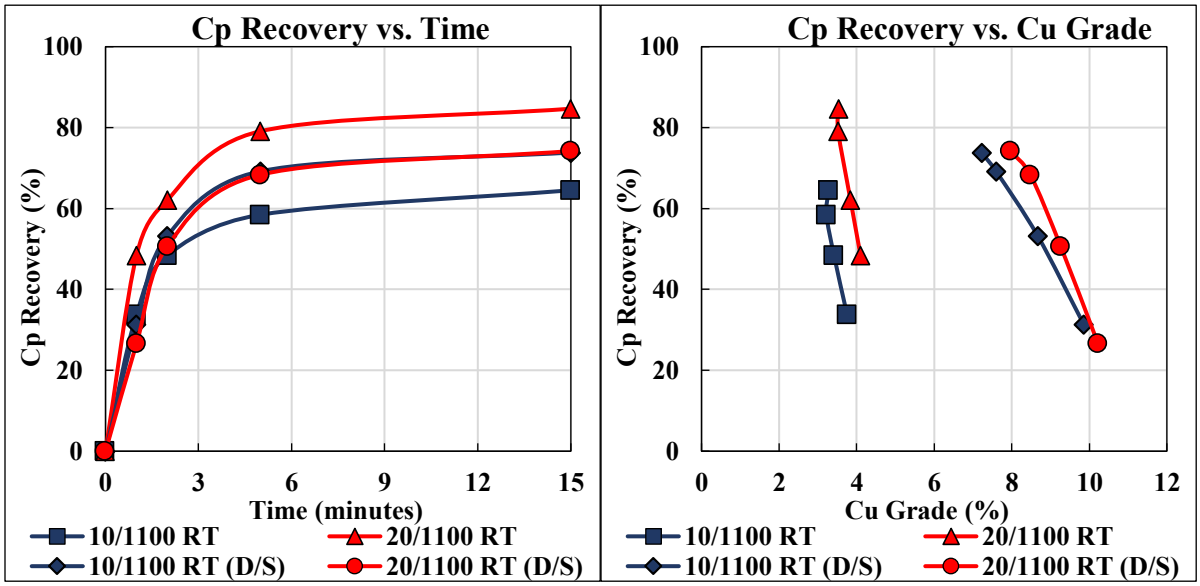

Figure 54: Chalcopyrite recovery over Time (left) and Chalcopyrite Recovery vs. Cu Grade (right) comparing Rushton HIC tests with and without DETA/SMBS (150/300 g/ton respectively) at various xanthate dosages.

The recovery of chalcopyrite with DETA/SMBS was relatively similar, regardless of xanthate addition. The MRC for Cp showed that DETA/SMBS slowed the flotation of chalcopyrite down in general, but the recovery was still quite high. Due to the low recovery of the other minerals, the grade with DETA/SMBS was considerably higher than Rushton HIC without DETA/SMBS.

Pentlandite Recovery for HIC with and without DETA/SMBS Addition

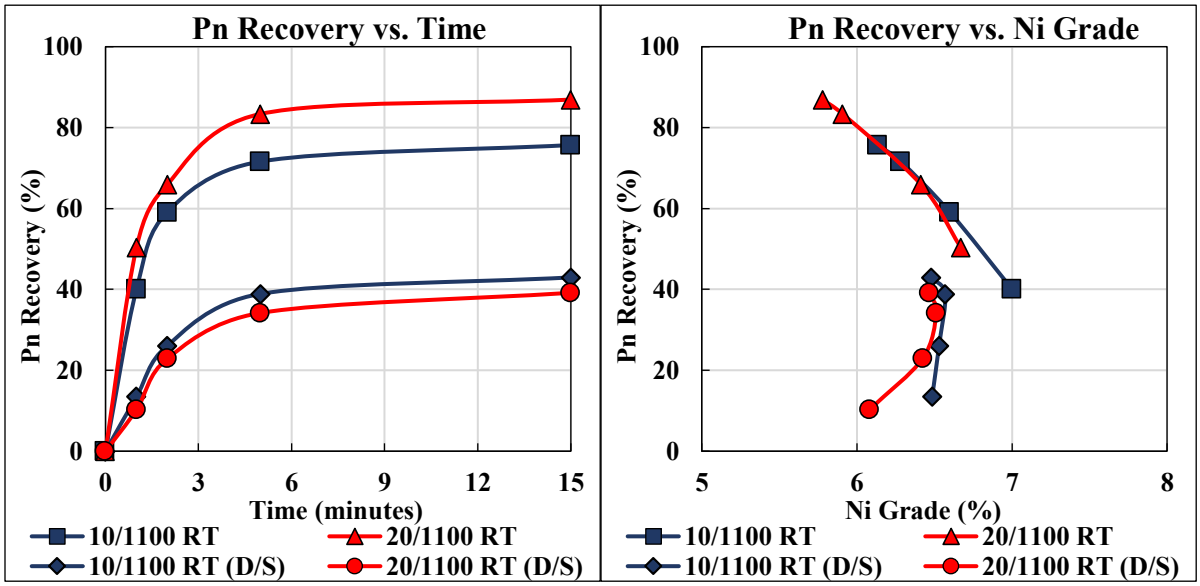

Figure 55: Pentlandite recovery (left) and Pentlandite Recovery vs. Ni Grade (right) comparing Rushton HIC tests with and without DETA/SMBS (150/300 g/ton respectively) at various xanthate dosages.

In general, the recovery of pentlandite was far better without the use of DETA/SMBS during Rushton HIC. The MRCs with DETA/SMBS drop to 30% of the values for Rushton HIC without DETA/SMBS.

Pyrrhotite Recovery for HIC with and without DETA/SMBS Addition

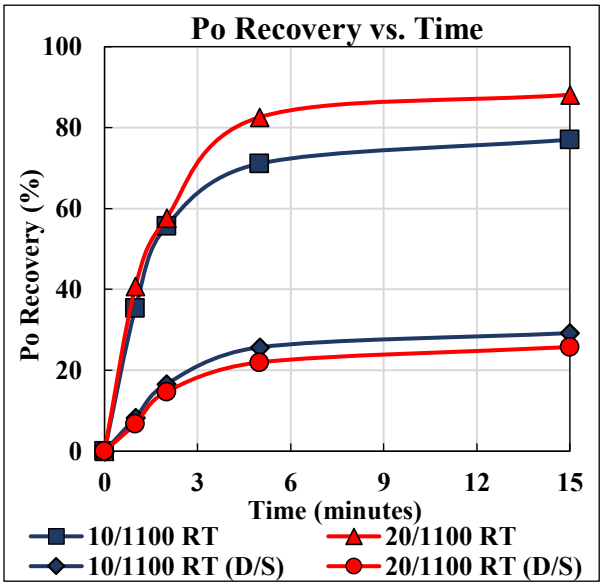

Figure 56: Pyrrhotite recovery comparing Rushton HIC tests with and without DETA/SMBS (150/300 g/ton respectively) at various xanthate dosages.

The recovery of pyrrhotite, like pentlandite, was drastically reduced with the use of DETA/SMBS. However, the pyrrhotite MRCs showed a greater degree of depression with values dropping to 20% of the Rushton HIC without DETA/SMBS.

Sulfide Selectivity during HIC with and without DETA/SMBS Addition

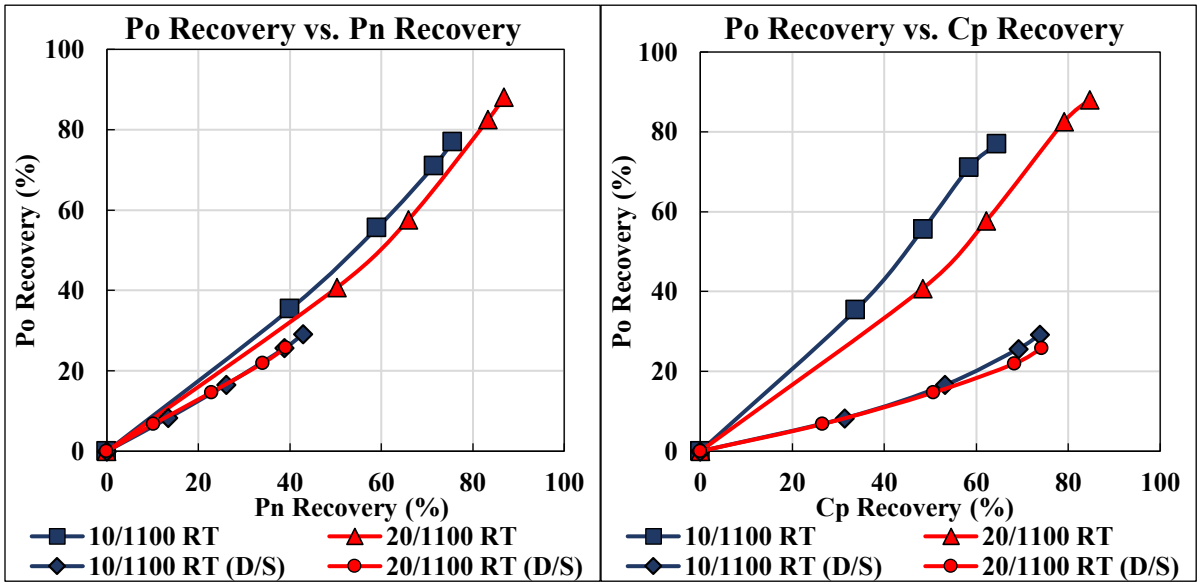

Figure 57: Pyrrhotite-pentlandite (left) and pyrrhotite-chalcopyrite (right) selectivity curves comparing various Rushton HIC tests and the use of DETA/SMBS (150/300 g/ton respectively) at various xanthate dosages.

The selectivity of both Po-Cp and Po-Pn curves are improved with the addition of DETA/SMBS. While chalcopyrite was largely resistant to the use of DETA/SMBS, pentlandite shows a dramatic reduction in recovery. The improved selectivity between pentlandite and pyrrhotite occurred largely due to pentlandite being depressed to a lesser degree than pyrrhotite when using DETA/SMBS.

Copper, Nickel and Iron Oxidation on the Concentrate Surface for HIC with and without DETA/SMBS Addition

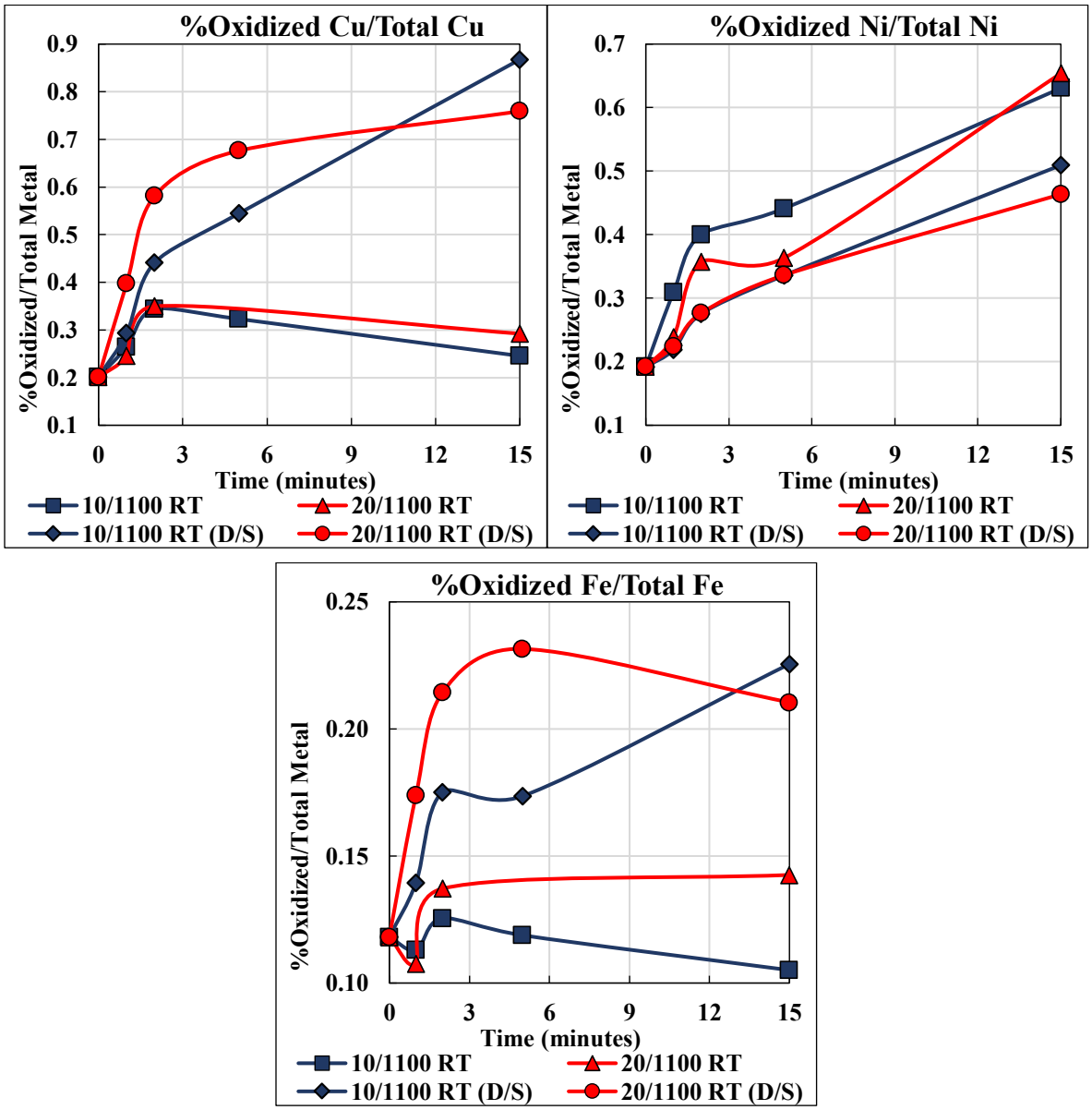

Figure 58: Copper Oxidation Levels (Top-Left), Nickel Oxidation Levels (Top-right) and Iron Oxidation Levels (Bottom-Left) for RT HIC with and without DETA/SMBS Addition. Oxidation levels were attained through EDTA extraction and AAS.

The copper and iron oxidation trends were quite similar, with iron oxidation showing generally higher levels. At higher xanthate additions, iron oxidation showed a general increase

over the course of the flotation. Copper showed similar trends, but the results between 10 and 20 g/ton xanthate dosage were much closer. With the addition of DETA/SMBS, the copper and iron oxidation greatly increased in both xanthate additions. However, this increased oxidation was much greater at 20 g/ton and likely contributed to the poor recovery of pentlandite.

Solution analysis was performed on the filtered liquid component of the slurry after HIC was performed, for both tests with and without DETA/SMBS. The samples were analyzed with ICP-MS. Testing the solution following the completion of the HIC stage, the nickel content and copper content were approx. 5-6 times higher when DETA/SMBS was used. The higher nickel/copper content in the DETA/SMBS tests makes sense due to the chelation of the ions with DETA.

Chapter 6 Discussion

The effect of high intensity conditioning on sulfides has not been well studied. The most exhaustive study was performed by Dr. Chen and his work was only on pentlandite. A real mixed sulfide ore system has not been investigated prior to this. Furthermore, the use of HIC on a mid-process concentrate hasn't been published or made publicly available. The presence of dixanthogen and oxidation species on the surface of the minerals complicates the study as typical tests rely on pristine samples before testing. As the goal of this work is to determine if HIC can be used to increase the recovery of pentlandite before it goes to the pyrrhotite regrind, creating more fines, improvement of the recovery of pentlandite is crucial. The recovery of pyrrhotite is detrimental to the optimization of the HIC process and so steps to understanding the means by which it becomes floatable is required.

6.1 Hydrofoil HIC

The initial studies in HIC were performed with a hydrofoil impeller (HF HIC). Traditionally, a Rushton impeller is used but there were a number of benefits that could impact its implementation into a plant flowsheet. These benefits were a lower power number for the hydrofoil impeller (energy savings during operation) and the axial flow pattern, which would assist to tank bottom cleaning.

The flotation tests using HF HIC showed a consistently negative impact on the hydrophobicity for all sulfide minerals. Increasing xanthate addition did improve the recovery of the minerals, but both pentlandite and pyrrhotite recoveries were worse than the No HIC tests. Chalcopyrite was the only mineral that showed slight improvements, upon the addition of xanthate, over the No HIC tests, although the increases were only 3% for both 10 and 20 g/ton of PIBX. The modified rate constants showed that the HF HIC tests had much slower flotation rates when compared to the No HIC tests for all sulfide minerals.

Adjusting the xanthate addition rate during HIC from 5% per minute to 20% per minute showed drastically poorer results, which further supported the theory that HF HIC had a negative effect on the hydrophobicity of the sulfide minerals over time.

Since all previous work in high intensity conditioning utilized high shear radial impellers, the failure of the low shear axial impeller, like the hydrofoil, supported the need of a high shear force within the slurry for HIC to function.

Additionally, the tank was changed to eliminate the formation of a vortex during HIC. While previous literature suggested vortexes were detrimental to optimal results with HIC, the explanation for this was never elaborated on and this requirement has been more of a standard that no study truly explained. Since a vortex would entrain gas, the power input into the slurry would likely decrease drastically. This would cause less particle-particle interactions that are essential for shear flocculation and more specifically pentlandite fine aggregation. Regarding sulfides, a vortex would also oxygenate the slurry and likely cause excessive oxidation of the surfaces.

The use of a Rushton turbine resulted in an immediate increase in power input with the slurry of 19 times when compared to the hydrofoil impeller. This is due to the different designs of each impeller and leads to the Rushton requiring 19 times the energy consumption when comparing a hydrofoil impeller of the same diameter. This increased power input is essential for HIC to function.

6.2 Rushton HIC

The use of HIC with a Rushton impeller (RT HIC) showed an immediate improvement in the flotation of all sulfide minerals over the No HIC tests, both in recovery and in the modified flotation rate constant. Both the impeller speed and xanthate addition had a drastic impact on the flotation tests. Each sulfide will be briefly discussed separately due to their unique responses.

6.2.1 Chalcopyrite

Chalcopyrite showed a preference for 900 RPM with RT HIC. This is likely why chalcopyrite floated reasonably well with HF HIC, due to the impeller's lower power number and therefor lower power input. When comparing RT HIC to No HIC tests, identical xanthate dosages resulted in RT HIC always recovering an additional 4.5% more chalcopyrite. Furthermore, the modified rate constant for chalcopyrite with RT HIC was twice that of the No HIC tests when xanthate was used. During RT HIC, an impeller speed of 1,400 RPM was detrimental for chalcopyrite recovery. At 10 g/ton of xanthate, chalcopyrite recovery with RT HIC at 1,400 RPM was lower than the No HIC tests. The use of HIC can improve the recovery of chalcopyrite, but an optimal response is only seen with lower power input when compared to pentlandite and pyrrhotite.

6.2.2 Pentlandite

The use of RT HIC was very effective at improving the flotation of pentlandite over the No HIC tests. The improvement was impressive enough that it took the No HIC tests double the xanthate addition to reach a similar recovery of pentlandite with RT HIC. An additional 9% more pentlandite was floated with RT HIC than the No HIC test at 20 g/ton of xanthate. Pentlandite showed a preference for higher impeller speeds. Impeller speeds of 1,100 and 1,400 RPM resulted in nearly identical recoveries at both 5 and 10 g/ton of xanthate. Due to the similar response, an optimal speed cannot be determined. Based on the modified rate constants, the pentlandite floated with RT HIC floated much faster than the No HIC tests.

6.2.3 Pyrrhotite

Pyrrhotite recovery was drastically improved with RT HIC. Using only 5 g/ton of xanthate during RT HIC, the pyrrhotite recovery was similar to the No HIC tests with 20 g/ton. With higher xanthate dosages, pyrrhotite recovery increases slightly. Like pentlandite, the best responses were seen at higher impeller speeds. Both 1,100 and 1,400 rpm were nearly indistinguishable regarding the recovery of pyrrhotite. The lowest impeller speed tested, 900 RPM, showed the lowest recovery of pyrrhotite observed with RT HIC. Copper activation is likely the reason for the enhanced flotation of the pyrrhotite recovery. This is discussed in the next section.

6.3 Metal Oxidation Levels of RT HIC Tests

The oxidation found on the sulfide surfaces of the Rushton HIC tests was removed via EDTA extraction and analyzed with AAS or ICP-MS. In general, increasing xanthate addition decreased all copper, nickel and iron oxidation levels in the immediately floatable minerals (within the first minute) and increased the recovery of all three sulfides. Each metal oxidation had a different, consistent trend during all flotations. Copper oxidation was always the highest in first few minutes and then rapidly decreased at the flotation progressed. Nickel oxidation always increased over time and generally had levels double or triple the initial oxidized nickel levels measured. Iron oxidation typically decreased over time. If sufficient levels of xanthate were used (10 g/ton PIBX) to promote surface competition, then the concentrate collected within the first minute had lower iron oxidation levels than the original feed sample, suggesting surface cleaning

has occurred. However, the iron oxidation levels increased considerably in the concentrate collected in the 1 to 2-minute duration. When comparing to the No HIC test of similar xanthate levels, RT HIC had overall more copper and nickel oxidation, but less iron oxidation. Each metal oxidation will be briefly discussed for their individual trends before the interrelated behavior is discussed. The effects of metal oxidation on pyrrhotite will be also described in this section as well.

It should be noted that the oxidation removed does not consider the surface area of the particles as a factor, but only the total calculated weight of the removed oxidation from the sampled portion of a concentrate or tails. Whether the particle size of the sample is fine or coarse could very impact the interpretation of the metal oxidation of the surface. A lack of certainty in the specific oxidation products and their distribution over the flotation was a challenge in this work. Furthermore, determining a particle size distribution for the test after flotation would require rendering the particles hydrophilic to be drawn into the Mastersizer. The degradation of the dixanthogen species to promote hydrophilicity would destroy the aggregates created through shear flocculation and skew the size distribution to a finer size, which would not be representative of the slurry during the flotation. Given the degree of oxidation during HIC eventually slows down due to a lack of oxygen (consumed during oxidation of the surface that is not replenished), which is noted in the reasonably consistent pulp potential drop after HIC, there is limit to the oxidation that can feasibly occur. While this is hardly a conclusive and satisfying answer, the allocation of the limited samples towards EDTA extraction or peroxide fusion was decided to be more important. Therefore, quantifying the surface area or particle size distribution was not attempted. An accurate means of measuring particle size distribution in situ was described by Chen [131] and would be recommended as an accompanying study if the available samples allows for such testing.

6.3.1 Copper Oxidation Levels

The oxidized copper levels are shown to be related to the speed of the Rushton impeller. With 10 g/ton of xanthate, reducing the impeller speed from 1,400 RPM down to 900 RPM (reduction factor of 4 in power input) increased overall chalcopyrite recovery by 12.4%. The EDTA extracted metals showed that the copper oxidation found on the concentrate surface was impacted by impeller speed and affected the recovery of chalcopyrite. The highest levels of

copper oxidation resulted in the lowest chalcopyrite recoveries. Increasing the dosage of xanthate from 5 to 10 g/ton showed a reduction in copper oxidation levels for all impeller speeds (Figure 41). At 5 and 10 g/ton of xanthate, increasing the RPM directly increased the oxidized copper levels. The copper oxidation level in the tails was always lower than in any concentrate collected during flotation. At 5 g/ton of xanthate, the oxidized copper levels in the tails were 70% lower than those seen in the final concentrate (15-minute mark). At 10 g/ton of xanthate, the oxidized copper levels in the tails were 50% of the final concentrate values.

6.3.2 Nickel Oxidation Levels

The levels of oxidized nickel followed a similar behavior to copper oxidation, as nickel oxidation levels increased as the impeller speed (or power input) increased. The nickel oxidation on the surface did not share any correlation to pentlandite recovery. In general, it could not be determined if nickel oxidation had a detrimental or beneficial effect on flotation. This is assumed to be due to iron and copper oxidation levels having a greater impact on flotation results and the effects of nickel oxidation being lost in the background. Nickel oxidation levels in the tails were dependent upon on the xanthate dosage. At 5 g/ton or below (no xanthate addition), nickel oxidation levels in the tails were approx. 20% lower than the final concentrate pulled. At 10 g/ton or higher, the oxidized nickel levels in the tails were about 25% higher than the levels measured in the final concentrate. These values are consistent for all RT HIC tests.

6.3.3 Iron Oxidation Levels

As the dosage of xanthate increases from 0 to 20 g/ton of xanthate, the initial oxidized iron levels seen in the first concentrate (within 1 minute) decreased. However, as the flotation progressed, the final oxidized iron levels were higher. This can be seen in Figure 30. When the impeller speed is varied from 900 to 1,400 RPM, oxidized iron levels generally increased as the impeller speed increased. Higher oxidized iron levels were shown to coincide with lower sulfide recoveries in the flotations. Conversely, reduced levels of iron oxidation allowed the sulfide minerals to float considerably faster, shown through the rate constants (see Table 8 and Table 9) as well comparisons of the relative sulfide amounts floated within in the first minute and the second minute. When considering the impact of the various metal oxidation species that are present, only higher iron oxidation levels could be related to a negative impact on the flotation.

Conversely, tests with lowest oxidized iron levels had the best flotation responses for their xanthate dosage. This suggests that iron oxidation plays a direct role in reducing sulfide hydrophobicity. The tails of all flotation experiments had higher oxidized iron levels than all concentrates taken during the flotation, typically 30 to 50% higher than the levels measured in the final concentrate.

6.4 Surface Competition for Metal Oxidation

At low xanthate levels, the surface area available for electrochemical reactions appeared to be in excess based on the EDTA extraction results. Specifically, oxidized iron levels increased with RPM and oxidized nickel levels were lower in the tails. Once the xanthate dosage increased to 10 g/ton, the oxidation behavior of these two metals changed dramatically. The reason for this change is the increased dixanthogen patch formation which blocked particle surface area. For the RT HIC test using 10 g/ton of xanthate, iron oxidation levels in the first concentrate (within 1 minute) were lower than the initial feed oxidized iron levels. This showed the immediately floatable material had less iron oxidation on average.

Additionally, the oxidized nickel levels were higher in the tails at 10 g/ton of xanthate. At lower xanthate doses, the competition for surface area was lower. Higher levels of oxidized nickel were found on the concentrates and less oxidized nickel was found in the tails.

The oxidized copper levels showed similar findings to previous RT HIC tests, but copper levels depleted much faster after 2 minutes of flotation than in lower xanthate doses. When looking at all three oxidized metal levels together, it became clear that copper oxidation was preferentially forming on the surface of the hydrophobic minerals before nickel or iron oxidation. This theory explains the lower iron and nickel oxidation levels in the 10/1400 RT HIC test where previous results would assume the oxidation levels increase as the impeller speed is increased. Furthermore, the lower oxidized copper levels in the tails suggests that copper plays an important role in promoting hydrophobicity in the sulfide minerals. Due to the large amount of pyrrhotite in the feed (54 wt.%), the most reasonable inference is that copper activation is responsible for improving the recovery of pyrrhotite. At 900 RPM, lower copper levels resulted in a reduction in the pyrrhotite being recovered. Though nickel activation is known to occur and is an effective way to activate pyrrhotite, analysis of the EDTA extractable oxides suggests that copper activation is the dominant mechanism.

The overall lower rate constant of pyrrhotite through all experiments suggests that while pyrrhotite recovery is quite high, it floats slower overall than both chalcopyrite and pentlandite. Due to the oxidized copper levels quickly dropping after the first couple of minutes, it may be possible than nickel activation plays a more important role in floating pyrrhotite later in the flotation. Approximately 70-80% of the chalcopyrite and pentlandite that was floated is collected in the first two minutes. Pyrrhotite, on the other hand, had only 55 to 65% of its overall concentrate collected in the first two minutes.

6.5 The Impact of DETA/SMBS on Sulfide Flotation

The use of DETA/SMBS had a negative impact on all sulfide minerals in both RT HIC and No HIC tests. Pentlandite and pyrrhotite were drastically impacted, with chalcopyrite being the most resistant to the effects of adding DETA/SMBS. Directly comparing the results between No HIC and RT HIC showed that RT HIC always had superior flotation results. In all tests, pyrrhotite was shown to be effectively depressed.

The reason for the poor flotation results can be explained with analyzing the EDTA extractable metal oxides. When comparing RT HIC tests, with and without DETA/SMBS, the oxidized iron levels with DETA/SMBS was shown to be double those of a standard RT HIC test. Nickel oxidation was slightly lower with DETA/SMBS, but copper oxidation was almost three times as high. Furthermore, oxidized copper levels continued to rise throughout the flotation which suggested no lack of copper ions for the surface to interact with.

The No HIC tests that used DETA/SMBS had nearly 2 to 3 times the amount of oxidized iron than its RT HIC counterpart. Similarly, high levels of oxidized copper and nickel were seen when comparing the RT HIC and No HIC tests. The high levels of iron oxidation on the surface of the minerals is likely the main factor that lead to the poor flotation of the sulfide minerals.

Solution analysis was performed on the RT HIC tests to determine the effect of DETA/SMBS on the copper and nickel ion concentration. Comparison of the solutions showed more than 5 to 10 times the amount copper and nickel in the solution, following the use of RT HIC and DETA/SMBS. As the chelated ions would be able to be analyzed in solution via ICP-MS, due to being water-soluble, the use of DETA/SMBS showed a massive degree of chelation had occurred. However, the removal of these metal ions from solution likely allowed for the

excessive oxidation of all minerals, due to the inability to limit the oxidation. This will be discussed in the next section.

It should be noted that DETA/SMBS was added to the HIC cell before RT HIC was started. It is unknown what the impact would have been if DETA/SMBS was added to the slurry just prior to flotation. It is likely the flotation results would have been more positive.

6.6 Metal Ion Generation during RT HIC

The use of high intensity conditioning was originally to clean the surfaces of the sulfide minerals in the slurry in the middle of the plant process. Due to the partial oxidation and other surface effects that will be present, it is difficult to reinvigorate the pentlandite surface for recovery. The only way to create new surfaces is from grinding which create more fines, reducing pentlandite recovery. The removal of oxidation from the surface through physical means with HIC and simultaneous flocculation of the fines should promote improved recovery of pentlandite. However, while HIC can remove the oxidation from the surface, the surface will continue to oxidize. This cycle of oxidation and removal via HIC likely increases the concentration of metal ions in solution. The proposed sequence of events is represented below in Figure 59 and can be described in 5 stages:

Stage A: Pentlandite particle is subjected to HIC and constant surface cleaning effects.

Stage B: The pentlandite particle surface forms an oxide layer.

Stage C: High intensity conditioning removes the oxide surface, resulting in nickel ions being ejected into the solution.

Stage D: Pentlandite particle continues to oxidize.

Stage E: The surface continues to be cleaned by HIC and subsequently re-oxidizing, pumping nickel ions into the solution

This occurs in EDTA extraction as well, where nitrogen in bubbled to lower pulp potential and drastically reduce continual surface oxidation[128]. While Figure 59 shows a uniform oxide layer around the particle, oxide formation would likely be in patches on the mineral surface.

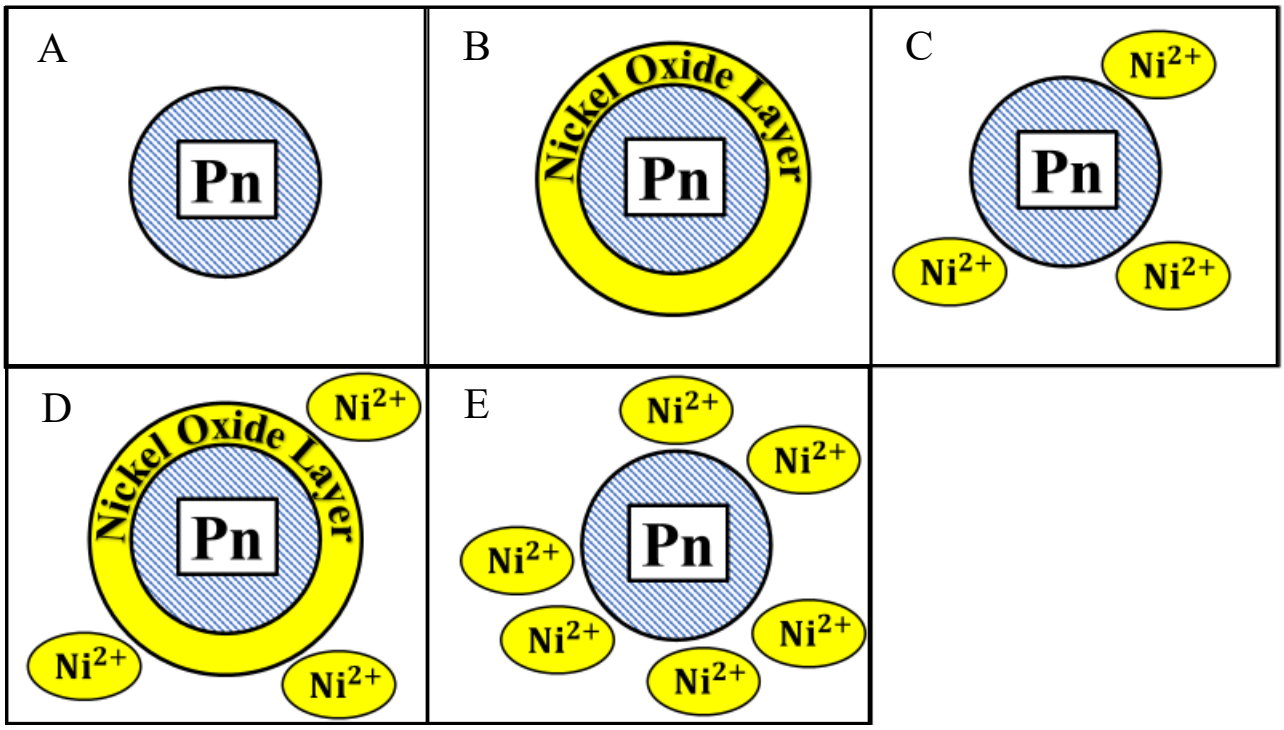

Figure 59: Representation of ion generation due to continual oxidation of the surface and removal of the oxide surface via HIC.

The activation of pyrrhotite via copper ions is complex and can occur from a variety of species. Below is Figure 60, a simple representation of one of the more well-known ways that copper can form a species that will precipitate onto the pyrrhotite surface. Below is an overview for the sequence of events that can result in activated pyrrhotite:

A. Chalcopyrite and pyrrhotite are present in a basic solution during high intensity conditioning.
B. During HIC, chalcopyrite is oxidized, and copper ions are released into solution.
C. As the copper concentration increases, copper hydroxide will begin to form as a means of balancing out the copper concentration.
D. As copper hydroxide is insoluble, it will precipitate onto the pyrrhotite surface. If xanthate is available, the pyrrhotite may activate via the copper ion.

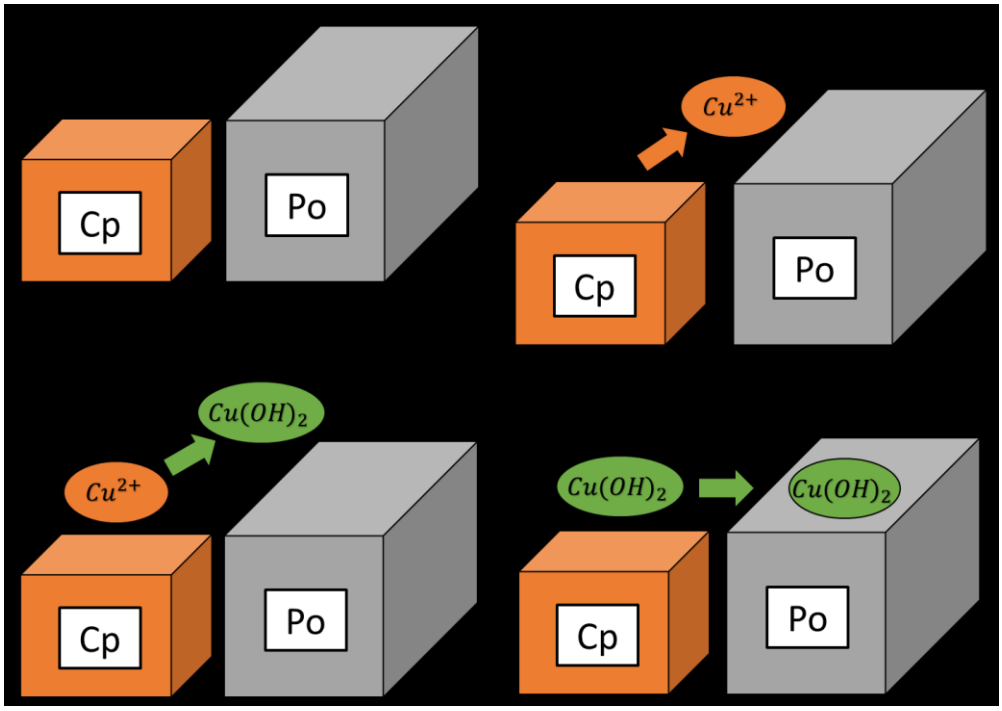

Figure 60: Representation of pyrrhotite activation due to HIC stage causing chalcopyrite to oxidize and release copper ions.

For pyrrhotite to activate, the hydroxide layer needs to be thin enough for electron transfer to occur. This is required for xanthate to oxidize onto the surface and later form dixanthogen. Once the layer becomes too thick for electron transfer, it can be considered hydrophilic.

6.7 Expansion of Dixanthogen Patch during HIC

The addition of xanthate was shown to decrease all metal oxidation while increasing all sulfide recovery. During HIC, dixanthogen patches are primarily valued for their hydrophobicity. However, the formation of a dixanthogen patch is also useful in protecting the surface from oxidation. In the case of pentlandite, the expansion of the dixanthogen patch requires a free adjacent nickel site, the formation of oxidation on the nickel site can effectively stop the formation of dixanthogen. The hydrophobicity that a dixanthogen patch imparts will increase as the surface area of the patch increases. Figure 61 shows how HIC can hypothetically extend a dixanthogen patch through the following steps:

A. The nickel site of the pentlandite crystal is blocked by an oxidation species.

B. During HIC, the oxidation is removed while the dixanthogen patch survives the shear force generated by the HIC.
C. Once the nickel site is cleaned, xanthate will be able to adsorb onto the surface if xanthate is available to do so.
D. Following the adsorption of the xanthate molecule onto the nickel site, a second xanthate molecule can oxidize between the two Ni-bonded xanthates and allowing the dixanthogen patch to continue increasing in size.

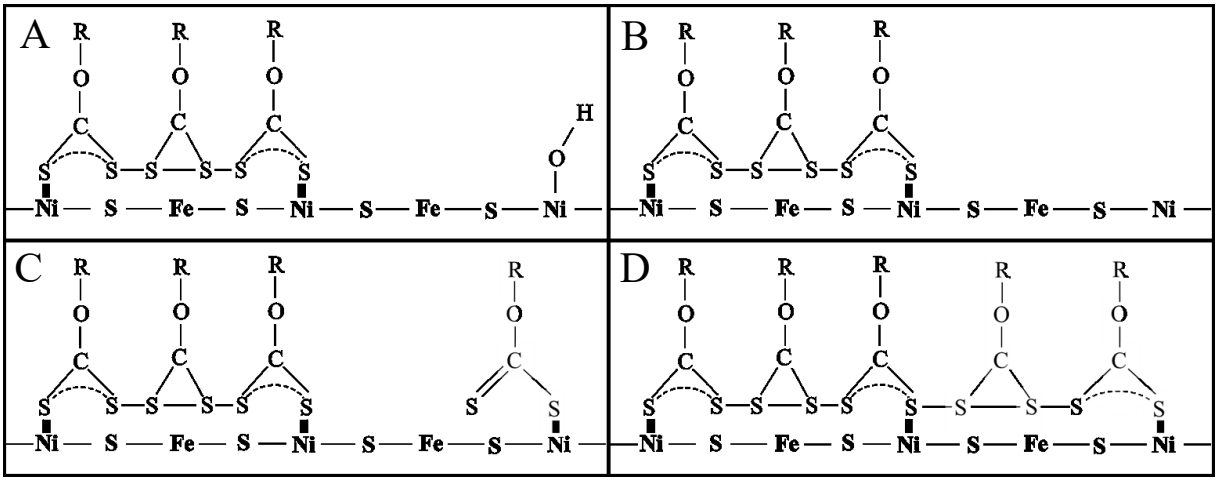

Figure 61: Representation of proposed dixanthogen patch extension during optimized HIC through surface cleaning and nickel site xanthate adsorption.

The success of the simultaneous surface cleaning and dixanthogen patch expansion relies on the stability of the dixanthogen patch during HIC. Longer chain xanthate molecules have improved the recovery of pentlandite during HIC, but are more susceptible to charged slimes such as serpentine fines [58]. As longer xanthate chains are less selective but more hydrophobic, creating dixanthogen patches during HIC may occur faster. Using a stronger, less selective collector may allow for greater collector consumption during HIC.

6.8 HIC Tank Analysis and Slurry Experimentation

Due to the detrimental effects of oxygen interaction with HIC and sulfides, the experimental setup needs to limit the oxidation that can occur. The design used allows the transfer of slurry from the HIC cell to the Denver cell for flotation in a less than optimal means (opening HIC cell and pouring slurry into Denver cell). The time is takes to complete this

transfer averaged 5 minutes between completing the HIC stage and starting the short conditioning time for flotation. In this time, the slurry is exposed to air and the pulp potential has shown to immediately increase by 50mv in the short amount of time. While the direct effects of this increase cannot be fully known, it would be reasonable to state that flotation should follow HIC as quickly as possible. In addition, the ability to control exposure to air would be useful in determining the range of effect.

The condition of the slurry should also be considered. The slurry used in this study was sampled into large buckets and was left in buckets. While the water layer kept the slurry from direct contact with the air, the pH of the solution dropped from above 8 to below a pH of 6. This pH depression is consistent with aging of the slurry and occurs even if the slurry is filtered immediately after extraction from the plant cell. The slurry becomes more challenging to float as a result, which is shown with the poor flotation of the slurry with no reagents or HIC used. Unfortunately, this cannot be easily remedied as engineers at the plant have said even nitrogen purging/freezing slurry samples does not allow for the flotation response to mirror the plant. It is likely that future testing should be performed near the plant to preserve the slurry conditions seen within the plant.

The minerals being overly oxidized by the two-week period required for shipping and the full day of exposure to air when vacuum filtering/homogenization of the filter cake in sampled bags. If fresh slurry was used, it is likely that the HIC duration could be reduced in length. As ion generation occurs over time through continual oxidation and surface cleaning (similar results are observed when performing EDTA extraction with nitrogen purging), reducing the HIC time may improve the overall flotation response.

Chapter 7 Conclusions and Recommendations for Future Work

7.1 Conclusion

High intensity conditioning is a process that has shown excellent results when testing on single sulfide systems in previous studies. This thesis studied the use of HIC on a filtered slurry sample from a concentrate within the plant process. The mineral sample had a wide degree of fine pentlandite and pyrrhotite along with coarse chalcopyrite. Rushton HIC showed promising improvements in the recovery of pentlandite and chalcopyrite, but unfortunately did little to improve the depression of pyrrhotite. The reasons for this can be described, but there is much about HIC that still needs to be developed. The key findings from the investigation are detailed below:

1. Chalcopyrite has the best recovery with RT HIC at lower power inputs. High power inputs lead to higher oxidized copper levels, lower chalcopyrite recovery and pyrrhotite activation.
2. Both pentlandite and pyrrhotite have improved recovery at higher power inputs. At lower power inputs, which resulted in lower oxidized copper levels, pyrrhotite recovery was reduced.
3. Copper oxidation was found to preferentially form on the sulfide surfaces within the first 2 minutes of flotation and decrease quickly afterwards. Nickel oxidation continued to increase throughout the flotation and iron oxidation decreased after 2 minutes.
4. Sulfide surface competition was observed to occur at 10 g/ton of xanthate, where the formation of surface species was limited and therefore based on preferential formation. Xanthate adsorption appeared to be the most preferential, as higher dosages decreased all metal oxidation in the concentrate pulled in the first minute. The oxidized iron levels in the first concentrate at 10 g/ton of xanthate or higher were lower than the feed iron levels, suggested the iron oxidation was replaced with either xanthate, copper or nickel oxidation.
5. The use of DETA/SMBS greatly reduced both pentlandite and pyrrhotite while only minorly impacting chalcopyrite recovery. In all DETA/SMBS tests, RT HIC had superior sulfide recovery when compared to the no HIC tests.

6. Nickel activation cannot be directly confirmed like copper activation. However, approximately 40% of pyrrhotite floated after the oxidized copper levels started to subside. Nickel oxidation levels continued to rise until the final concentrate was collected, so nickel activation may be a kinetically slower mechanism in conjunction with copper activation.

7.2 Recommendations for Future Work

Based on the findings from this investigation, several suggestions for improving HIC studies for mixed mineral sulphides are provided below:

1. Due to the evidence that chalcopyrite is responsible for activating pyrrhotite during HIC, separation of chalcopyrite from pyrrhotite would likely have an immediate impact on reducing pyrrhotite recovery. Pentlandite has a better flotation response at high power inputs, while chalcopyrite benefits from lower power inputs (at least 4x lower with RT HIC was tested).
2. Longer chain xanthate molecules are less selective and are a stronger collector. Faster xanthate adsorption to pentlandite/chalcopyrite during HIC will consume xanthate faster and will protect surface from oxidation. Improving dixanthogen patch expansion during HIC will lead to improving the selectivity between pentlandite and pyrrhotite.
3. Nickel activation needs to be kinetically compared to copper activation. As nickel ions are in excess past 10 g/ton, quantifying the activation of pyrrhotite would provide valuable information into the combination activation of both copper and nickel ions.
4. Regarding HIC tank design, improvements toward floating the slurry following an HIC stage quickly and without oxygenating the slurry would likely yield positive results.
5. Future studies of sulfide slurries should be coordinated with plant, so the surface of the sulfide minerals is representative of the condition in the plant. The slurry is this study was had severe oxidation and therefore required an aggressive strategy to clean. A less intensive HIC stage (lower power input or duration) may allow for greater control over the slurry's final state. For example, the residual xanthate present in the plant pulp may be enough for HIC and therefore no additional xanthate may be needed.
6. HIC studies that focus on the shear flocculation of mixed sulfides would be incredibly helpful in determining the degree that aggregates consist of pentlandite, chalcopyrite

and/or pyrrhotite. Chen's study used an in-situ method to analyze the particle size distribution which is likely the best means of seeing the growth or breakage of aggregates as a function of time. The goal is to determine whether shear flocculation of pentlandite fines are possible to recover before they are inevitably lost in the pyrrhotite tails. Considering the regrind would create even more fines, a means of restoring their floatability without grinding would be very beneficial.

High intensity conditioning has shown to be ability to restore the floatability of a heavily oxidized sulfide slurry. A direct comparison between flotations with No HIC and with RT HIC showed that both chalcopyrite and pentlandite recoveries were always substantially higher with RT HIC. Due to excessive oxidation and ion generation, pyrrhotite was also heavily activated. Further refinement of the HIC stage will improve the selectivity between pentlandite and pyrrhotite. With further improvements, this technique can be used to extend standard pentlandite recovery from the intermediate range into the fine particle size range.

Bibliography

[1] R. C. Hochreiter, D. C. Kennedy, W. Muir, and A. I. Wood, "Platinum in South Africa (Metal Review Series no. 3)," *J. South African Inst. Min. Metall.*, vol. 85, no. 6, pp. 165–185, 1985.

[2] J. D. Miller, J. Li, J. C. Davidtz, and F. Vos, "A review of pyrrhotite flotation chemistry in the processing of PGM ores," *Miner. Eng.*, vol. 18, no. 8, pp. 855–865, 2005.

[3] R. H. Yoon, C. I. Basilio, M. A. Marticorena, A. N. Kerr, and R. Stratton-Crawley, "A study of the pyrrhotite depression mechanism by diethylenetriamine," *Miner. Eng.*, vol. 8, no. 7, pp. 807–816, 1995.

[4] S. M. Bulatovic, *Handbook of Flotation Reagents*. Elsevier, 2007.

[5] M. Becker, "The Mineralogy and Crystallography of Pyrrhotite From Selected Nickel and PGE Ore Deposits and its Effect on Flotation Performance," University of Pretoria, 2009.

[6] R. S. Multani, "The Flotation Characteristics of Magnetic/4C (Fe7S8) and Non–magnetic/5C (Fe9S10) Pyrrhotite Superstructures," McGill University, 2018.

[7] G. D. Senior, L. K. Shannon, and W. J. Trahar, "The flotation of pentlandite from pyrrhotite with particular reference to the effects of particle size," *Int. J. Miner. Process.*, vol. 42, no. 3–4, pp. 169–190, 1994.

[8] R. G. Arnold, "Range in composition and structure of 82 natural terrestrial pyrrhotites," *Can. Mineral.*, vol. 9, no. 1, pp. 31–50, 1967.

[9] J. F. Riley, "The pentlandite group (Fe,Ni,Co)9S8: New data and an appraisal of structure-composition relationships," *Mineral. Mag.*, pp. 345–349, 1977.

[10] A. R. Ramsden, "Compositions of coexisting pyrrhotites, pentlandites and pyrites at spargoville, western australia," *Can. Mineral.*, vol. 13, pp. 133–137, 1975.

[11] J. E. Hawley and V. A. Haw, "Intergrowths of pentlandite and pyrrhotite," *Econ. Geol.*, vol. 52, no. 2, pp. 132–139, Mar. 1957.

[12] R. W. Shewman, "Pentlandite Phase Relations in the Fe-Ni-S System and the Stability of the Pyrite-Pentlandite Assemblage," McGill University, 1967.

[13] R. S. Multani and K. E. Waters, "A review of the physicochemical properties and flotation of pyrrhotite superstructures (4C – Fe7S8/ 5C – Fe9S10) in Ni-Cu sulphide mineral processing," *Can. J. Chem. Eng.*, vol. 96, no. 5, pp. 1185–1206, 2018.

[14] C. Francis, M. Fleet, K. Misra, and J. R. Craig, "Orientation of exsolved pentlandite in natural and synthetic nickeliferous pyrrhotite," *Am. Mineral.*, vol. 61, no. 1929, pp. 913–920, 1976.

[15] A. P. Batt, "Nickel Distribution in Hexagonal and Monoclinic Pyrrhotite," *Can. Mineral.*, vol. 11, pp. 892–897, 1972.

[16] S. C. Gordon and A. M. McDonald, "A study of the composition, distribution, and genesis of pyrrhotite in the copper cliff offset, sudbury, Ontario, Canada," *Can. Mineral.*, vol. 53,

no. 5, pp. 859–878, 2016.

[17] B. A. Wills and J. A. Finch, “Chapter 12 - Froth Flotation,” in *Wills’ Mineral Processing Technology (Eighth Edition)*, Eighth Edi., B. A. Wills and J. A. Finch, Eds. Boston: Butterworth-Heinemann, 2016, pp. 265–380.

[18] R. D. Crozier, “Sulphide collector mineral bonding and the mechanism of flotation,” *Miner. Eng.*, vol. 4, no. 7–11, pp. 839–858, 1991.

[19] H. Khoshdast, “Flotation Frothers: Review of Their Classifications, Properties and Preparation,” *Open Miner. Process. J.*, vol. 4, no. 1, pp. 25–44, 2011.

[20] S. Farrokhpay, “The significance of froth stability in mineral flotation - A review,” *Adv. Colloid Interface Sci.*, vol. 166, no. 1–2, pp. 1–7, 2011.

[21] T. V. Subrahmanyam and E. Forssberg, “Froth stability, particle entrainment and drainage in flotation — A review,” *Int. J. Miner. Process.*, vol. 23, no. 1–2, pp. 33–53, May 1988.

[22] V. Bozkurt, “Pentlandite/pyrrhotite interactions and xanthate adsorption,” McGill University, 1997.

[23] C. E. Gibson and S. Kelebek, “Sensitivity of pentlandite flotation in complex sulfide ores towards pH control by lime versus soda ash: Effect on ore type,” *Int. J. Miner. Process.*, vol. 127, pp. 44–51, 2014.

[24] F. Göktepe, “Effect of pH on pulp potential and sulphide mineral flotation,” *Turkish J. Eng. Environ. Sci.*, vol. 26, pp. 309–318, 2002.

[25] N. P. Finkelstein, “The activation of sulphide minerals for flotation: a review,” *Int. J. Miner. Process.*, vol. 52, no. 2–3, pp. 81–120, Dec. 1997.

[26] R. J. Pugh, “Macromolecular organic depressants in sulphide flotation-A review, 1. Principles, types and applications,” *Int. J. Miner. Process.*, vol. 25, no. 1–2, pp. 101–130, 1989.

[27] V. Bozkurt, Z. Xu, and J. A. Finch, “Effect of depressants on xanthate adsorption on pentlandite and pyrrhotite: Single vs mixed minerals,” *Can. Metall. Q.*, vol. 38, no. 2, pp. 105–112, 1999.

[28] E. A. Agorhom, W. Skinner, and M. Zanin, “Diethylenetriamine depression of Cu-activated pyrite hydrophobised by xanthate,” *Miner. Eng.*, vol. 57, pp. 36–42, 2014.

[29] R. A. Hayes and J. Ralston, “The collectorless flotation and separation of sulphide minerals by Ehcontrol,” *Int. J. Miner. Process.*, vol. 23, no. 1–2, pp. 55–84, 1988.

[30] R. A. Hayes, D. M. Price, J. Ralston, and R. W. Smith, “Collectorless Flotation of Sulphide Minerals,” *Miner. Process. Extr. Metall. Rev.*, vol. 2, no. 3, pp. 203–234, 1987.

[31] V. M. Lepetic, “Flotation of Chalcopyrite Without Collector After Dry, Autogenous Grinding,” *Can Min Met. Bull*, vol. 67, pp. 71–77, 1974.

[32] P. J. Harris and N. P. Finkelstein, “Interactions between sulphide minerals and xanthates, I. The formation of monothiocarbonate at galena and pyrite surfaces,” *Int. J. Miner.*

Process., vol. 2, no. 1, pp. 77–100, Mar. 1975.

[33] G. W. Heyes and W. J. Trahar, "The natural flotability of chalcopyrite," *Int. J. Miner. Process.*, vol. 4, no. 4, pp. 317–344, Dec. 1977.

[34] J. R. Gardner and R. Woods, "An electrochemical investigation of the natural flotability of chalcopyrite," *Int. J. Miner. Process.*, vol. 6, no. 1, pp. 1–16, Jun. 1979.

[35] R. S. C. Smart, M. Jasieniak, K. E. Prince, and W. M. Skinner, "SIMS studies of oxidation mechanisms and polysulfide formation in reacted sulfide surfaces," *Miner. Eng.*, vol. 13, no. 8–9, pp. 857–870, Aug. 2000.

[36] Y. Hu, W. Sun, and D. Wang, *Electrochemistry of Flotation of Sulphide Minerals*. Berlin, Heidelberg: Springer Berlin Heidelberg, 2009.

[37] W. T. Thompson, M. H. Kaye, C. W. Bale, and A. D. Pelton, "Pourbaix Diagrams for Multielement Systems," in *Uhlig's Corrosion Handbook*, Hoboken, NJ, USA: John Wiley & Sons, Inc., 2011, pp. 103–109.

[38] J. D. Verink, "Simplified Procedure for Constructing Pourbaix Diagrams," *Uhlig's Corros. Handb. Third Ed.*, pp. 93–101, 2011.

[39] B. Beverskog, "Revised Pourbaix Diagrams for Copper at 25 to 300°C," *J. Electrochem. Soc.*, vol. 144, no. 10, p. 3476, 1997.

[40] J. L. Bowden and C. A. Young, "Xanthate chemisorption at copper and chalcopyrite surfaces," *J. South. African Inst. Min. Metall.*, vol. 116, no. 6, pp. 503–508, 2016.

[41] S. Kelebek and B. Nanthakumar, "Characterization of stockpile oxidation of pentlandite and pyrrhotite through kinetic analysis of their flotation," *Int. J. Miner. Process.*, vol. 84, no. 1–4, pp. 69–80, 2007.

[42] M. Hodgson and G. E. Agar, "Electrochemical Investigations into the Flotation Chemistry of Pentlandite and Pyrrhotite: Process Water and Xanthate Interactions," *Can. Metall. Q.*, vol. 28, no. 3, pp. 189–198, Jul. 1989.

[43] K. Heiskanen, V. Kirjavainen, and H. Laapas, "Possibilities of collectorless flotation in the treatment of pentlandite ores," *Int. J. Miner. Process.*, vol. 33, no. 1–4, pp. 263–274, 1991.

[44] P. J. Guy and W. J. Trahar, "The influence of grinding and flotation environments on the laboratory batch flotation of galena," *Int. J. Miner. Process.*, vol. 12, no. 1–3, pp. 15–38, Jan. 1984.

[45] W. J. Trahar, "A laboratory study of the influence of sodium sulphide and oxygen on the collectorless flotation of chalcopyrite," *Int. J. Miner. Process.*, vol. 11, no. 1, pp. 57–74, 1983.

[46] R. H. Yoon, "Collectorless flotation of chalcopyrite and sphalerite ores by using sodium sulfide," *Int. J. Miner. Process.*, vol. 8, no. 1, pp. 31–48, 1981.

[47] S. Chander and A. Khan, "Effect of sulfur dioxide on flotation of chalcopyrite," *Int. J. Miner. Process.*, vol. 58, no. 1–4, pp. 45–55, 2000.

[48] Z. Ekmekci, A. Aslan, and H. Hassoy, “Effects of EDTA on selective flotation of sulphide minerals,” *Physicochem. Probl. Miner. Process.*, vol. 38, pp. 79–94, 2004.

[49] M. C. Fuerstenau and B. J. Sabacky, “On the natural floatability of sulfides,” *Int. J. Miner. Process.*, vol. 8, no. 1, pp. 79–84, Mar. 1981.

[50] G. Chen, “The Mechanisms of High Intensity Conditioning on Mt. Keith Nickel Ore,” University of South Australia, 1998.

[51] G. Heyes and W. J. Trahar, “Flotation of Pyrite and Pyrrhotite in the Absence of Conventional Collectors,” *Proc. - Electrochem. Soc.*, vol. 84, pp. 219–232, 1984.

[52] X. Cheng and I. Iwasaki, “Pulp Potential and Its Implications to Sulfide Flotation,” *Miner. Process. Extr. Metall. Rev.*, vol. 11, no. 4, pp. 187–210, 1992.

[53] M. Becker, J. De Villiers, and D. Bradshaw, “The flotation of magnetic and non-magnetic pyrrhotite from selected nickel ore deposits,” *Miner. Eng.*, vol. 23, no. 11–13, pp. 1045–1052, 2010.

[54] D. L. Legrand, G. M. Bancroft, and H. W. Nesbitt, “Oxidation of pentlandite and pyrrhotite surfaces at pH 9.3: Part 2. Effect of xanthates and dissolved oxygen,” *Am. Mineral.*, vol. 90, no. 7, pp. 1055–1061, 2005.

[55] F. W. Tveter, E.C. McQuiston, “Plant Practice in Sulfide Mineral Flotation,” in *Froth Flotation 50th Anniversary Volume*, R. Fuerstenau, M.C. Jameson, G., Yoon, Ed. Littleton: Society of Mining, Metallurgy and Exploration, Inc., 2013, pp. 382–426.

[56] C. R. Edwards, W. B. Kipkie, and G. E. Agar, “The effect of slime coatings of the serpentine minerals, chrysotile and lizardite, on pentlandite flotation,” *Int. J. Miner. Process.*, vol. 7, no. 1, pp. 33–42, 1980.

[57] Y. Peng and D. Seaman, “The flotation of slime-fine fractions of Mt. Keith pentlandite ore in de-ionised and saline water,” *Miner. Eng.*, vol. 24, no. 5, pp. 479–481, 2011.

[58] B. Feng, Q. Feng, Y. Lu, and P. Lv, “The effect of conditioning methods and chain length of xanthate on the flotation of a nickel ore,” *Miner. Eng.*, vol. 39, pp. 48–50, 2012.

[59] D. L. Legrand, G. M. Bancroft, and H. W. Nesbitt, “Oxidation/alteration of pentlandite and pyrrhotite surfaces at pH 9.3: Part 1. Assignment of XPS spectra and chemical trends,” *Am. Mineral.*, vol. 90, no. 7, pp. 1042–1054, 2005.

[60] A. E. C. Peres, “The interaction between xanthate and sulphur dioxide in the flotation of nickel-copper sulphide ores,” 1979.

[61] M. McNeil, S. R. Rao, and J. A. Finch, “Oxidation of Amyl Xanthate by Pentlandite,” *Can. Metall. Q.*, vol. 33, no. 2, pp. 165–167, Apr. 1994.

[62] J. Leja, *Surface Chemistry of Froth Flotation*, vol. 39, no. 5. Boston, MA: Springer US, 1981.

[63] V. Bozkurt, Z. Xu, and J. A. Finch, “Pentlandite/pyrrhotite interaction and xanthate adsorption,” *Int. J. Miner. Process.*, vol. 52, no. 4, pp. 203–214, Feb. 1998.

[64] N. K. Mendiratta, “Kinetic Studies of Sulfide Mineral Oxidation and Xanthate Adsorption,” Virginia Polytechnic Institute and State University, 2000.

[65] J. O. Leppinen, C. I. Basilio, and R. H. Yoon, “In-situ FTIR study of ethyl xanthate adsorption on sulfide minerals under conditions of controlled potential,” *Int. J. Miner. Process.*, vol. 26, no. 3–4, pp. 259–274, 1989.

[66] J. O. Leppinen, “FTIR and flotation investigation of the adsorption of ethyl xanthate on activated and non-activated sulfide minerals,” *Int. J. Miner. Process.*, vol. 30, no. 3–4, pp. 245–263, 1990.

[67] V. Bozkurt, Z. Xu, and J. A. Finch, “Pentlandite/pyrrhotite interaction and xanthate adsorption,” *Int. J. Miner. Process.*, vol. 52, no. 4, pp. 203–214, Feb. 1998.

[68] P. Page *et al.*, “Electrochemical Behaviour of Pyrite, Pyrrhotite, Pentlandite and Chalcopyrite,” University of London, 1988.

[69] G. Winter and R. Woods, “The Relation of Collector Redox Potential to Flotation Efficiency: Monothiocarbonates,” *Sep. Sci.*, vol. 8, no. 2, pp. 261–267, Apr. 1973.

[70] A. Khan and S. Kelebek, “Electrochemical aspects of pyrrhotite and pentlandite in relation to their flotation with xanthate. Part-I: Cyclic voltammetry and rest potential measurements,” *J. Appl. Electrochem.*, vol. 34, no. 8, pp. 849–856, 2004.

[71] S. A. Allison and C. T. O’Connor, “An investigation into the flotation behaviour of pyrrhotite,” *Int. J. Miner. Process.*, vol. 98, no. 3–4, pp. 202–207, 2011.

[72] T. Chimbganda, M. Becker, J. L. Broadhurst, S. T. L. Harrison, and J. P. Franzidis, “A comparison of pyrrhotite rejection and passivation in two nickel ores,” *Miner. Eng.*, vol. 46–47, pp. 38–44, 2013.

[73] G. Mishra, K. S. Viljoen, and H. Mouri, “Influence of mineralogy and ore texture on pentlandite flotation at the nkomati nickel mine, south Africa,” *Miner. Eng.*, vol. 54, pp. 63–78, 2013.

[74] S. Kelebek and C. Tukel, “The effect of sodium metabisulfite and triethylenetetramine system on pentlandite-pyrrhotite separation,” *Int. J. Miner. Process.*, vol. 57, no. 2, pp. 135–152, 1999.

[75] C. Weisener and A. Gerson, “Investigation of the Cu(II) adsorption mechanism on pyrite by ARXPS and SIMS,” *Miner. Eng.*, vol. 13, no. 13, pp. 1329–1340, 2000.

[76] A. M. Buswell M.J. Nicol, “Some aspects of the electrochemistry of the flotation of pyrrhotite,” *J. Appl. Electrochem.*, vol. 32, no. 12, pp. 1321–1329, 2002.

[77] C. Tukel and S. Kelebek, “Modulation of xanthate action by sulphite ions in pyrrhotite deactivation/depression,” *Int. J. Miner. Process.*, vol. 95, no. 1–4, pp. 47–52, 2010.

[78] S. Tukel, C., Kelebek, “Separation of nickeliferous hexagonal pyrrhotite from pentlandite in Ni-Cu sulphide ores: Recovery by size performance,” *Miner. Eng.*, vol. 125, pp. 223–230, Aug. 2018.

[79] V. Malysiak, C. T. O’Connor, J. Ralston, A. R. Gerson, L. P. Coetzer, and D. J. Bradshaw,

"Pentlandite-feldspar interaction and its effect on separation by flotation," *Int. J. Miner. Process.*, vol. 66, no. 1–4, pp. 89–106, 2002.

[80] M. Xu and S. Wilson, "Investigation of seasonal metallurgical shift at inco's clarabelle mill," *Miner. Eng.*, vol. 13, no. 12, pp. 1207–1218, Oct. 2000.

[81] M. R. Thornber, "Mineralogical and electrochemical stability of the nickel-iron sulphides-pentlandite and violarite," *J. Appl. Electrochem.*, vol. 13, no. 2, pp. 253–267, Mar. 1983.

[82] J. Bard, A.J., Parsons, R. and Jordan, *Standard Potentials in Aqueous Solution*. New York: IUPAC-Marcel Dekker Inc., 1985.

[83] A. Cushing, A. Ghahreman, and S. Kelebek, "Electrochemical characteristics of iron sulfide minerals in the presence of SMBS and TETA and the case for their joint action," 2017.

[84] V. Lawson, G. Hill, L. Kormos, and G. Marrs, "The Separation of Pentlandite from Chalcopyrite , Pyrrhotite and Gangue in Nickel Projects Throughout the World," in *Proceedings 12th AusIMM Mill Operators' Conference 2014 (The Australasian Institute of Mining and Metallurgy: Melbourne*, 2014, pp. 153–162.

[85] L. Bard, A., Faulkner, *Electrochemical Methods Fundamentals and Applications*. New York: John Wiley & Sons, Inc., 2001.

[86] K. Adam, K. A. Natarajan, and I. Iwasaki, "Grinding media wear and its effect on the flotation of sulfide minerals," *Int. J. Miner. Process.*, vol. 12, no. 1–3, pp. 39–54, 1984.

[87] V. Kirjavainen, N. Schreithofer, and K. Heiskanen, "Effect of some process variables on flotability of sulfide nickel ores," *Int. J. Miner. Process.*, vol. 65, no. 2, pp. 59–72, 2002.

[88] B. Nanthakumar, S. Kelebek, and P. D. Katsabanis, "Impact of oxidation on flotation of Ni–Cu sulphide ore with respect to grinding," *Miner. Process. Extr. Metall.*, vol. 116, no. 3, pp. 197–206, 2007.

[89] G. Berglund, "Pulp chemistry in sulphide mineral flotation," *Int. J. Miner. Process.*, vol. 33, no. 1–4, pp. 21–31, 1991.

[90] Y. Peng, "Grinding environment studies in the control of oxidation and interaction between sulphide minerals and grinding media," University of South Australia, 2003.

[91] Y. Peng, S. Grano, D. Fornasiero, and J. Ralston, "Control of grinding conditions in the flotation of chalcopyrite and its separation from pyrite," *Int. J. Miner. Process.*, vol. 69, no. 1–4, pp. 87–100, Mar. 2003.

[92] M. Azizi, A., Shafaei, S., Noaparast, M., Karamoozian, "Investigation of the electrochemical factors affecting the grinding environment of a porphyry copper sulphide ore," *J. Min. Metall.*, vol. 45, no. 1, pp. 45–55, 2013.

[93] S. Kelebek, "The Effect of Oxidation on the Flotation Behaviour of Nickel-Copper Ores," *XVlll lntemational Miner. Process. Congr.*, no. May, pp. 999–1006, Vol 4, 1993.

[94] C. J. Martin, R. E. McIvor, J. A. Finch, and S. R. Rao, "Review of the effect of grinding media on flotation of sulphide minerals," *Miner. Eng.*, vol. 4, no. 2, pp. 121–132, 1991.

[95] A. J. H. Newell and D. J. Bradshaw, “The development of a sulfidisation technique to restore the flotation of oxidised pentlandite,” *Miner. Eng.*, vol. 20, no. 10, pp. 1039–1046, 2007.

[96] S. Richardson and D. J. Vaughan, “Surface alteration of pentlandite and spectroscopic evidence for secondary violarite formation,” *Mineral. Mag.*, vol. 53, no. 370, pp. 213–222, Apr. 1989.

[97] A. N. Buckley and R. Woods, “Surface composition of pentlandite under flotation-related conditions,” *Surf. Interface Anal.*, vol. 17, no. 9, pp. 675–680, Aug. 1991.

[98] D. L. Legrand, G. M. Bancroft, and H. W. Nesbitt, “Surface characterization of pentlandite, (Fe,Ni)9S8, by X-ray photoelectron spectroscopy,” *Int. J. Miner. Process.*, vol. 51, no. 1–4, pp. 217–228, Oct. 1997.

[99] N. Belzile, Y. W. Chen, M. F. Cai, and Y. Li, “A review on pyrrhotite oxidation,” *J. Geochemical Explor.*, vol. 84, no. 2, pp. 65–76, 2004.

[100] A. N. Buckley and R. Woods, “X-ray photoelectron spectroscopy of oxidized pyrrhotite surfaces,” *Appl. Surf. Sci.*, vol. 22–23, pp. 280–287, May 1985.

[101] M. F. Cai, Z. Dang, Y. W. Chen, and N. Belzile, “The passivation of pyrrhotite by surface coating,” *Chemosphere*, vol. 61, no. 5, pp. 659–667, 2005.

[102] R. S. C. Smart, J. Amarantidis, W. M. Skinner, C. A. Prestidge, L. La Vanier, and S. R. Grano, “Surface Analytical Studies of Oxidation and Collector Adsorption in Sulfide Mineral Flotation,” vol. 12, no. 4, 2003, pp. 3–62.

[103] M. P. Janzen, R. V. Nicholson, and J. M. Scharer, “Pyrrhotite reaction kinetics: Reaction rates for oxidation by oxygen, ferric iron, and for nonoxidative dissolution,” *Geochim. Cosmochim. Acta*, vol. 64, no. 9, pp. 1511–1522, 2000.

[104] R. V. Nicholson and J. M. Scharer, “Laboratory Studies of Pyrrhotite Oxidation Kinetics,” in *Environmental Geochemistry of Sulfide Oxidation*, 1993, pp. 14–30.

[105] I. Bunkholt and R. A. Kleiv, “Pyrrhotite oxidation and its influence on alkaline amine flotation,” *Miner. Eng.*, vol. 71, pp. 65–72, 2015.

[106] A. Chopard, M. Benzaazoua, B. Plante, H. Bouzahzah, and P. Marion, “Kinetic tests to evaluate the relative oxidation rates of various sulfides and sulfosalts,” *Proc. 10th Int. Conf. Acid Rock Drain. IMWA Annu. Conf. Santiago, Chile*, p. 10, 2015.

[107] I. C. Hamilton and R. Woods, “An investigation of surface oxidation of pyrite and pyrrhotite by linear potential sweep voltammetry,” *J. Electroanal. Chem. Interfacial Electrochem.*, vol. 118, pp. 327–343, Feb. 1981.

[108] J. M. Nicholson, Ronald V. Scharer, “Laboratory Studies of Pyrrhotite Oxidation,” Waterloo, 1998.

[109] W. Lv *et al.*, “A kinetic study on oxidation of ferrous sulfide (FeS) in mixtures of CO 2 and H 2 O,” *Proc. Combust. Inst.*, vol. 36, no. 2, pp. 2173–2180, 2017.

[110] J. Goode, *Canadian Milling Practice*. Montreal: Canadian Institute of Mining, Metallurgy,

and Petroleum, 2001.

[111] D. Todorović, M. Trumic, L. Andrić, V. Milosevic, and M. Trumić, "A quick method for bond work index approximate value determination," *Fizykochem. Probl. Miner. - Physicochem. Probl. Miner. Process.*, vol. 53, pp. 321–332, 2017.

[112] H. Cho, J. Kwon, K. Kim, and M. Mun, "Optimum choice of the make-up ball sizes for maximum throughput in tumbling ball mills," *Powder Technol.*, vol. 246, pp. 625–634, 2013.

[113] G. D. Senior, W. J. Trahar, and P. J. Guy, "The selective flotation of pentlandite from a nickel ore," *Int. J. Miner. Process.*, vol. 43, no. 3–4, pp. 209–234, 1995.

[114] R. S. Multani, H. Williams, B. Johnson, R. Li, and K. E. Waters, "The effect of superstructure on the zeta potential, xanthate adsorption, and flotation response of pyrrhotite," *Colloids Surfaces A Physicochem. Eng. Asp.*, vol. 551, no. April, pp. 108–116, Aug. 2018.

[115] S. M. Bulatovic and R. S. Salter, *High intensity conditioning — a new approach to improving flotation of mineral slimes*. The Canadian Institute of Mining and Metallurgy, 1989.

[116] L. J. Warren, "Shear-flocculation of ultrafine scheelite in sodium oleate solutions," *J. Colloid Interface Sci.*, vol. 50, no. 2, pp. 307–318, 1975.

[117] L. J. Warren, *Shear-flocculation*, vol. 12. Elsevier B.V., 1992.

[118] L. J. Warren, "Flocculation of stirred suspensions of cassiterite and tourmaline," *Colloids and Surfaces*, vol. 5, no. 4, pp. 301–319, Dec. 1982.

[119] S. Bilgen and B. A. Wills, "Shear flocculation — A review," *Miner. Eng.*, vol. 4, no. 3–4, pp. 483–487, Jan. 1991.

[120] P. K. Weissenborn, L. J. Warren, and J. G. Dunn, "Selective flocculation of ultrafine iron ore 2. Mechanism of selective flocculation," *Colloids Surfaces A Physicochem. Eng. Asp.*, vol. 99, no. 1, pp. 29–43, 1995.

[121] L. Valderrama and J. Rubio, "High intensity conditioning and the carrier flotation of gold fine particles," *Int. J. Miner. Process.*, vol. 52, no. 4, pp. 273–285, 1998.

[122] E. Tabosa and J. Rubio, "Flotation of copper sulphides assisted by high intensity conditioning (HIC) and concentrate recirculation," *Miner. Eng.*, vol. 23, no. 15, pp. 1198–1206, 2010.

[123] B. Feng, J. Peng, W. Zhang, G. Luo, and H. Wang, "Removal behavior of slime from pentlandite surfaces and its effect on flotation," *Miner. Eng.*, vol. 125, no. January, pp. 150–154, 2018.

[124] Y. Chen, Q. Shi, Q. Feng, Y. Lu, and W. Zhang, "The Effect of Conditioning on the Flotation of Pyrrhotite in the Presence of Chlorite," *Minerals*, vol. 7, no. 7, p. 125, 2017.

[125] R. S. C. Smart, "Surface layers in base metal sulphide flotation," *Miner. Eng.*, vol. 4, no. 7–11, pp. 891–909, Jan. 1991.

[126] B. A. Wills and K. Atkinson, “The development of minerals engineering in the 20th century,” *Miner. Eng.*, vol. 4, no. 7–11, pp. 643–652, Jan. 1991.

[127] M. C. Pietrobon, S. R. Grano, S. Sobieraj, and J. Ralston, “Recovery mechanisms for pentlandite and MgO-bearing gangue minerals in nickel ores from Western Australia,” *Miner. Eng.*, vol. 10, no. 8, pp. 775–786, 1997.

[128] J. a. Rumball and G. D. Richmond, “Measurement of oxidation in a base metal flotation circuit by selective leaching with EDTA,” *Int. J. Miner. Process.*, vol. 48, no. 1–2, pp. 1–20, 1996.

[129] W. J. Trahar and L. J. Warren, “The flotability of very fine particles - A review,” *Int. J. Miner. Process.*, vol. 3, no. 2, pp. 103–131, 1976.

[130] M. D. Engel, P. D. Middlebrook, and G. J. Jameson, “Advances in the study of high intensity conditioning as a means of improving mineral flotation performance,” *Miner. Eng.*, vol. 10, no. 1, pp. 55–68, 1997.

[131] G. Chen, S. Grano, S. Sobieraj, and J. Ralston, “The effect of high intensity conditioning on the flotation of a nickel ore. Part 1: Size-by-size analysis,” *Miner. Eng.*, vol. 12, no. 10, pp. 1185–1200, Oct. 1999.

[132] G. Chen, S. Grano, S. Sobieraj, and J. Ralston, “The Effect of High Intensity Conditioning on the Flotation of a Nickel Ore, Part 2: Mechanisms,” *Miner. Eng.*, vol. 12, no. 11, pp. 1359–1373, Nov. 1999.

[133] E. J. Wellham, L. Elber, and D. S. Yan, “The role of carboxy methyl cellulose in the flotation of a nickel sulphide transition ore,” *Miner. Eng.*, vol. 5, no. 3–5, pp. 381–395, Mar. 1992.

[134] Y. Peng, B. Wang, and D. Bradshaw, “Pentlandite oxidation in the flotation of a complex nickel ore in saline water,” *Miner. Eng.*, vol. 24, no. 1, pp. 85–87, 2011.

[135] E. Paul, V. Atiemo-Obeng, and S. M. Kresta, *Handbook of Industrial Mixing*. Hoboken, NJ, USA: John Wiley & Sons, Inc., 2003.

[136] R. Multani, “Email Correspondence for Slurry sampling,” 2018.

[137] X. Manqiu, “Email Correspondence for Slurry sampling.” 2018.

[138] P. Clarke, D. Fornasiero, J. Ralston, and R. S. C. Smart, “A study of the removal of oxidation products from sulfide mineral surfaces,” *Miner. Eng.*, vol. 8, no. 11, pp. 1347–1357, 1995.

[139] M. Xu, “Modified flotation rate constant and selectivity index,” *Miner. Eng.*, vol. 11, no. 3, pp. 271–278, 1998.

[140] X. Bu, G. Xie, Y. Peng, L. Ge, and C. Ni, “Kinetics of flotation. Order of process, rate constant distribution and ultimate recovery,” *Physicochem. Probl. Miner. Process.*, vol. 53, no. 1, pp. 342–365, 2017.

Appendix A: Pulp Potential and pH Measurements during HIC and Froth Flotation

Table 14: Measured Pulp Potential and pH during 0/1100 HF Experiment.

0/1100 HF			
Stage	Time (minute)	pH	Eh
HIC	2	9.2	35
	16	8.8	58
	Add Lime	9.14	48
	22	8.9	57
	27	8.83	61
Froth Flotation	1	8.91	67
	4	8.85	69
	10	8.61	75
	15	8.56	67

Table 15: Measured Pulp Potential and pH during 10/1100 HF Experiment.

10/1100 HF			
Stage	Time (minute)	pH	Eh
HIC	23	9	54
Froth Flotation	5	8.82	64
	15	8	68

Table 16: Measured Pulp Potential and pH during 20/1100 HF Experiment.

20/1100 HF			
Stage	Time (minute)	pH	Eh
HIC	1	9.3	40
	5	8.85	57
	14	9.04	59
	27	8.73	65
Froth Flotation	3	8.86	67
	12	8.65	75
	15	8.59	72

Table 17: Measured Pulp Potential and pH during 0/No HIC Experiment.

0/No HIC			
Stage	Time (minute)	pH	Eh
Froth Flotation	15	8.5	90

Table 18: Measured Pulp Potential and pH during 20/1100 HF (20%) Experiment.

20/1100 HF (20%)			
Stage	Time (minute)	pH	Eh
HIC	3	9.75	15
	6	9.61	22
	8.75	9.74	24
	12.5	9.55	25
	17	9.38	33
	20	9.37	33
	22	9.34	34
	25	9.34	35
	27.5	9.31	37
	29.5	9.28	38
Froth Flotation	2.5	9.47	32
	5.75	9.42	35
	7.5	9.28	40
	11.25	9.12	46
	13.5	9.02	44
	15	8.99	48

Table 19: Measured Pulp Potential and pH during 10/No HIC Experiment.

10/No HIC			
Stage	Time (minute)	pH	Eh
Froth Flotation	0	9.12	29
	3	8.72	54
	6	8.65	60
	9.5	8.53	64
	13	8.53	65
	15.5	8.43	69

Table 20: Measured Pulp Potential and pH during 20/No HIC Experiment.

20/No HIC			
Stage	Time (minute)	pH	Eh
Froth Flotation	1.5	8.78	50
	3	8.73	57
	5.3	8.61	47
	7.5	8.6	58

Table 21: Measured Pulp Potential and pH during 0/1100 RT Experiment.

0/1100 RT			
Stage	Time (minute)	pH	Eh
HIC	Before HIC	9.16	36
	After HIC	8.44	32
Froth Flotation	3.5	8.46	60
	8.5	8.5	64
	8.29	8.29	69

Table 22: Measured Pulp Potential and pH during 10/1100 RT Experiment.

10/1100 RT			
Stage	Time (minute)	pH	Eh
HIC	Before HIC	9.3	30
	After HIC	8.65	16
	After transfer and Lime	9.25	35
Froth Flotation	6	8.89	42
	12	8.61	32

Table 23: Measured Pulp Potential and pH during 20/1100 RT Experiment.

20/1100 RT			
Stage	Time (minute)	pH	Eh
HIC	Before HIC	9.25	16
	After HIC	8.43	32
	After transfer and Lime	9.2	28
Froth Flotation	6	8.97	37
	10	7.78	50
	14	8.59	54
	15	8.59	54

Table 24: Measured Pulp Potential and pH during 10/900 RT Experiment.

10/900 RT			
Stage	Time (minute)	pH	Eh
HIC	Before HIC	9.21	38
	After HIC	8.52	26
	After transfer and Lime	9.23	19
Froth Flotation	2	8.97	35
	4	8.87	32
	6	8.79	42
	12	8.5	52
	15	8.44	55

Table 25: Measured Pulp Potential and pH during 10/1400 RT Experiment.

10/1400 RT			
Stage	Time (minute)	pH	Eh
HIC	Before HIC	9.37	33
	After HIC	8.49	13
	After transfer and Lime	9.18	7
Froth Flotation	2	8.98	25
	8.5	8.66	40
	15	8.36	56

Table 26: Measured Pulp Potential and pH during 5/900 RT Experiment.

5/900 RT			
Stage	Time (minute)	pH	Eh
HIC	Before HIC	9.2	38
	After HIC	8.72	34
	After transfer and Lime	9.3	3
Froth Flotation	2	9.07	29
	8.5	8.72	48
	15	8.49	59

Table 27: Measured Pulp Potential and pH during 5/1100 RT Experiment.

5/1100 RT			
Stage	Time (minute)	pH	Eh
HIC	Before HIC	9.27	40
	After HIC	8.4	24
	After transfer and Lime	9.21	2
Froth Flotation	1	8.99	38
	6	8.71	48
	11	8.52	57
	15	8.36	62

Table 28: Measured Pulp Potential and pH during 5/1400 RT Experiment.

5/1400 RT			
Stage	Time (minute)	pH	Eh
HIC	Before HIC	9.3	40
	After HIC	8.04	24
	After transfer and Lime	9.24	2
Froth Flotation	6	8.69	44
	14	8.5	52
	15	8.45	54

Table 29: Measured Pulp Potential and pH during 10/No HIC + DETA/SMBS Experiment.

10/No HIC + DETA/SMBS			
Stage	Time (minute)	pH	Eh
Froth Flotation	0	9.24	10
	3	8.75	35
	6	8.64	37
	10	8.56	40
	15	8.5	45

Table 30: Measured Pulp Potential and pH during 20/No HIC + DETA/SMBS Experiment.

20/No HIC + DETA/SMBS			
Stage	Time (minute)	pH	Eh
Froth Flotation	0	9.21	0
	3	8.8	30
	6.5	8.69	33
	10	8.68	37
	15	8.6	42

Table 31: Measured Pulp Potential and pH during 10/1100 RT + DETA/SMBS Experiment.

10/1100 RT + DETA/SMBS			
Stage	Time (minute)	pH	Eh
HIC	Before HIC	9.3	6
	After HIC	8.25	-9
	After transfer and Lime	9.19	18
Froth Flotation	3	8.98	30
	6	8.9	33
	11	8.7	37

Table 32: Measured Pulp Potential and pH during 20/1100 RT + DETA/SMBS Experiment.

20/1100 RT + DETA/SMBS			
Stage	Time (minute)	pH	Eh
HIC	Before HIC	9.23	6
	After HIC	8.34	-9
	After transfer and Lime	9.21	0
Froth Flotation	3	8.99	30
	10	8.77	35
	13	8.7	37
	15	8.63	37

Appendix B: EDTA Extraction and Oxidized Metal % for Various Experiments

Table 33: Oxidized Metal Levels for Concentrates and Tails From 10/No HIC Experiment.

10/No HIC	Oxidized Element (%w /w Element)		
	Mass of Cu	Mass of Ni	Mass of Fe
Feed	0.2013	0.1919	0.1181
T1C1	0.3030	0.2459	0.1324
T1C2	0.2632	0.2883	0.1334
T1C3	0.2557	0.3545	0.1263
T1C4	0.3012	0.4454	0.1205
T1Tails	0.1418	0.6015	0.1207

Table 34: Oxidized Metal Levels for Concentrates and Tails From 0/1100 RT Experiment.

0/1100 RT	Oxidized Element (%w /w Element)		
	Mass of Cu	Mass of Ni	Mass of Fe
Feed	0.2013	0.1919	0.1181
T2C1	0.4077	0.4259	0.1673
T2C2	0.3561	0.3799	0.1289
T2C3	0.3762	0.4054	0.1224
T2C4	0.3066	0.5317	0.1220
T2Tails	0.1456	0.4117	0.1082

Table 35: Oxidized Metal Levels for Concentrates and Tails From 10/1100 RT Experiment.

10/1100 RT	Oxidized Element (%w /w Element)		
	Mass of Cu	Mass of Ni	Mass of Fe
Feed	0.2013	0.1919	0.1181
T3C1	0.2642	0.3090	0.1130
T3C2	0.3437	0.4001	0.1255
T3C3	0.3230	0.4412	0.1188
T3C4	0.2455	0.6306	0.1051
T3Tails	0.1446	0.8197	0.1900

Table 36: Oxidized Metal Levels for Concentrates and Tails From 20/1100 RT Experiment.

20/1100 RT	Oxidized Element (%w /w Element)		
	Mass of Cu	Mass of Ni	Mass of Fe
Feed	0.2013	0.1919	0.1181
T4C1	0.2451	0.2390	0.1076
T4C2	0.3499	0.3572	0.1372
T4C3		0.3633	
T4C4	0.2922	0.6540	0.1425
T4Tails	0.2270	0.8534	0.1439

Table 37: Oxidized Metal Levels for Concentrates and Tails From 10/900 RT Experiment.

10/900 RT	Oxidized Element (%w /w Element)		
	Mass of Cu	Mass of Ni	Mass of Fe
Feed	0.2013	0.1919	0.1181
T5C1	0.1880	0.2230	0.0942
T5C2	0.2840	0.3241	0.1189
T5C3	0.2747	0.3830	0.1149
T5C4	0.2481	0.4679	0.1049
T5Tails	0.1433	0.5291	0.1328

Table 38: Oxidized Metal Levels for Concentrates and Tails From 10/1400 RT Experiment.

10/1400 RT	Oxidized Element (%w /w Element)		
	Mass of Cu	Mass of Ni	Mass of Fe
Feed	0.2013	0.1919	0.1181
T6C1	0.3212	0.2588	0.0979
T6C2	0.4691	0.3173	0.1152
T6C3	0.4418	0.3656	0.1034
T6C4	0.2720	0.4356	0.0894
T6Tails	0.1022	0.5373	0.1232

Table 39: Oxidized Metal Levels for Concentrates and Tails From 5/900 RT Experiment.

5/900 RT	Oxidized Element (%w /w Element)		
	Mass of Cu	Mass of Ni	Mass of Fe
Feed	0.2013	0.1919	0.1181
T7C1	0.3637	0.3936	0.1432
T7C2	0.4301	0.3739	0.1269
T7C3	0.4234	0.4837	0.1264
T7C4	0.2987	0.7481	0.1053
T7Tails	0.1188	0.5057	0.1314

Table 40: Oxidized Metal Levels for Concentrates and Tails From 5/1100 RT Experiment.

5/1100 RT	Oxidized Element (%w /w Element)		
	Mass of Cu	Mass of Ni	Mass of Fe
Feed	0.2013	0.1919	0.1181
T8C1	0.3107	0.2996	0.1278
T8C2	0.3593	0.3633	0.1146
T8C3	0.4136	0.3951	0.1105
T8C4	0.2778	0.4927	0.0971
T8Tails	0.1203	0.4117	0.1324

Table 41: Oxidized Metal Levels for Concentrates and Tails From 5/1400 RT Experiment.

5/1400 RT	Oxidized Element (%w /w Element)		
	Mass of Cu	Mass of Ni	Mass of Fe
Feed	0.2013	0.1919	0.1181
T9C1	0.4102	0.3805	0.1507
T9C2	0.5320	0.5210	0.1787
T9C3	0.4710	0.6074	0.1461
T9C4	0.3884	0.9447	0.1621
T9Tails	0.1011	0.7328	0.1504

Table 42: Oxidized Metal Levels for Concentrates and Tails From 10/No HIC + DETA/SMBS Experiment.

10/No HIC + DETA/SMBS	Oxidized Element (%w /w Element)		
	Mass of Cu	Mass of Ni	Mass of Fe
Feed	0.2013	0.1919	0.1181
T1C1	0.5544	0.5029	0.3127
T1C2	0.8609	0.6791	0.4434
T1C3	1.0319	0.7574	0.4647
T1C4	1.6213	0.9196	0.5550
T1Tails	0.4518	0.6892	0.1547

Table 43: Oxidized Metal Levels for Concentrates and Tails From 20/No HIC + DETA/SMBS Experiment.

20/No HIC + DETA/SMBS	Oxidized Element (%w /w Element)		
	Mass of Cu	Mass of Ni	Mass of Fe
Feed	0.2013	0.1919	0.1181
T2C1	0.4772	0.3379	0.2129
T2C2	0.6916	0.4851	0.3230
T2C3	0.7125	0.5460	0.3078
T2C4	1.1936	0.9150	0.4663
T2Tails	0.4810	0.3289	0.0974

Table 44: Oxidized Metal Levels for Concentrates and Tails From 10/1100 RT + DETA/SMBS Experiment.

10/1100 RT + DETA/SMBS	Oxidized Element (%w /w Element)		
	Mass of Cu	Mass of Ni	Mass of Fe
Feed	0.2013	0.1919	0.1181
T3C1	0.2935	0.2187	0.1395
T3C2	0.4414	0.2754	0.1751
T3C3	0.5447	0.3358	0.1736
T3C4	0.8676	0.5094	0.2255
T3Tails	0.6234	0.4358	0.1105

Table 45: Oxidized Metal Levels for Concentrates and Tails From 20/1100 RT + DETA/SMBS Experiment.

20/1100 RT + DETA/SMBS	Oxidized Element (%w /w Element)		
	Mass of Cu	Mass of Ni	Mass of Fe
Feed	0.2013	0.1919	0.1181
T4C1	0.3973	0.2242	0.1740
T4C2	0.5812	0.2766	0.2144
T4C3	0.6761	0.3363	0.2315
T4C4	0.7589	0.4636	0.2104
T4Tails	0.5161	0.4328	0.0942